Dissertation presented to the Instituto Tecnológico de Aeronáutica, in partial fulfillment of the requirements for the degree of Master of Science in the Program of Aeronautics and Mechanical Engineering of Materials, Manufacturing and Automation Area.

Nathianne de Moura de Andrade

DYNAMIC BEHAVIOR OF POWER LOSSES IN A POWER-CIRCULATING RIG FOR GEAR TESTING

Dissertation approved in its final version the signatories below:

Prof. Dr. Jefferson de Oliveira Gomes
Advisor

Prof. Dr. Ronnie Rodrigo Rego
Co-advisor

Prof. Dr. Pedro Teixeira Lacava
Pro-Rector of Graduate Courses

Campo Montenegro
São José dos Campos, SP – Brazil
2019

BIBLIOGRAPHIC REFERENCE

ANDRADE, N. M. **Dynamic behavior of power losses in a power-circulating rig for gear testing**. 2019. 124p. Dissertation of Master of Science in Materials, Manufacturing and Automation Area – Instituto Tecnológico de Aeronáutica, São José dos Campos.

CESSION OF RIGHTS

AUTHOR NAME: Nathianne de Moura de Andrade
PUBLICATION TITLE: Dynamic behavior of power losses in a power-circulating rig for gear testing
PUBLICATION KIND/YEAR: Dissertation / 2019

_____
Nathianne de Moura de Andrade
Praça Marechal Eduardo Gomes, 50 - Vila das Acacias.
CEP: 12228 - 900, São José dos Campos - SP

DYNAMIC BEHAVIOR OF POWER LOSSES IN A POWER-CIRCULATING RIG FOR GEAR TESTING

Nathianne de Moura de Andrade

Thesis Committee Composition:

Prof. Dr.	Anderson Vicente Borille	Chairperson	-	ITA
Prof. Dr.	Jefferson de Oliveira Gomes	Advisor	-	ITA
Prof. Dr.	Ronnie Rodrigo Rego	Co-advisor	-	ITA
Prof. Dr.	Ricardo Sutério	Internal Examiner	-	ITA
Prof. Dr.	Izabel Fernanda Machado	External Examiner	-	USP

ITA

I dedicate this work to the inspiring women in my family.

Acknowledgment

First of all, I thank God for the many opportunities I have been given until here and for the parents to whom I have been entrusted. Without their unconditional support, many of these opportunities would have be in vain in my path.

I thank my aunts, my uncles, my grandmother and my cousins. Although we were not together as frequently as we wished, our reunions and phone calls were my safe haven during those years. Thank you for being my purest source of happiness and motivation.

I thank Pedro Teruel for the offered partnership before this challenge. Thank you for all the emotional support, technical discussions and help provided.

I thank my mentor, Jefferson de Oliveira Gomes, and my co-counselor, Ronnie Rodrigo Rego, who have guided me during the development of this project. I thank my colleagues from the Group of Gear Innovation, André d'Oliveira, Lucas Robatto, Thiago Neves, Rodrigo Metzger, Marcos Campos, Artur Cantisano and Ângelo Carvalho for the fellowship and availability offered. I also thank for all the support I received from those who are part of the Competence Center in Manufacturing (CCM-ITA). In addition to all the contributions during my Master course, this team's work enabled a remarkable achievement for the present work: a masters dissertation presentation was broadcast online at CCM-ITA for the first time.

Finally, I thank CNPq for supporting the Brazilian scientific research, including the present work.

"What is not started today is never finished tomorrow".

(GOETHE, Johann).

Resumo

Este trabalho apresenta uma investigação estruturada cujo objetivo são medições mais confiáveis da eficiência de transmissão em uma bancada de recirculação de potência. A Associação Alemã de Pesquisa em Tecnologia de Transmissões (FVA) estabeleceu um método para medição de eficiência de transmissões em bancadas que apresentam esse conceito construtivo, assumindo que cada uma das duas caixas de engrenagens dissipa 50% da potência entregue ao sistema pelo motor. Uma investigação experimental foi delineada e conduzida para verificar os impactos de caixas de transmissão com perdas diferentes entre si no comportamento dinâmico das perdas de potência dentro da malha fechada de potência. Uma bancada de recirculação de potência foi concebida com medições de torque dentro da malha e dotada de um sistema capaz de induzir perdas controladas independentemente em cada caixa de transmissão. Um experimento Fatorial Completo 2^4 foi usado para identificar fatores e interações significantes e o plano experimental foi aplicado em duas condições: com e sem torque aprisionado. A partir dos resultados experimentais, foi possível estabelecer o sentido do fluxo de potência e derivar conclusões sobre a relação entre as perdas das caixas de transmissão. Na bancada usada para esse estudo, foi mostrado que perdas de potência nas caixas dependem das variações de perda de potência em outras caixas pertencentes à malha fechada, principalmente daquelas situadas antes da caixa observada, em relação ao sentido estabelecido pelo fluxo de potência. Notavelmente, uma das caixas se mostrou menos suscetível às variações em outras caixas. Uma hipótese para a determinação do ponto menos sensível às variações em outros pontos da malha fechada foi proposta com base na revisão de literatura e nas observações experimentais.

Abstract

This work presents a structured investigation whose objective is more reliable efficiency measurements at a power-circulating rig. The German Research Association for Drive Technology (FVA) has established a method to measure gear efficiency for this rig concept, assuming that each of the two boxes dissipates half of the amount of power delivered by the motor. An experimental investigation was designed and conducted in order to verify the impacts of transmission boxes with different power losses over the dynamic behavior of the power losses inside the loop. A power-circulating rig was conceived with torque measurements inside the power loop and with a system able to induce controlled losses independently on each transmission box. A 2^4 full factorial design was used to identify significant factors and interactions and this experiment plan was applied under two conditions: with and without locked-in torque. From the experiment results, it was possible to establish the power flow direction and draw conclusions about the relation among the transmission boxes' losses. In the test rig used for this study, it was shown that losses on boxes depend on loss variations on other boxes belonging to the power loop, mainly on those located upstream with relation to the power flow direction. Remarkably, one of the boxes was less susceptible to other boxes' loss variations. A hypothesis for the determination of the less susceptible point to variations in other points of the loop was proposed based on the literature review and the experimental observations.

List of Figures

List of Tables

List of Acronyms

ANOVA   *Analysis of Variance*

DoE   *Design of Experiments*

FVA   *German Research Association for Drive Technology*

FZG   *Forschungsstelle für Zahnräder und Getriebebau*

IEEE   *Institute of Electrical and Electronics Engineers*

ISO   *International Organization for Standardization*

ITA   *Aeronautics Institute of Technology*

PRILs   *Power-Circulating Rig with Induced Losses*

List of Symbols

$^\circ$	Degree
BL_i	Torque loss on box i
C_1, C_2	Gear center points
CO_2	Carbon dioxide
d_{w1}, d_{w2}	Gear pitch diameters
E_A	Effect due to factor A in relation to all effects
F_0	Reference value from an F-distribution
$F_{fric,i}$	Friction force on disk i
g	Gram
g	Acceleration due to gravity
g/km	Grams per kilometer
Hz	Hertz
i	Gear ratio
J	Joule
KWh	Kilowatt Hour
m	Mass
M_i	Mass added onto box i
min	Minute
mm	Milimeter
MS_A	Mean square of factor A
MS_T	Mean square of all experimental runs

mV	Milivolt
N	Total number of degrees of freedom
N.m	Newton meter
N_A	Number of degrees of freedom of factor A
N_i	Normal force on disk i
ºC	Grades Celsius
P_{in}	Power input
P_L	Power loss
P_{out}	Power output
rpm	Rotations per minute
SS_A	Sum of squares due to factor A
SS_E	Sum of squares due to experimental error
SS_T	Sum of squares due to all effects
T_i	Torque on measurement point i
T_{in}	Torque input
T_{out}	Torque output
V	Volt
V_g	Gear instantaneous tangential velocity
V_{gn}	Normal to gear surface velocity
V_{gt}	Tangential to gear surface velocity
V_p	Pinion instantaneous tangential velocity
V_{pn}	Normal to pinion surface velocity
V_{pt}	Tangential to pinion surface velocity
β	Statistical level of confidence

η	Gear efficiency
η_T	Transmission efficiency
ϑ_{oil}	Oil temperature
υ_1, υ_2	Degrees of freedom of the numerator and denominator of an F-distribution
Ω	Ohm
ω_{in}	Input rotation speed
ω_{out}	Output rotation speed

Summary

1   Introduction

Fossil fuel usage and greenhouse gas emission will be still an issue for the next decades (CONTI, 2016). The world energy demand is expected to grow about 48% by 2040, compared to what was recorded in 2012, and fossil fuels will fulfill even 78% of this estimated demand. Forecasts from International Energy Outlook 2016 indicate that the demand for petroleum and other liquid fuels is expected to grow from 90 million barrels per day in 2012 to 121 million barrels per day in 2040 and world energy-related CO_2 emissions will increase from 32.3 billion metric tons to 43.2 billion metric tons for the same period.

This scenario, along with a prognosis of oil scarcity for the next decades (SHAFFFIE and TOPAL 2017; BRITISH PETROLEUM, 2016), has stimulated greater rationalization of the use of this non-renewable energy source and efforts towards the improvement of technologies based on alternative sources (DRESSELHAUS, 2001). Some sectors play important roles in this scenario. Since, anthropogenic emissions of carbon come primarily from the combustion of fossil fuels, power generation sector is in the center of this discussion. Alongside there are intense energy-consuming sectors, such as transport, which is responsible for 26% of the world energy demand and whose main energy source is oil, since it attends to 78% of the transport sector's total demand.

Some of the direct consequences of this finding are the increasing incidence of government intervention for the reduction of energy consumption and emission of greenhouse gases (ZHANG et al., 2011; ZHANG et al., 2014) and for the increase of the use of clean and renewable sources of energy (SWART et al., 2009). The European Union has adopted legislation to guide the technological development of cars with less environmental impact: the average emission of cars produced after 2015 should be lesser than 130 g/km (EUROPEAN PARLIAMENT AND THE COUNCIL OF THE EUROPEAN UNION, 2009) and after 2020 lesser than 95 g/km (EUROPEAN PARLIAMENT, 2014). The European Union also proposed a target corresponding to 20% share of renewable energies in overall Community energy consumption by 2020 (SWART et al., 2009).

Transmissions are used to convert torque and speed in all kind of vehicles, with combustion or electric engines, aircraft and watercraft included (LECHNER and NAUMHEIMER, 1999). They are also present in renewable energy generating process, such as wind energy generating, by the reason of common generator require that the rotor speed be

multiplied, and the rotor torque be reduced. Since transmission are closely related to transport sector, one of the most intense energy consuming sector and associated with greenhouse emission, and with wind energy, their efficiency is of central importance with respect to greenhouse emission, fuel consumption and electric energy generating.

The automotive industry has the challenge of developing vehicles with lower rates of fuel consumption and emission of polluting gases. One of the three main trends pointed out by Chiara and Canova (2013) to increase car's efficiency is managing transmission losses, what accounts for 5,5% of total fuel energy in a passenger car with manual gear transmission. Additionally, the transmission system position, after the engine output, is strategic for energy savings: every 1 J of energy saved in the transmission box means a saving of 4 J in fuel (HÖHN et al, 2009). The wind power industry was also affected by this global trend, since this wind energy is pointed as one of the most relevant energy sources for global energy sustainability and its contribution is expected to grow 3.4 times by 2040, as can be seen in Figure 1.1 below (CONTI, 2016).
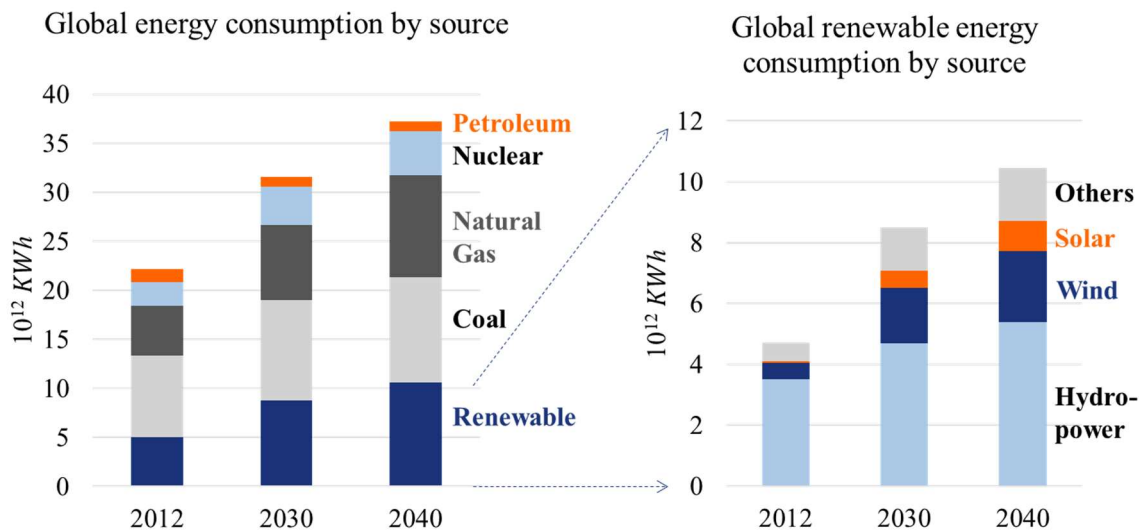
Figure 1.1: Global energy demand foresee until 2040 by source. Adapted from Conti et al. (2016).

Although gear efficiency is already very high when compared to other mechanical transmission system (JUVINALL and MARKESH, 1991), accordingly to the given context and the following examples, gear efficiency is still subject of current studies. Some gear applications imply trade-offs between efficiency and other specific requirements, such as the electric vehicles' challenge relative to gear noise (LI, 2009). For others, even a small increase

in gear torque efficiency represents significant energy savings or reductions of emission, such as production of renewable energy from wind, due to the high total available power and the increasing number of wind farms (MARQUES et al, 2014), or combustion engine vehicle, since current world fleet account for 16,5% of the fossil fuel consumption (THIES et al., 2014) and it is expected to be the largest transportation fuel for the next decades (CONTI et al., 2016).

A conventional method of studying gear torque efficiency using gear test samples is by means of a power-circulating test rig. This type of rig normally has two identical gearboxes, and each gear is connected by a shaft to its correspondent on the other box. This concept's most notable features are the locked-in torque is applied statically by twirling the flexible shafts and fixing the system under this condition, and an electrical engine, which is arranged outside the loop and connected to one of the gearboxes, provides the demanded energy to spin all the system (ISO, 2006; WARD JR., 2001; DOLESCHEL, 2002).

The German Research Association for Drive Technology (FVA) has established for this rig concept, by means of the report 345, a method to measure gear efficiency assuming the power delivered by the motor is equal to the total loss, which is measured outside the loop and divided between the two gearboxes. The statement depends heavily on similarity among other sources of power loss belonging to the gearboxes, such as bearings, seals, gears and other components (HÖHN et al, 2009), besides natural variability on assemblage. For more complex rig configurations of the same testing concept, with three or four gearboxes, this assumption should be contested, since one cannot guarantee the elements' similarity and unvarying assembly.

Andersson et al. (2014) and Wang et al. (2018) contributed to improve the method proposed by FVA 345. Andersson et al. (2014) introduced a new method to disregard the thermal effect over the efficiency measure. Wang et al. (2018) presented a calculation method to identify the losses of a power loop test rig coming from different sources, such as gears, bearings and churning of lubricant, accordingly to its characteristics. However, their studies still did not investigate whether there is interaction among the boxes' power losses, whether the boxes present unequal efficiencies or how the power flows through the system.

Maia et al. (2014) investigated the dynamic behavior of the losses in a power-circulating gear test rig. This work focused on the development of a Multiphysics analysis model to evaluate the dynamic behavior of a gear test bench in a power-circulating system in order to specify the electrical motor capable of driving the bench. This development also required simplifications, such as the power flow behavior, since not much was known about the studied phenomenon.

Nowadays, the dynamic behavior of power loss distribution in the gearboxes is simplified. The objective of this study is more reliable power losses measurements in a power-circulating test rig. In order to achieve this objective, it is necessary to know the distribution of the power losses among the gearboxes when whether variability on other boxes losses may affect the losses on the box of interest. Three questions were proposed to guide this work forwards the objective:

• Which experimental procedure is suitable to achieve the objective?

• Is one box's torque efficiency affected by the power losses of other boxes belonging to the power loop?

• Is it possible to quantify the relation between one box's torque efficiency and the power losses of other boxes belonging to the power loop?

In order to study this behavior, a power recirculating test rig was conceived at the Aeronautics Institute of Technology (ITA), in Brazil, considering a mechanism capable of individual induction of power losses in each transmission box and other simplifications, such as synchronized pulleys and belts instead of gear. Its design and construction were the objective of a course conclusion work at ITA.

This test rig, called PRILs, has two possible assembly configurations: two-box power loop and four-box power loop. The four-box configuration was chosen to the present investigation, since there is a test rig for gear testing at ITA with this same feature. It is expected that the results obtained with PRILs will support studies about gear efficiency conducted at the other rig.

The study of the dynamics of the torque loss distribution among the transmission boxes will be based on the strain on both shafts of each box. The strain will then be correlated with the input and output torque, and the difference between these measurements is the definition of transmission power losses. Strain gauge sensors will be used for this purpose.

1.1   Structure

The structure of the present work is summarized in Figure 1.2. The second chapter "Literature Review" provides relevant information for discussions in the following chapters, including the definition of the objective of this work and the proposed research questions. Topics about sources of power losses in power transmission systems, experimental methodology for gear testing and design of experiments are addressed there.
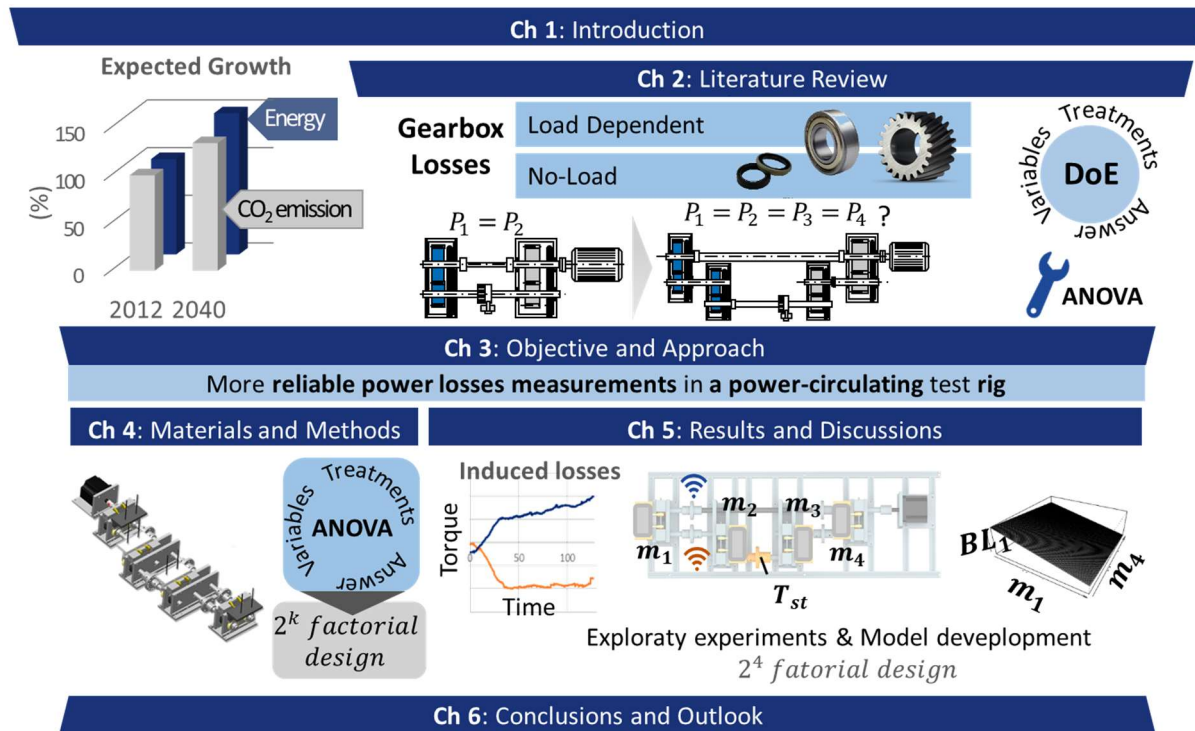
Figure 1.2: Structure of the dissertation and main addressed topics.

Based on the background offered in the previous section, the third chapter presents the objective of a novel method for determining the power loss distribution on a four-box power-circulating test rig. The forth chapter "Materials and Methods" presents the tools used for the proposed investigation. The power loop test rig designed for the present purpose and the experimental plan designed for the other questions will be presented here. Additionally, preliminary test' results are also included on the planning description. They allowed the determination of limitation for the following investigations, such as applied torque, speed and amount of induced losses.

The fifth chapter "Results and discussion" shows the results of the investigations resulting from the research questions. A test procedure, demanded by the first question, was develop based on specific literature and preliminary tests. A 2^4 full factorial design was applied to identify factors and interactions that influence on the studied behavior, which is the matter of the second question; and another 2^4 fractional factorial design was used to obtain the models for losses and efficiency, including the locked-in torque effect, in order to answer the third question.

The chapter "Conclusion and Outlook" summarizes the main outcomes of this work and future applications for the acquired knowledge. Also, potentially relevant limitations and new questions derived from the present study are also pointed out as possible subjects of further investigations.

1.2   Contributions

The work presented here studies the dynamic behavior of a power-circulating rig at different conditions of power loss distribution. The results obtained may help to achieve greater accuracy in the measurements of transmission efficiency by showing some features of the dynamic behavior of the losses and by suggesting new points for torque measuring.

1.3   Scope boundaries

The present work contains the theoretical comparison among method of evaluation of gear efficiency and an experimental investigation of topics, which were not covered by the used references. This work does not cover assessment of improvements of gear efficiency, methods to predict gear efficiency or power losses model of transmission parts.

2   Literature Review

This chapter is divided into two parts. The first part consists on the review of theory about gear efficiency as well as established methods and test rigs for gear efficiency measurement. The theory of power losses in transmission gearboxes will provide the motivation of this study, also representing the base for the definition of the requirements for the methods and materials adopted in the further investigations. The second part presents the fundamentals used for the design of the experiments. That includes statistical definitions and methods used for data analysis.

2.1   Transmission power losses

Transmission efficiency is defined as the ratio between the power output (P_{out}) and the power input (P_{in}) of a transmission system, or even in terms of power loss (P_L) In terms of torque, torque efficiency can be defined as showed in Equation 2.1 (LECHNER and NAUMHEIMER, 1999):

$$\eta_T = \frac{P_{out}}{P_{in}} = \frac{P_{in} - P_L}{P_{in}} = 1 - \frac{P_L}{P_{in}} \qquad \text{Eq. 2.1}$$

Gearboxes are largely applied for vehicle transmissions and for wind generators, besides many other applications. This kind of transmission presents some advantages in comparison to other commons transmissions (belts and chain), such as toughness and maintainability. Additionally, a pair of spur gears, the most applied kind, generally presents a value of torque efficiency as high as 98% (JUVINALL and MARKESH, 1991).

The power losses in gearboxes cause a reduction deduction on the torque output, in relation on what was expected considering the torque input and the transmission ratio. If the gear geometry is still not affected by any side effect of the power losses, none reduction of the speed output is expected due to the transmission efficiency.

In a transmission gearbox, there are three main sources of power losses: gear, bearings and seals (HÖHN et al., 2009). Gears and bearings present losses even when there is no load.

Therefore, gear and bearing losses can be divided in load dependent and load independent losses. Figure 2.1 shows the distribution of losses among the transmission box' elements and accordingly with its nature.
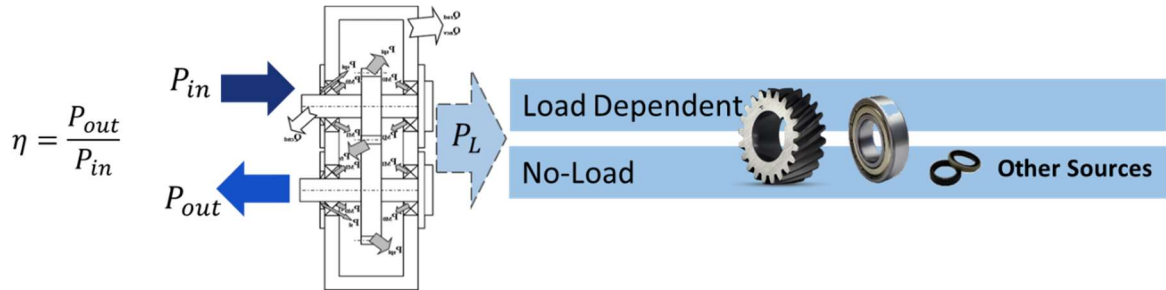
Figure 2.1: Power losses in a gearbox accordingly with their sources and nature (MARTINS et al., 2006).

When power losses of gears, bearings and seals are compared under an overall perspective, the first one produces the largest losses (LECHNER and NAUMHEIMER, 1999). Lechner and Naumheimer (1999) provide an example of how the power losses are distributed among the cited sources in a common automotive gearbox. Figure 2.2 shows that the load dependent losses coming from gears are larger than the no-load losses coming from bearings and gears and the load dependent losses coming from bearings together.
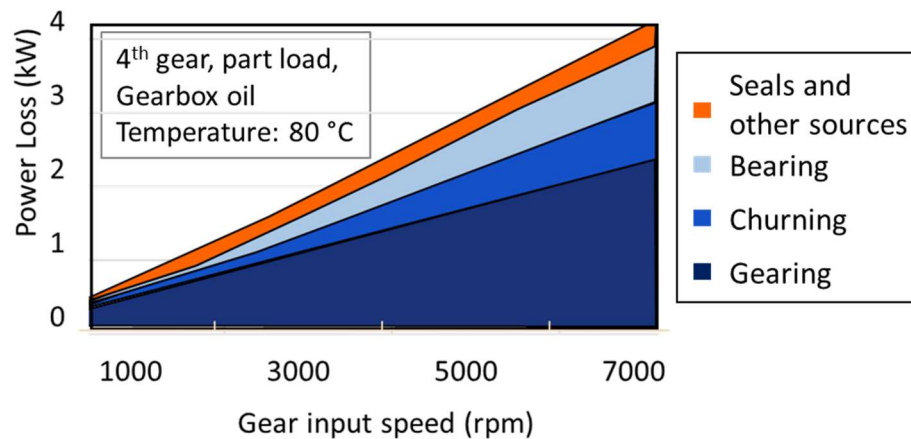
Figure 2.2: Distribution and size of power losses of a coaxial 6-speed manual gearbox in 4th gear at the condition of 50% of part load (LECHNER and NAUMHEIMER, 1999).

The power losses on those components vary accordingly to temperature, speed and lubricant properties (HÖHN et al., 2009). Besides the operational conditions, there is also variation on the power losses due to variance on the assembly process (ANDERSSON et al., 2014).

2.1.1 Gear efficiency

Gear efficiency is defined similarly to the definition presented for transmission efficiency: as the ratio between the power output and the power input (XU, 2005). It is unavoidable that some energy be lost due to the gearing, since some phenomena like friction and drag resistance are characteristic of this mechanism. Equation 2.2 shows the used formula to define gear efficiency:

$$\eta = \frac{P_{out}}{P_{in}} = \frac{P_{in} - P_L}{P_{in}} = 1 - \frac{P_L}{P_{in}}$$
Eq. 2.2

Gear efficiency can be also expressed in terms of torque input and output (T_{in} and T_{out}, respectively) and gear ratio (i) (XU, 2005), accordingly to Equation 2.3:

$$\eta = \frac{P_{out}}{P_{in}} = \frac{T_{out}\omega_{out}}{T_{in}\omega_{in}} = \frac{T_{out}i\omega_{in}}{T_{in}\omega_{in}} = i \cdot \frac{T_{out}}{T_{in}}$$
Eq. 2.3

Gear power losses are divided in two categories: the losses that occur even when there is no load on the system and the losses that depend on the load applied. Load independent gear losses normally are related to the churning and splashing of the lubricant and drag force of the fluid present on the gear surroundings (XU, 2005). These losses depend on lubricant properties and on how deep the gears are immersed into the lubricant and another fluid without the lubrication purpose.

Load dependent losses are related to the body solid and to the shearing of the lubricant film between the gear flanks (JOACHIM et al., 2004). This kind of power loss usually increases with the normal force and the surfaces relative velocity (HÖHN et al., 2009). However, it also

depends on the load; on the temperature; on the lubrication regime, which is not constant and generally mixed; and on the surface roughness (JOACHIM et al., 2004).

Both kind of losses are closely related with the engaging dynamics. The most notable characteristic of the involute gears is the capability to provide constant angular velocity ratios (JUVINALL and MARKESH, 1991). The tooth flank shape is primarily designed to coincide with a portion of the involute curve. One of the main features of this engaging is that all the points of contact are on a line. This line is called action line. The point C in Figure 2.3 is the intersecting point between the action line and the center-to-center line segment (C_1 and C_2). This point belongs also to both pitch circles, which diameter are d_{w1} and d_{w2}. The angle between the action line and the tangent on pitch circles is the pressure angle and the line across the flank of the tooth that also contains C is called pitch line.
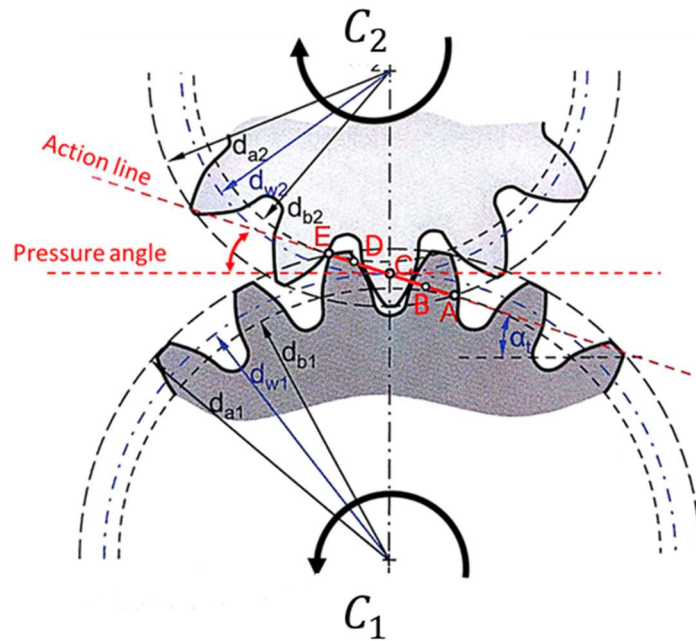
Figure 2.3: Action line A-B-C-D-E (KLOCKE and BRECHER, 2016).

V_p and V_g are the instantaneous tangential velocities of the pinion and gear in the figure C, respectively. These velocities are tangent the center of the gears. V_{pn} and V_{gn}, the normal to the surface velocities, are always the same, otherwise the contact would be lost, or the teeth

would be crushed. V_{pt} and V_{gt} are the tangential to the surface velocities and their difference represent the relative speed between the surfaces, what is known as sliding velocity.

The situation presented in Figure 2.4 (b) shows the contact in an ordinary point between A and C. The difference between the instantaneous tangential velocities (V_p and V_g) causes a non-zero sliding velocity. In other words, there are sliding and rolling moves. Figure 2.4 (a) shows the moment when the contact point is at the pitch circles. At this moment, V_p and V_g are equal and tangent to the pitch circles. V_{pt} and V_{gt} are also equal and the sliding velocity is null. Thus, at the pitch circle there is only rolling move.
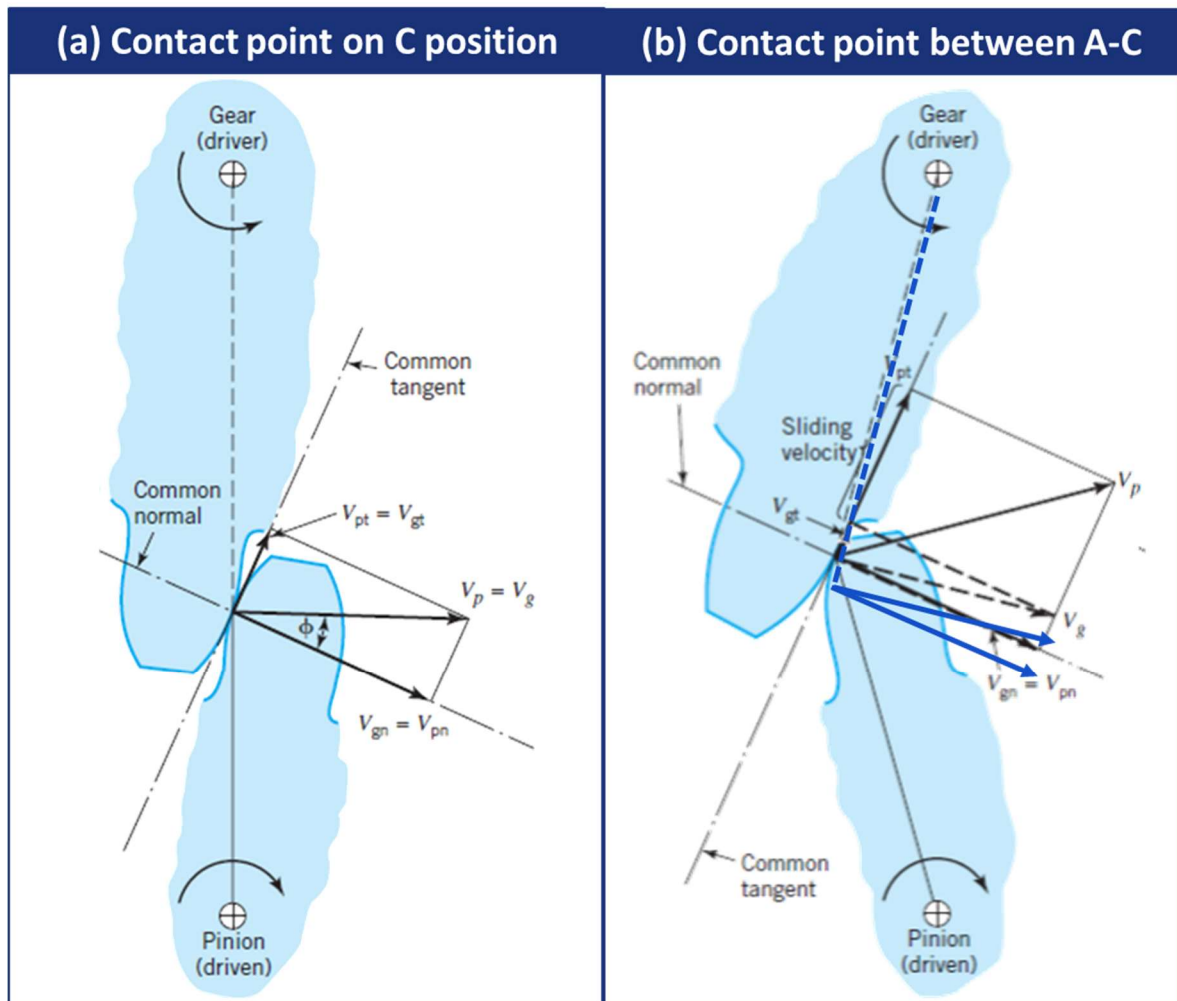
Figure 2.4: Kinematics and dynamics of gear engaging (JUVINALL and MARKESH , 1991).

Around the pitch line, the contact pressures are higher, since the normal forces are higher and the rolling forces lower. Therefore, this region is favorable to contact fatigue mechanisms, as can be seen in Figure 2.5. The sliding velocity gets higher as the contact goes

farther from the pitch line. High sliding velocity and pressure affect the lubrication regime, the generated heat and the temperature. All these effects combined create a worse lubrication condition, what may damage the surface integrity (JUVINALL and MARKESH, 1991).
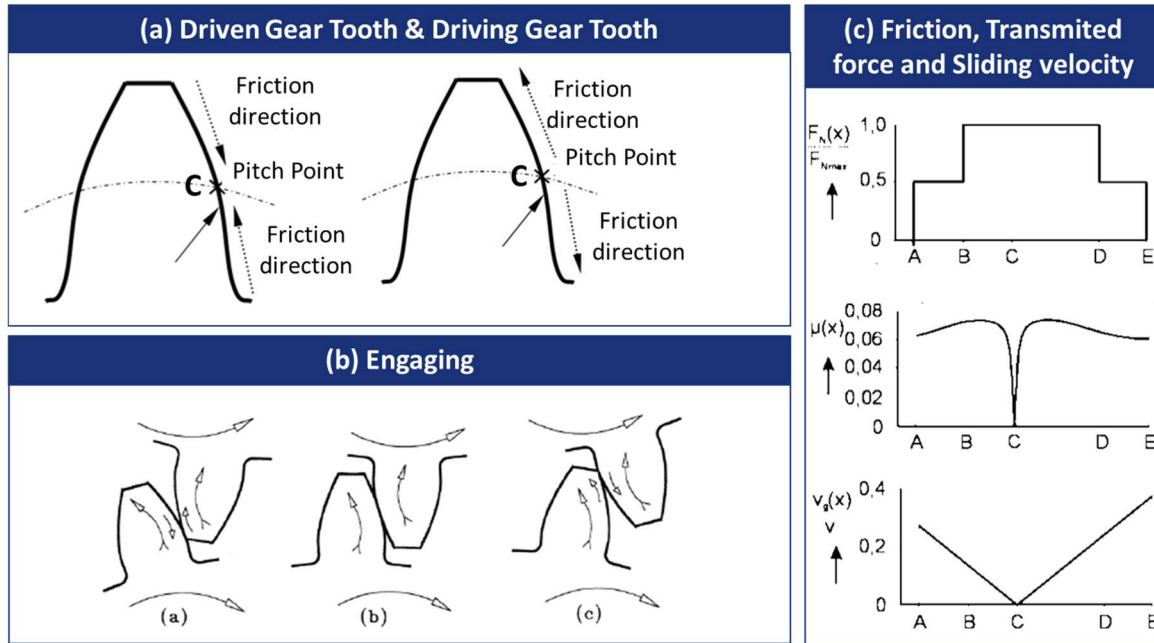
Figure 2.5: Engaging kinematics and some related gear failures (HÖHN et al., 2009; LI et al., 2014).

From what has been described, gear efficiency depends on lubrication properties, velocity, torque and temperature. Additionally, it is possible to conclude that improvements in gear efficiency can be achieved shrinking the losses caused by drag forces, churning lubricant and friction forces. Although, current gear improvements occur at small steps (LECHNER and NAUMHEIMER, 1999) and trade-offs between gear efficiency and other requirements must be observed (LI et al., 2009).

2.1.2 Investigation on gear efficiency: simulation and experiments

There are two main approaches for studying gear torque efficiency: simulation and experimentation. The former approach offers a more suitable aid for the project phase and can reproduce conditions that might be hard to control during testing, such as assembly errors. Although, the current techniques are still limited due to the required computational power and to the usual model simplifications (PETRY-JOHNSON et al., 2008). In addition, it is expected

the simulation models to be crosschecked and even adjusted with experimental test. Thus, the experimental investigation plays a very important role in gear efficiency research area.

Tribology tests are also performed in order to analyze the tribological behavior of alternative tribosystems, which can be used for gear application in order to improve efficiency. Generally, this kind of investigations is focused on the load dependent losses, since the load independent losses depend on the gear and gearbox geometries and on the gears' surroundings, such as the amount of lubricant and other lubricant's properties. Additionally, tribological tests generally can reproduce just a part of the gear engagement process, since this mechanism presents variation on the ratio between the rolling and sliding movement (Höhn et al., 2001).

Höhn et al. (2001) presents a comparative study between the observed frictional behaviors obtained from tests performed in different test facilities: a twin disk machine and a power-circulating gear test rig. Both facilities are able to simulate a movement with sliding and rolling components. Twin disk bench is a test facility in which two rolling discs are pressed one against the other. According to the selection of the rotational speed and the disk's diameters, it is possible to simulate a well-defined condition of movement including sliding and rolling components (DAVIS, 2005; MENEGHETTI et al., 2016). This machine can be seen in Figure 2.6.

FZG-FVA power-circulating test rig
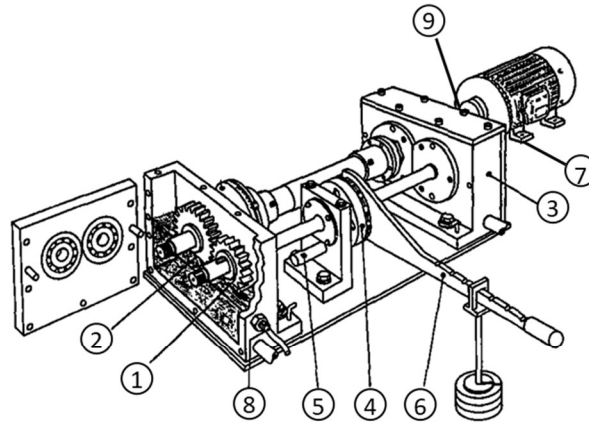
① Test Pinion	⑤ Locking Pin
② Test Wheel	⑥ Load Lever and Weights
③ Slave Gear	⑦ Variable Speed Engine
④ Load Clutch	⑧ Temperature Sensor
	⑨ Measuring Torque Clutch

Twin-disk test
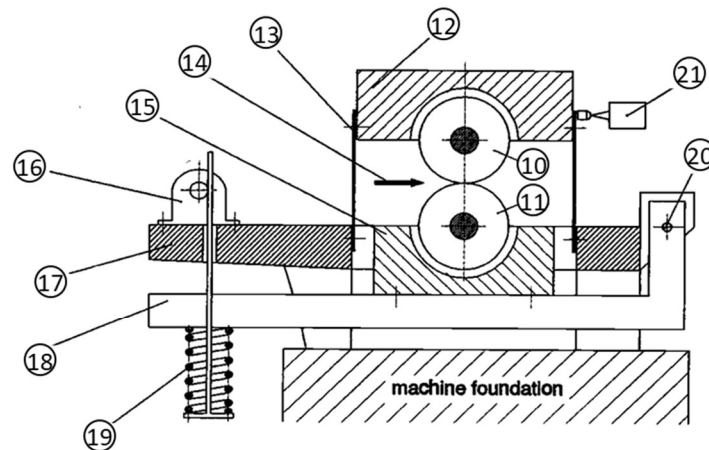
⑩ Disk	⑭ Oil Injection	⑱ Pivot-arm
⑪ Disk	⑮ Lower Bench	⑲ Helical Spring
⑫ Upper Bench	⑯ Actuating Drive for Load	⑳ Pivot
⑬ Flat Springs	⑰ Frame	㉑ Load Cell (Frictional Force)

Figure 2.6: Test benchs (HÖHN et al., 2001).

Tribological behavior observed in benches that only reproduce conditions of 100% sliding rate are not comparable to the frictional behavior of gears observed in a power-circulating gear test rig. The twin disk bench results can be related to the power-circulating gear test rig results, due to its capability of reproducing a condition with rolling and sliding movements. Höhn et al. (2001) obtained a good relative and absolute correlation between the twin disk test results and power-circulating gear test rig results.

Despite their limitations, tribological tests are very attractive and suitable to preliminary investigations on gear efficiency, since they are fast, simple and less expensive when compared to gear testing (HÖHN et al., 2001, MICHAELIS et al., 2004).

A gear tester machine that uses power-circulating concept are also known by back-to-back test rig or FZG test rig. These rigs have two gearboxes, a test box and a slave box. Each box contains a one-stage gear mesh, pointed out as 1, 2 and 3 in Figure 2.6. The test box and the slave box have the same transmission ratio and center-to-center distance, and the gears of each box have the same number of teeth (DOLESCHEL, 2002, ISO 14635-1).

Power-circulating test rig is a rig for testing gear samples and the FZG model can be seen in Figure 2.6. Procedures for testing gear endurance and gear efficiency have been developed using this kind of rig (DOLESCHEL, 2002; HÖHN et al. 2009; ISO 14635-1).

The power-circulating concept is such as that each gear of the box is connected to the corresponding gear of the other box, as illustrated on the Figure 2.6. There is a split coupling, here called Load Clutch (item 4 in Figure 2.6), mounted on one of the shafts. The Load Clutch is used to apply the locked-in load on the system: one of its halves is clamped by the Locking Pin (number 5 in Figure 2.6) while Load Lever and the Weights (number 6 in Figure 2.6) twist the shafts, loading both gear meshes. The power loop is closed by fixing the Load Clutch halves and taking out the Locking Pin. In order to reproduce dynamic tests, there is an engine outside the power loop. It provides just the energy required to spin the system (DOLESCHEL, 2002; HÖHN et al. 2009; ISO 14635-1).

The explained concept requires a less powerful engine to test gear with the same load, since, it is partially applied by the torsion of the system and the engine supplies just the energy dissipated during the operation (DOLESCHEL, 2002; PETRY-JOHNSON et al., 2008).

2.1.3 FZG-FVA gear efficiency test and further investigation

FZG-FVA efficiency test is a widespread method for assessing gear efficiency with a power-circulating test rig (ISO 14635-1). The objective of this method is to compare the tribological behavior of formulated lubricant system. The procedure for this kind of test considers that efficiency depends on five variables: temperature, torque, speed, lubricant and method of lubrication, such as dip lubrication. By means of it, several runs are conducted with different levels of the first three variables, while the lubricant is kept (DOLESCHEL, 2002). Different lubricants can be compared using the lubricant coefficients results of the runs. The levels of torque, tangential speed and temperature are shown in Figure 2.7. The diagram bellow shows the order of runs to conduct experimental procedure prescribed by FVA n° 345 (DOLESCHEL, 2002). Each line contains the runs that should be conducted in order at the same condition of temperature and load. There are three standard run duration: 5 minutes (white dot), 15 minutes (black dot) and 5 hours (black square). Each run should be done at a defined speed, that could be seen in Figure 2.7. The temperature (ϑ_{oil}) is specified in the second column and the load (KS) at the third one. KS0 represents no locked-in toque applied. KS5, KS7 and KS9 represent, respectively, 94.1 N.m, 183.4 N.m and 302.0 N.m.
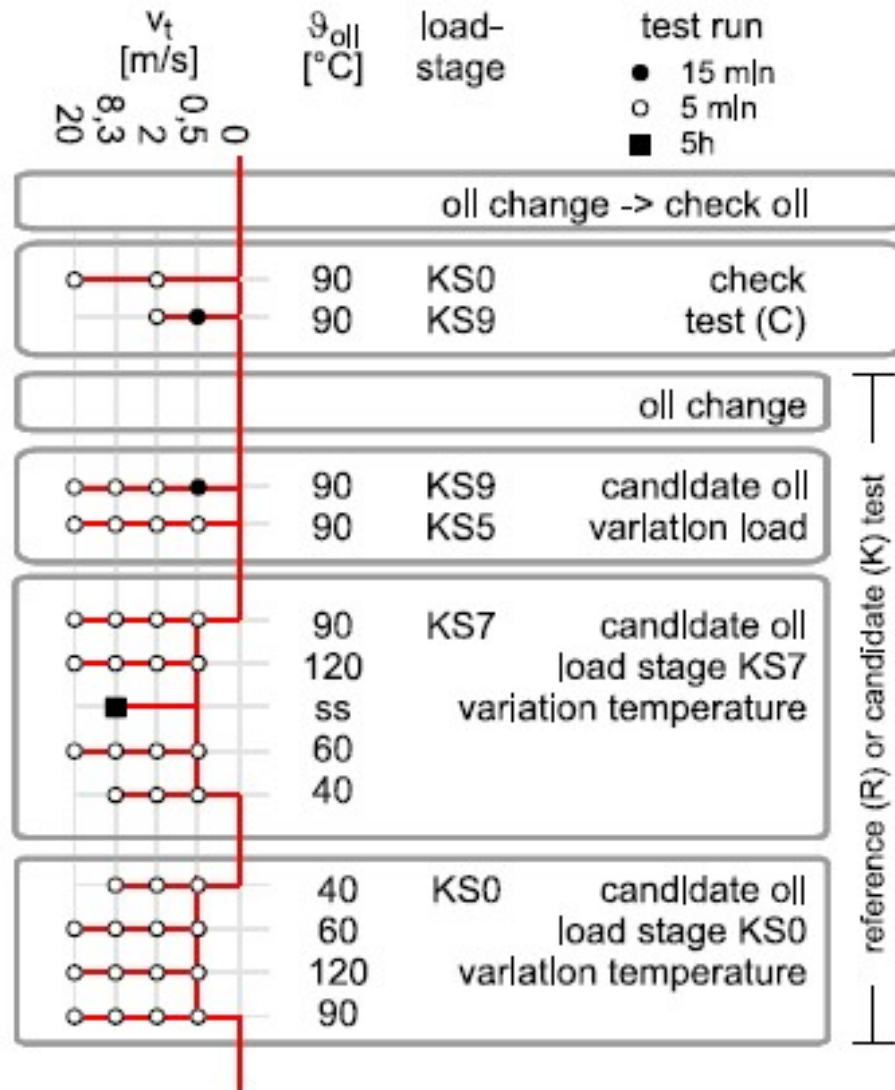
Figure 2.7: The FZG-FVA efficiency test. KS0 represent no-load applied. KS5, KS7 and KS9 represent, respectively, an applied load of 94.1 N.m, 183.4 N.m and 302.0 N.m (DOLESCHEL, 2002; ISO 14635-1).

The FVA-FZG efficiency test uses a modified FZG gear test, which is a commercial model of power circulating gear test rig. The required sensors and actuators features required by Doleschel (2002) are:

- Variable speed motor from 0 rpm to 4000 rpm;
- Loss torque meter at the engine output shaft with nominal load of 30 Nm. The required accuracy of 0.03 Nm and temperature stability of 0.001 Nm/°C. Torque transducers are commonly used for this end;

- Boxes' oil temperature control from 0 °C to 200 °C. The required accuracy is $\pm$ 2 °C. The most common method to control the oil temperature is inducing heat through the boxes body;

- Speed measurement for the output engine shaft from 50 rpm to 4000 rpm. The accuracy should be $\pm$ 2 rpm.

In order to characterize the load dependent losses, the method assesses the total losses in several conditions of load, temperature and speed and also performs those runs without load. The load dependent losses are obtained through the subtraction of the no-load losses from the total losses. Additionally, it is shown how to deduce the losses coming from bearings and seals (DOLESCHEL, 2002).

Finally, this report also provides a method to assess gearbox losses. Since all the engine power is dispersed during the operation, it corresponds to the total losses. Thus, the total losses is the power engine output, obtained from the multiplication of the engine output torque and the engine shaft speed (DOLESCHEL, 2002; ISO 14635-1).

The losses coming from each of the boxes are not directly measured. Only the total losses are measured, and it is supposed that both boxes lost the same amount of power. Some of the method requirements support this assumption: the boxes, including the gear pair, should be identical, as well as, the oil volume and the boxes' temperature. The described simplication is illustrated in Figure 2.8 for the traditional two-box power-circulating test rig. The measurement of the engine output torque and the engine output speed at different conditions of speed, temperature and load produces maps of how much power is dispersed at the considered conditions (DOLESCHEL, 2002).
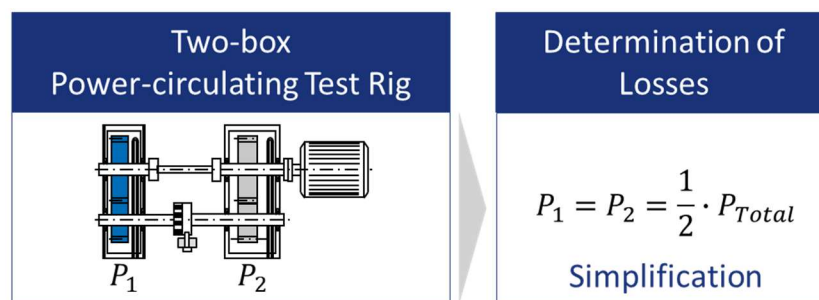
Figure 2.8: Simplication suggested by the report FVA nº 345 (DOLESCHEL, 2002)

The summarized concerns about the rig sensing are to guarantee the reliability of the efficiency measurements: it is required that all the conditions that change the gearbox efficiency be well controlled in order to obtain comparable runs. Although, the reliability of the

assumption about the boxes' efficiency depends heavily on the similarity among all the sources of power loss belonging to the gearboxes, such as bearings, seals, gears and other components (HÖHN et al, 2009), besides other sources of variability.

Andersson et al. (2014) investigated the effect of some common sources of variability on the efficiency measurements at power-circulating gear test rigs. The used equipment was a FZG power-circulating test rig. The analyzed sources were: assemblage, loading process, control of the oil level and pre-heating duration. Each test gives an overall torque loss (measured outside the power loop) and it is a sequence of five minutes long runs with different speeds at the same load and temperature condition. For each analyzed configuration, 5 replicates were realized and then they were used to calculate the configuration variability.

In order to analyze the variability of the assembly process, four configurations (1, 2, 3 and 4) were tested. Those configurations were equal except by the assembly process: for each configuration, the same operator disassembled and reassembled the rig with the objective of minimize the process variability. In order to analyze the variability of the loading process, one configuration (4UN) was tested. The conditions were the same used for the four first configuration except by the loading process: the load was applied, unapplied and then applied again (ANDERSSON et al.,2014). This configuration was compared to the formers.

The variability of the control of oil level was analyzed by means of the comparison among the configuration 1, 2, 3 and 4, in which the oil level was controlled by just observing if the oil level was at the middle of the shafts, and configuration 6 and 7, in which the oil level was controlled my measuring its level from the bottom of the box, with the precision of ± 1 mm (ANDERSSON et al.,2014). The configurations 8 and 9 were performed at the same temperature as the configurations 1, 2, 3 and 4. However, the rig was pre-heated at the test temperature for twelve hours. Also, the oil level was measured for 8 and 9 configurations.

The conclusion of this study is that the assembly process changes the variability and the mean of the test (comparison among configurations 1, 2, 3 and 4). The alternative loading process does not change the mean of the test, but reduces the variability of the answers (comparison among configurations 1, 2, 3, 4 and 4UN). The measured control of the oil level changes the mean of the experiments for higher speeds and reduces the variability (comparison among the configurations 1, 2, 3, 4, 6 and 7). Finally, the pre-heating process changes the mean and increases the variability (among the configurations 1, 2, 3, 4, 8 and 9). The results can be seen in the figure bellow. The changes on the mean of the tests were also compared to the uncertainty of the rig sensing, thus it was possible to assure that variability coming from the

assemblage process, control of the oil level and pre-heating have influence on the results of the efficiency test (ANDERSSON et al.,2014).

2.1.4 The four-box power-circulating gear test rig: ITA test rig

A variant of the presented power-circulating concept is available at ITA (Aeronautics Institute of Technology). It was designed to be a gear test center, enabling to perform durability, efficiency, noise, and vibration gear tests. Although presenting the same power-circulating concept, its configuration is still more complex, as shown in Figure 2.8. In order to be able to test two different center distances, the power loop includes four gearboxes.
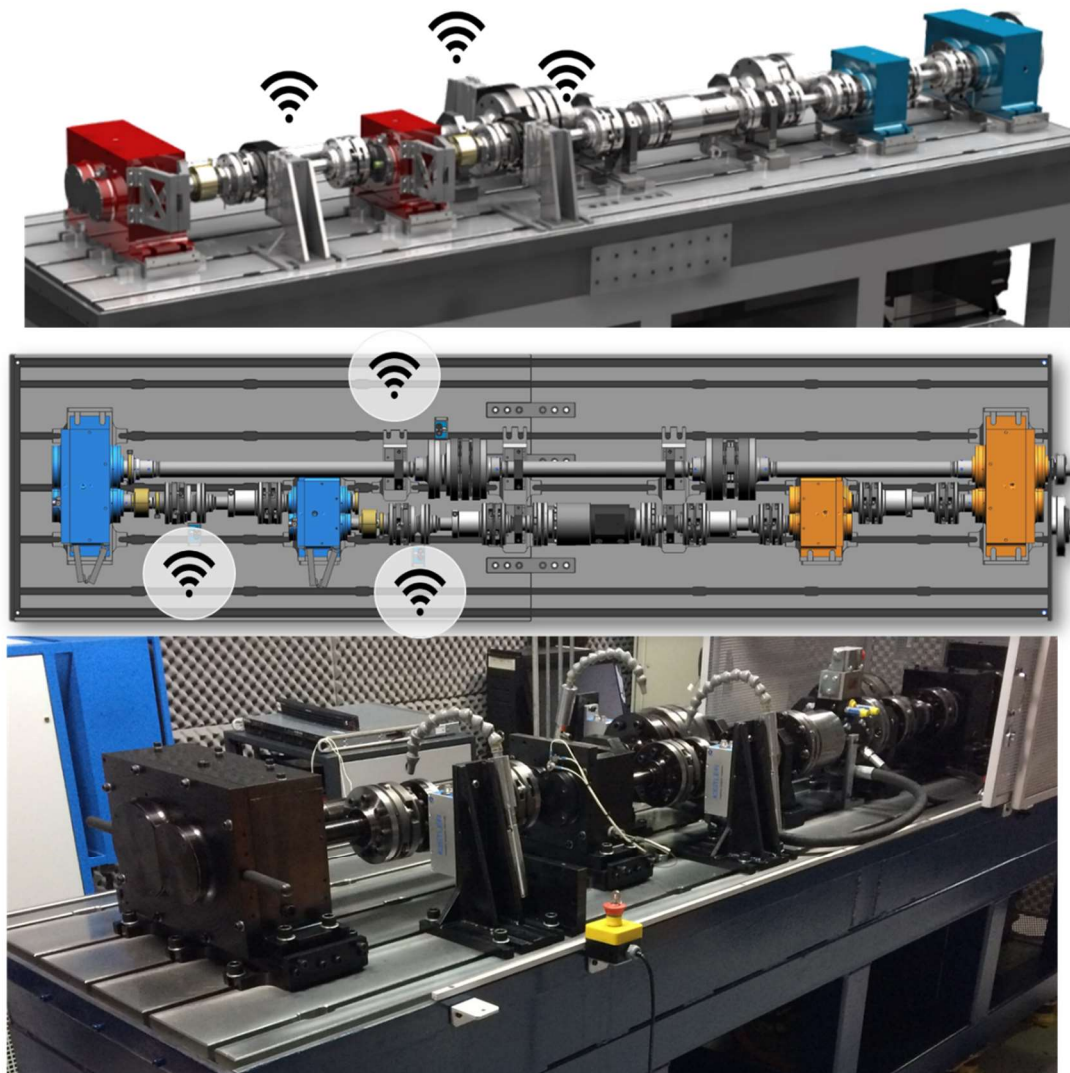
📶Points of torque measuring instaled

Figure 2.9: ITA test rig

It has been described that changes on gearbox or gear body geometries, such as number of teeth, diameter or module, change gear efficiency (CHANGENET and VELEX, 2008; LI et al. 2009). It was also showed that assembly process has a relevant effect on the measurement of gear efficiency in a power-circulating test rig (ANDERSSON et al. 2014). Considering this four-box configuration, it is unlikely that all the four boxes present the same efficiency, thus the hypothesis that the gearboxes are equally efficient should be contested, as illustrated in Figure 2.10.
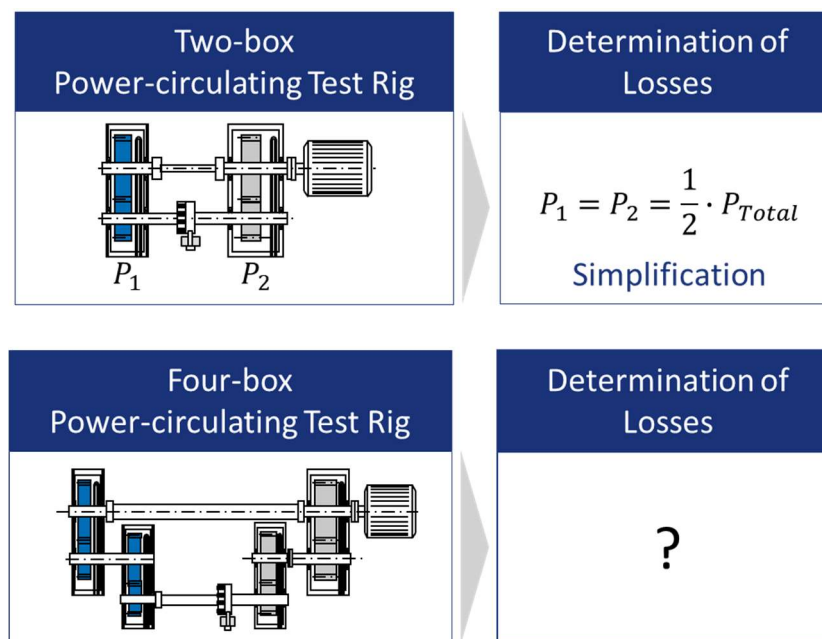
Figure 2.10: Two configurations of power-circulating gear test rig. The determination of losses for the four-box configuration is not approached by the report FVA nº 345 (DOLESCHEL, 2002).

For this reason, ITA test rig has 3 torque measuring points inside the power loop, instead of one measurement point as instructed by Doleschel (2002). The three measurements points at ITA Test rig can be seen in Figure 2.9. On the other hand, this acquisition system has not yet been validated for gear efficiency assessment and it brings a new challenge: the current acquisition system is enough to measure gear efficiency without knowing how the power flows through this more complex power loop system and how the losses are related to one another inside this loop.

2.2   Design of full factorial and fractional factorial experiments

Experiments aim to enable the observation and even to quantify the effects of some variables, called factors, on something measurable, called response. Tests are performed with different values of the variables, what are named levels. The classic experimental procedure states that the effect of each factor on the response must be observed singly, while all other factors are kept constant. This simple approach does not allow to identify effects which depend on two or more factors at the same time. Those effects, called interactions, can be studied by different designs of experiments, such as factorial designs (MONTGOMERY, 2013).

The interactions between two factors are called two-factor interactions or second order interactions. The interactions among k factors are called k-factors interactions or k^{th} order interactions. The notation used for interaction among factors is the factors themselves with ":" between each two of them.

Montgomery (2013) presents the sparsity principle. This principle affirms that most systems are dominated by some of the main effects and low-order interactions, thus high-order interaction are negligible. The designs of experiments and the statistical treatment used for this work will be explained in the following sections.

2.2.1   ANOVA and residuals analysis

ANOVA (analysis of variance) is a statistical method used to test differences among means. It is used to investigate whether the factors have influence on the response variable of interest. It analyzes if the mean of the response varies for different levels of the factors by partitioning the total variability (SS_T) into components relative to the considered factors ($SS_{Factors}$) and to the experimental error (SS_E).

$$SS_T = SS_{Factors} + SS_E$$

Eq. 2.4

SS_T is the sum of all squared distances of the measured responses to the overall mean. $SS_{Factors}$ is the sum of all variability of the factors. For a hypothetical factor A, SS_A is the sum of the squared distances of the mean of each level to the overall mean. This quantity is the sum of the variability due the levels of the factor A.

SS_E is the sum of all squared distances of the measured responses to the mean of the considered level. That is SS_E is the variability around the mean of the considered level. These quantities are graphically showed in Figure 2.11 for a particular case of just one factor, three levels of treatment and three measurements of each level.
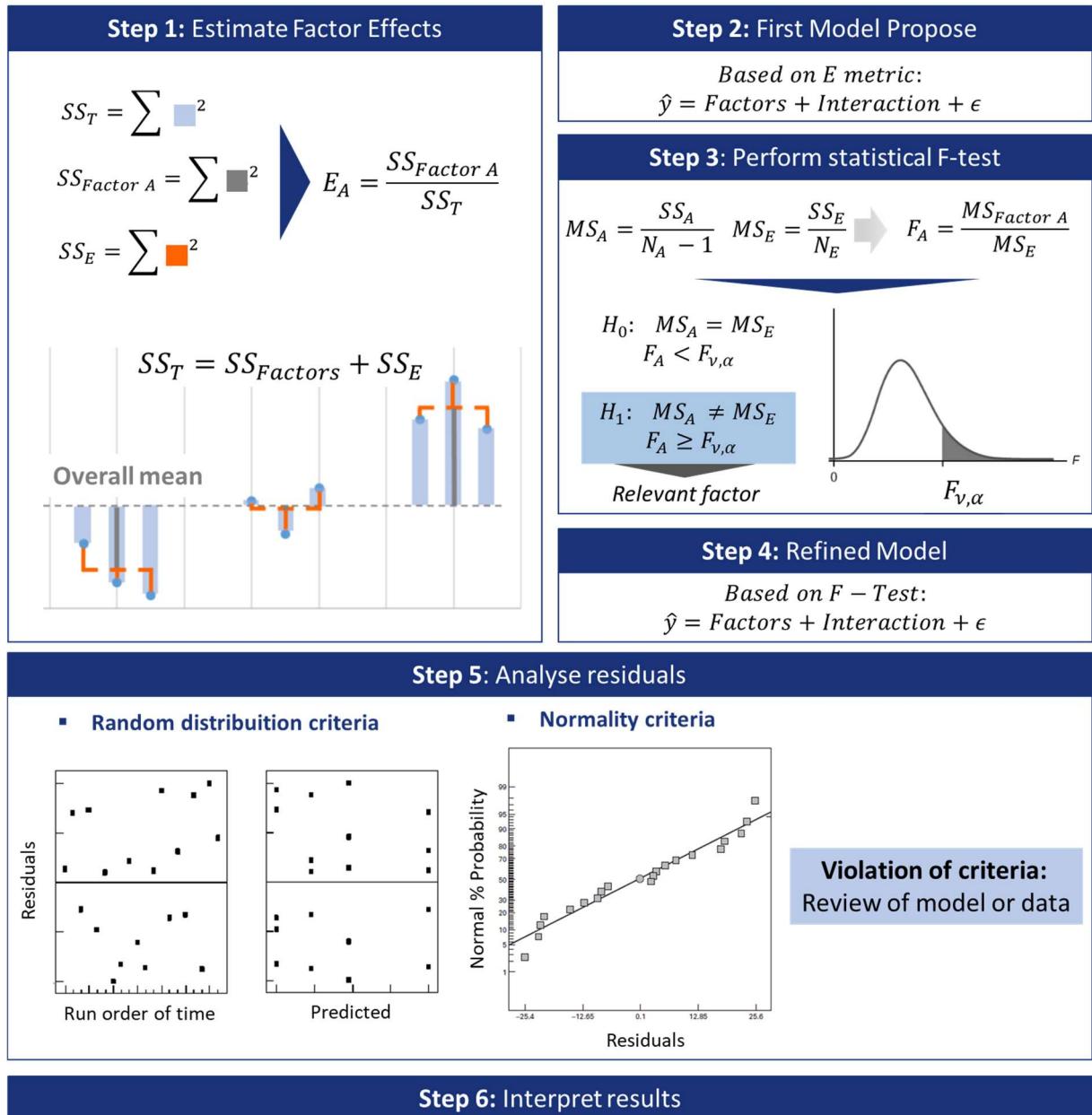
Figure 2.11: 6-step ANOVA Method

The effects of the factors are used for the first selection of relevant factors and interaction. The effects are estimated by the quantity called mean square (MS), which is a mean of the variability by the number of tests used to calculate the variability. The effects of a factor

A (E_A) is the reason between the mean square of the factor A (MS_A) and the mean factor of all the runs (MS_T).

$$MS_A = \frac{SS_A}{N_A - 1}$$

<div align="right">Eq. 2.5</div>

$$MS_T = \frac{SS_T}{N - 1}$$

<div align="right">Eq. 2.6</div>

$$E_A = \frac{MS_A}{MS_T}$$

<div align="right">Eq. 2.7</div>

The variability that is not related to the factors is attributed to the experimental error, also known as residuals. The residuals are the model representation of the error inherent from experimental processes. The criteria used to determine whether an effect is relevant to the response is a comparison between the mean square of the factor and the mean square of the residuals. If the variance due to the factor is almost equal to the variance of the experimental error, it cannot be classified as relevant in this case.

The statistical test used for comparison of two variances is a hypothesis test known as F-test for comparison of variances. The null hypothesis is that the variances are equal. The alternative hypothesis is that the variances are unequal. The reason between the variance due to the factor and the variance due to the error is calculated. A limit value (F_0) is obtained from F-distribuition, for a given level of confidence (β) and a given set of numerator and denominator degrees of freedom (v_1 e v_2). If the reason is bigger than F_0, the alternative hypothesis is accepted. This process is showed graphically in figure 4.

The level of confidence of the test is the probability of supporting the alternative hypothesis when it is true. Further information about the F-test for comparison of variances can be found in (MONTGOMERY, 2013).

Other important criteria must be applied to the residuals. Since they represent experimental error, it is expected that appropriate models have the residuals with normal and random distribution. This condition must be verified for the proposed model. The normal probability plot (MONTGOMERY, 2013) allows the verification of the normal distribution. If the residuals have a normal distribution, this plot resembles a straight line, as shown in Step 5 in Figure 2.11. Besides the normal probability plot, there are other ways to verify if some

sample comes from a normally distributed population. A useful tool for this purpose is the *Shapiro-Wilk* test. The null hypothesis for the *Shapiro-Wilk* test is that the data are normally distributed, considering a determined confidence level. If the output test, which is also called p-value, is smaller than the quantity of a unit minus the confidence level (α), then the null hypothesis that the data are normally distributed is rejected. If the p-value is greater than α, then the null hypothesis is not rejected.

In order to verify whether the residuals are structureless, it is useful to plot them versus the fitted values and in time order. Neither trend nor correlation is expected in these plots. Residuals with non-normal or non-random distribution indicate systematic errors on the experimental process or relevant factors missing in the model. For this case, further investigations and model review are recommended.

2.2.2 2^k Full factorial experiments

A 2^k Full factorial design of experiments is design in which the k factors are fixed into two levels, the response is one-dimensional, and the runs are done in a total randomized way to avoid noises originated from a non-random order.

This design is suitable to explore systems which still little is known and with relatively many factors to be considered (MONTGOMERY, 2013). 2^k Runs are necessary to perform this experiment without replicates and considering all the factors and their interactions. It is also possible to perform several statistical analyses using the same data base in order refine the model by removing, systematically, not relevant factors or interaction of the analysis.

Besides its advantages, one of the limitations of this analysis is that it cannot identify non-linear behaviors. It must be assumed that the response is linear over the range of the levels chosen. Therefore, for this work, it will be used for the investigations proposed by the second research question, whose objective is identifying the relevant factors and interactions.

The required data is the 2^k measured values of the responses and the corresponding factors levels. Step 1 (Estimate factor effects) quantifies the variance of the responses due to variation on the factors, and also the variance which is not related to any factor, but to the inherent variability of experimental procedures. The metric used to quantify is MS.

Since the effects were quantified, in Step 2 (First model proposal) the relevant factors and interaction are chosen based on the comparison among the mean square. This selection is the first version of the model. In Step 3 (Perform statistical testing), a statistical test is performed

to compare the variance due to the factor with the variance due to the error (MONTGOMERY, 2013). The method used at that step is ANOVA, already discussed in the previous section.

Accordingly, with the result of the statistical tests, the choice of the relevant factors and interactions can be rethought, and the model can be refined. That is the Step 4. The conditions about the residuals are verified in Step 5, accordingly with the methods explained previously. Conclusions are drawn in Step 6, based on the created model, the results from the statistical analysis and their graphic representations. This procedure is illustrated in Figure 2.11.

2.3   Summary

Power losses are inherent to torque transmission system. Gears power losses manifest themselves as a deduction in the expected output torque, since the angular velocity is theoretically constant. This deduction is due to the energy loss caused by friction, drag force and churning of the surrounding fluids.

A conventional method of studying gear torque efficiency is by means of a power-circulating test rig, described in ISO 14635-1, Ward Jr. et al. (2001) and Doleschel (2002). This established method assumes that the power delivered by the motor is equal to the total loss, which is measured outside the loop and divided between the two gearboxes. The statement depends heavily on similarity among other sources of power loss belonging to the gearboxes, such as bearings, seals, gears and other components (HÖHN, 2009), besides natural variability on assemblage. For more complex rig configurations of the same testing concept, with three or four gearboxes, this assumption should be contested, since one cannot guarantee the elements' similarity and unvarying assemblage (ANDERSSON et al., 2014). Additionally, the models developed to simulate the dynamic behavior of power losses demanded the knowledge about the power flow direction (MAIA et al., 2014; WANG et al, 2018), which was presupposed in order to build the models, but is still not well-defined.

For more reliable torque efficiency measurements, it is necessary to know the distribution of the power losses among the gearboxes. Nowadays, the dynamic behavior of power loss distribution in the gearboxes is simplified. In order to study a more complex case, a four-box power loop test rig was conceived, considering a mechanism capable of individual induction of power losses in each transmission box.

3   Objective and Approach

From the reviewed methods and test benches applied for assessing gear efficiency, it is possible to conclude that the existent experimental methods do not follow appropriately the rising demands on torque efficiency investigations. Considering that the expected improvements on gear efficiency are the same order to the current simplifications, these one should be further researched.

The objective of this work is a more reliable power losses measurements in a power-circulating test rig. Considering the nature of the problem, three research questions were elaborated to organize the entire investigation, since the development of proper method and tool until the elaborating of a model for the studied behavior. The questions wordings can be seen in Figure 3.1.
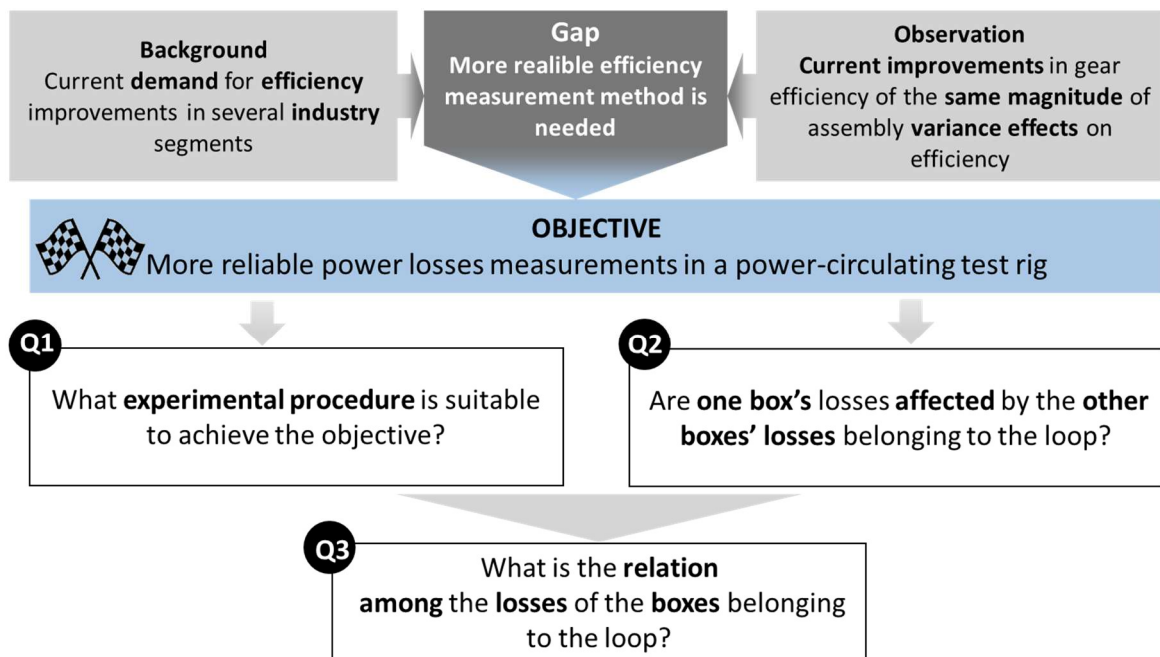
Figure 3.1: The objective is approached by investigating the proposed questions about experimental procedure and development of a model for the dynamic behavior.

The investigation starts by identifying the simplifications entrenched in the already developed experimental procedure presented in report FVA 345. The previous chapter pointed that the most established method to evaluate gear efficiency using power-circulating test rig

simplifies its value by the arithmetic mean of the total losses and relies heavily on the boxes' symmetry. Additionally, earlier studies pointed out that gear efficiency depends on five factors (transmitted load, speed, temperature, lubricant and kind of lubrication).

Considering what has been said, the first research question concern about the development of a tool and a method that will allow the achievement of the objective: **"Which experimental procedure is suitable to achieve the objective?"** In order to answer appropriately this question, several aspects should be considered for the designs of the tool and experiments. It is necessary to define how to measure what is currently ignored and identify experimental conditions, including new unavoidable simplifications. This discussion will be detailed in the fourth and fifth chapter, where the preliminary results are shown too.

Initially, efficiency testing at ITA test rig will focus on just the test gearboxes and not on the "slaves" gearboxes. Therefore, it is possible to focus on the test box' dynamic behavior and on how it is related to the other boxes' losses. So, the second question aims to determine whether losses in the other stages impact on efficiency on the stage of interest. The second research question wording is: **Are one box's losses affected by the other boxes' losses belonging to the loop?"**

After the first question investigation, what factors that influence the dynamic behavior of the power losses of the studied system are still unknown. This fact leads to the need of identify them. Additionally, it is possible that some interaction among those factors has also influence on the behavior. Considering that a quantitative approach at this point possibly requires a high number of experiments, an exploratory qualitative investigation of the effects is the proposed approach for the second question.

When the second analysis indicates there is an interaction among the boxes' efficiencies and the relevant factors and interactions among them, a third investigation towards the evaluation of the observed effects should be done. Thus, the third research question is: **"Is it possible to quantify the relation among the power losses of the boxes belonging to the power loop?"**

A quantitative approach, required to the third question, needs a higher number of tests, accordingly to the theory exposed in the following chapter. Although, the number of experiments can be optimized since the relevant factors were identified previously. Thus, the design of experiments for the last investigation should be based on design of fractional factorial experiments theory.

4   Materials and Methods

This chapter presents the materials and methods used for reaching the objective, as can be seen in Figure 4.1. Firstly, it is presented PRILs, a power-circulating rig with unique features able to induce controlled power losses. It was designed for the investigation proposed by this study and it was where the experimental investigation was done. Secondly, the methods used for each research question investigation are described. The first method discusses what PRILs characteristics may affect experiments repeatability and reproductivity, pointing out investigations about PRILs performance that helps the development of a robust experimental procedure.
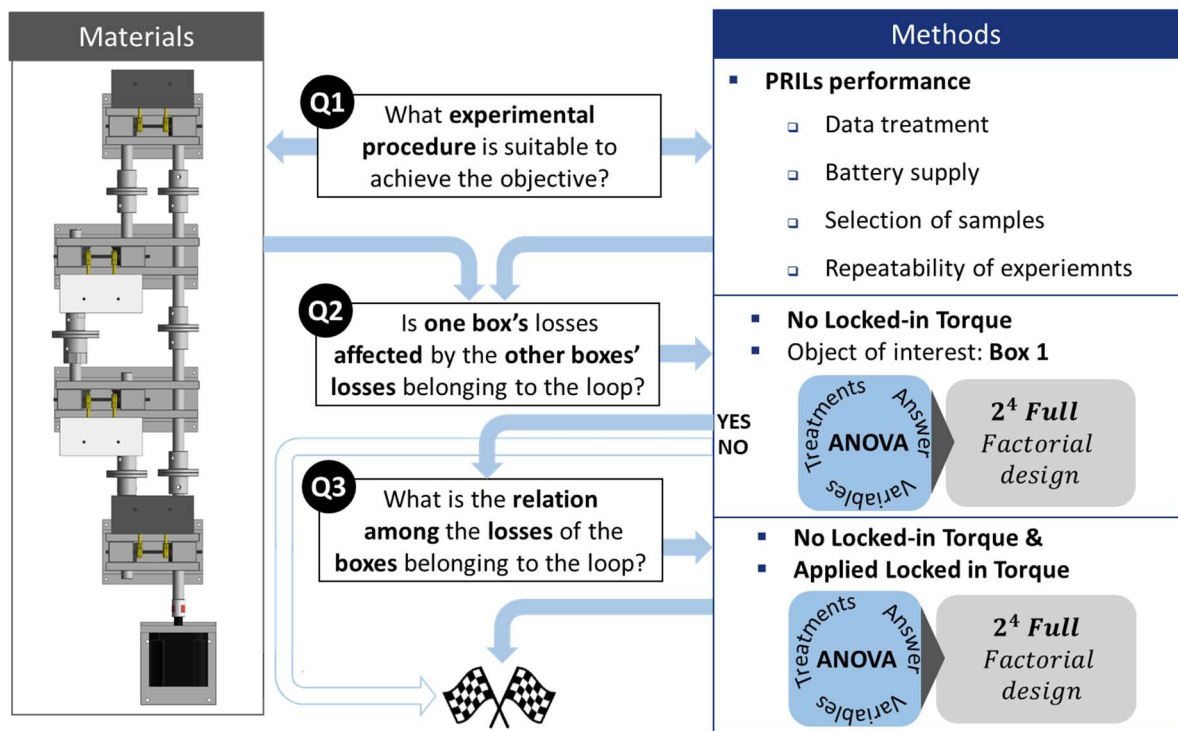
Figure 4.1: Materials and Methods

The second and the third methods are related to the second and the third research question. In order to answer the second research question, an experimental plan is designed based on the theory exposed along the second chapter. The definition of responses, variables and treatments are conducted with the purpose to identify if a box loss depends on other boxes' losses. In order to simplify this investigation, the locked-in torque is not considered in this plan.

When the losses dependency is identified, the third investigation is needed to achieve the objective: a new experimental plan is designed, including locked-in torque application, in order to quantify this relation. The theoretical base used for this plan is the design of fractional factorial experiments, since the majority of the relevant factors has been identified during the second investigation.

4.1   Power-circulating rig with induced losses

The design and building of Power-circulating Rig with Induced Losses (PRILs) consisted in a final graduation work for the undergraduate course of Mechanical Engineering at ITA in 2017. This previous study focused on designing and building PRILs, while the present study aims to use PRILs as a tool for investigating the dynamic behavior of power losses at a power-circulating rig. PRILs, showed in Figure 4.2, and its main features will be discussed ahead, and more details of this project can be found in Andrade (2017).

N°	Part
1	Stepper Motor
2 and 3	Losses Induction System
4	Pre-Load Coupling
5	Measurement Points
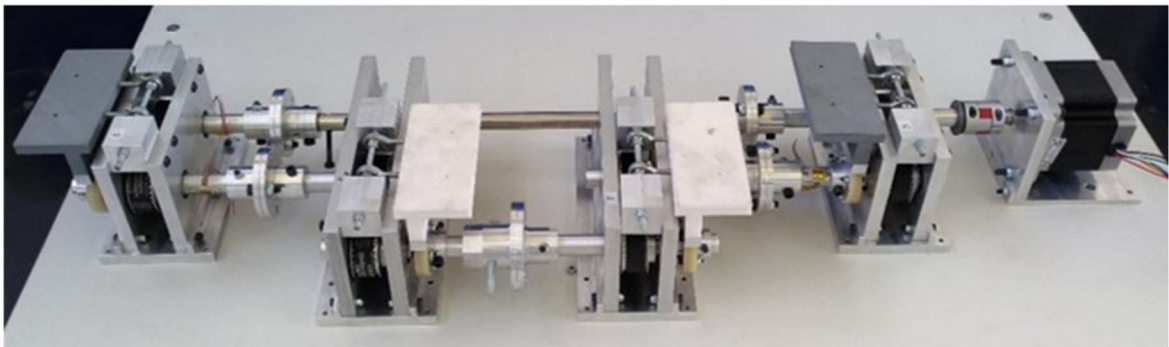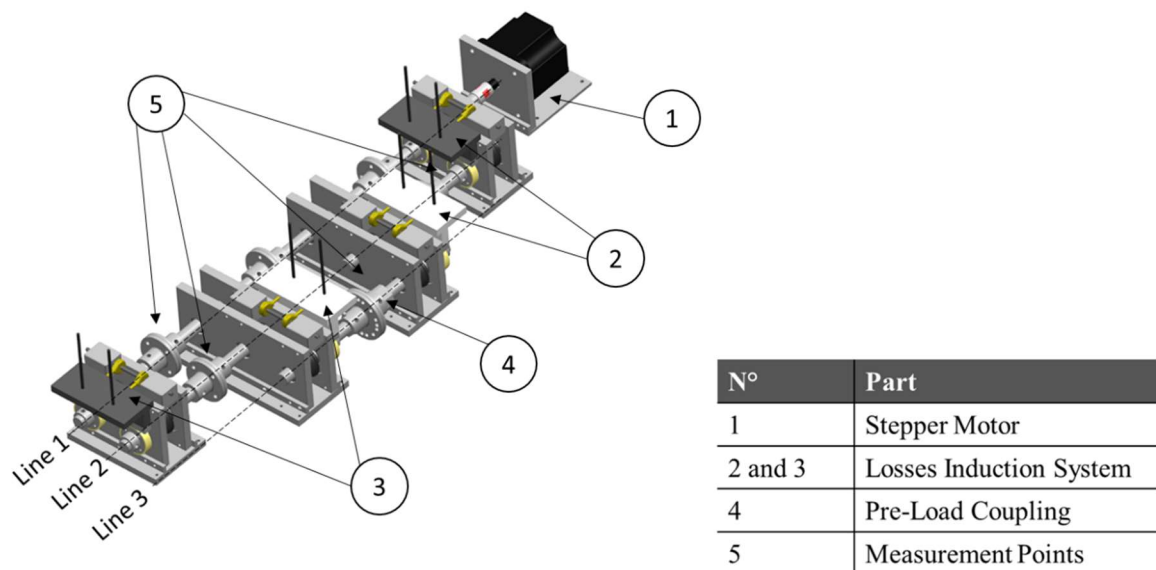
Figure 4.2: The power recirculating testrig with induced losses (PRILs).

PRILs was designed to perform the necessary experimentation to investigate the research questions. It aims to understand the dynamic behavior of the losses in a power loop test rig. The four-box configuration was chosen to the present investigation due to the possibility to validate the model at the original ITA gear test rig, hereafter named as "ITA test rig" (Figure 4.3), which is a natural continuation of the herein presented study. A stepper motor is employed to insert rotation into the system. As the locked-in torque is imprisoned into the loop manually, the torque delivered by the motor is numerically equal to the total loss.
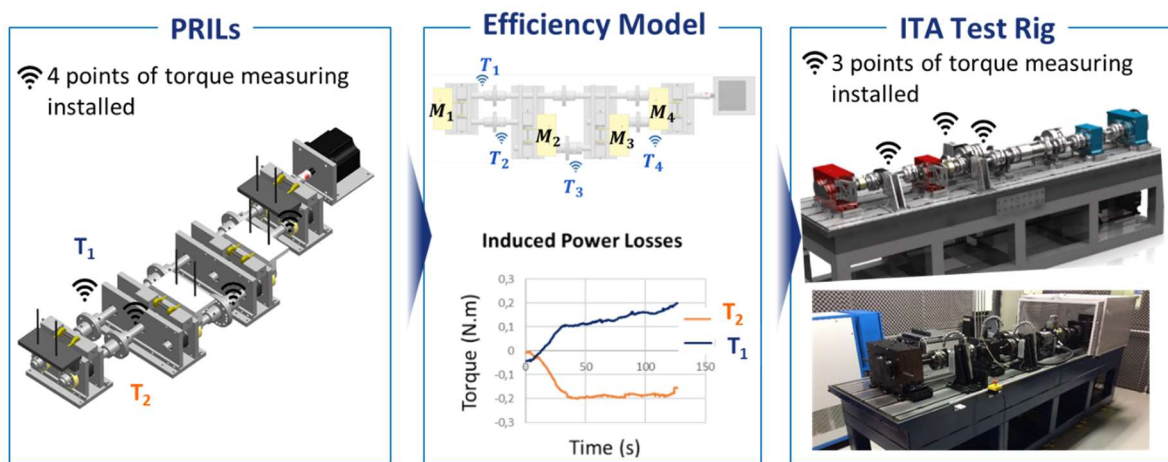
Figure 4.3: PRILs test rig and ITA test rig.

Locked-in torque is applied manually on a flanged joint. It can also be static loaded. There is a flange coupling in which one of the flanges can be clamped to the table while the other is connected to one lever in order to apply the torsion manually. The described mechanism can be seen in Figure 4.4. Three different sets of bore holes were used to define the different torsion levels. Also, a torquemeter was used as lever, which allowed for the verification of the load applied at each run.
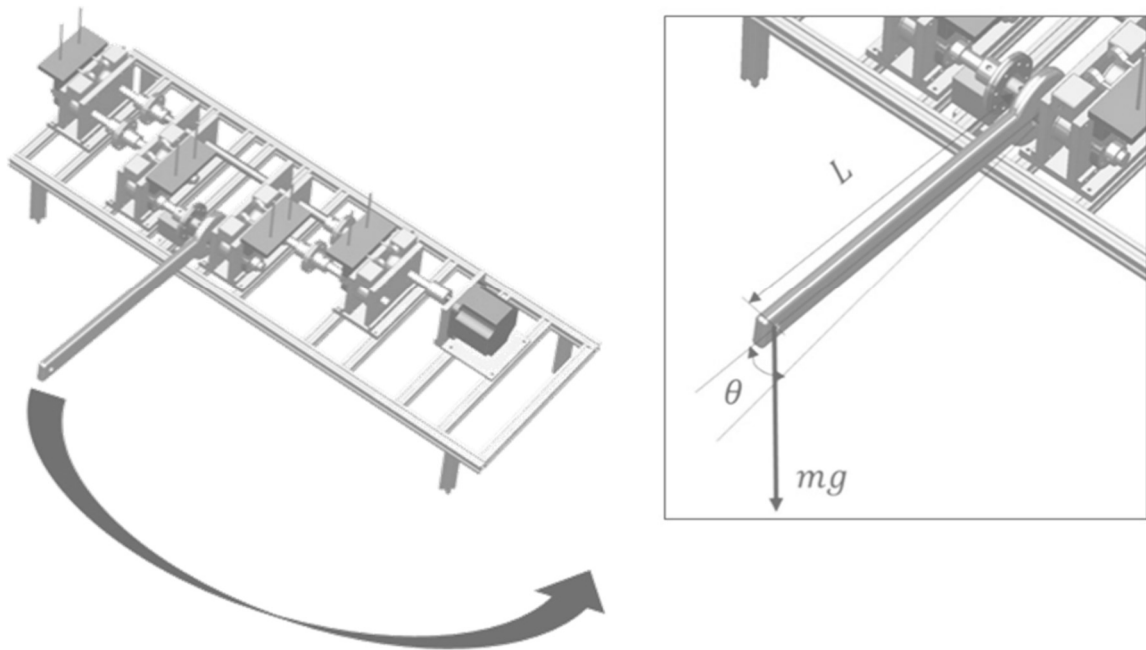
Figure 4.4: Manual load application

Besides configuration and functional similarities between the test rigs, PRILs has some unique features. The investigations must analyze the dynamic behavior of different combinations of induced losses on the transmission boxes. Thus, it is required an equipment able to induce different losses on the boxes in a controlled way. PRILs' most characteristic feature is a system for inducing losses by friction. Losses are independently induced on each box with the use of a disc-bar friction platform that can be seen in figure below. It operates independently on each box and its fixing was projected to be present lower variability on the load application, meeting the high repeatability. The current system, shown in Figure 4.5, with two ball-joints, presents just one more constraint than the necessary to define the system position (ANDRADE, 2017). Additionally, the system is flexible with regard to how much loss is induced, which can the defined according to the acquisition system accuracy.
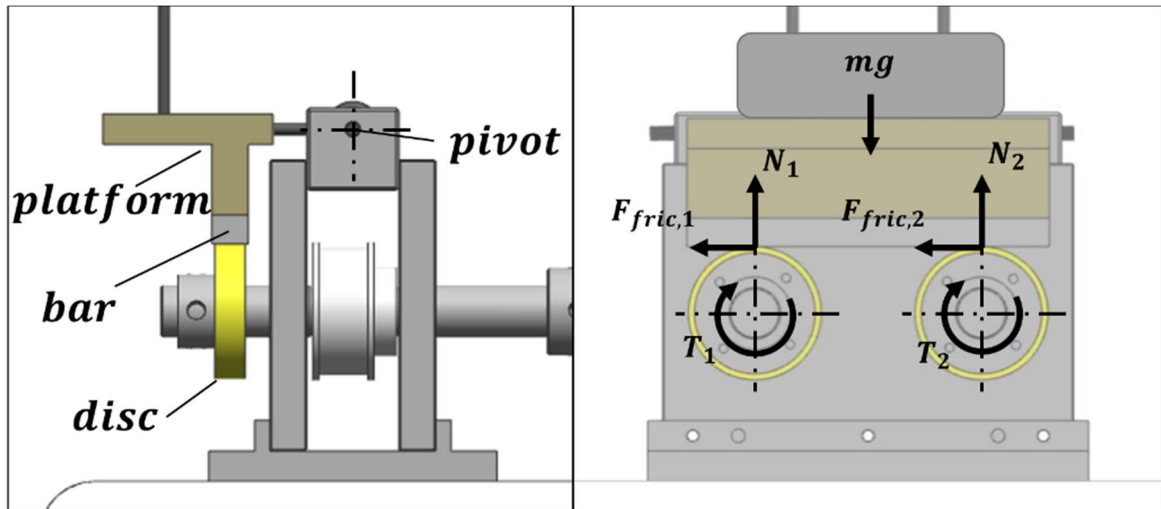
Figure 4.5: Losses induction system are present on each box, in order to induce losses in an independent way.

PRILs was designed using toothed belt drives, which are OEM parts, instead of regular gears. This eliminates the need for coolant fluids and oils, thus removing a possible source of noise and simplifying the rig design, but still ensures no transmission errors due to slipping will occur. Losses coming from gear features which are not present at PRILs, such as churning losses, can be reproduced by induced friction losses.

The main simplification investigated by this work is the equal distribution of the losses among the boxes suggested by the report 345 from FVA. For this reason, PRILs has four points of torque measurement inside the loop instead of one point outside the loop. There is at least one point on each transmission line in Figure 4.2. The sensors used are strain gauges in a ½ *Wheatstone* bridge configuration, which specification can be seen on Table 4.1. Each sensor has two mesh with an angular offset of 90°. This configuration was selected to measure torque since it allows to compensate flexion effects on the measurement (DALLY and RILEY, 1965). Temperature effects are compensated by the integrated circuit embedded on the axis (ANDRADE, 2017).

Table 4.1: Strain Gauge properties

Strain Gauge Properties	Unit	Value
Resistance	Ω	350
Nº of meshes	-	2
Angle between the meshes	°	45
Gauge factor in measuring points 1, 2 and 4	-	1.94
Gauge factor in measuring point 3	-	2.03

The selected sensors present a very simple architecture. Therefore, their operation requires a custom-made signal conditioning and a wireless transmission circuit. The ½ *Wheatstone* bridge must be completed with two high-precision 350 Ω resistors and powered by a battery installed on the instrumented shaft. The signal coming from the circuit bridge is very low and needs to be filtered and amplified before been transmitted.

Cable data transmission is not compatible with the rotational application. The data transmission is wireless between an antenna assembled to the rotational shaft and another static antenna. The static antenna is called master antenna and is connected to a computer, where the data is monitored in real time and saved. The transmission technology used is *IEEE 802.15.4* suitable to data transmission within ten meters. In addition, a speed control system was applied to the engine.

The amplifier and transmission circuits were built on a circuit board. Each measure point includes a strain sensor with two meshes, a circuit board and a battery all assembled on the shaft. The battery used produces 9 V voltage. The correct operation of the system requires a minimal battery voltage. This limit was investigated for the first question and will be approached in the chapter "Results and Discussions". During the tests, the battery voltage is monitored using a multimeter.

There are conditions which must be controlled during the execution of the experiments, such as the room temperature and the position of the masses, as it will affect the distribution of friction force. For this reason, a thermometer is used for monitoring the room temperature and a digital caliper will be used for monitoring the disc wear.

4.2   Testing for experimental procedure development

The first research question indicates that some preliminary observations are required in order to develop an appropriate procedure to perform the planned experiments based on DoE principles and techniques. It is expected that the procedure states ways to minimize the variability from undesirable sources: environmental conditions, noisy operation conditions, deteriorate components and electric signal variation along the time. Additionally, the signal coming from PRILs' sensing system should be treated before used to answer the second and the third question.

4.2.1   Data treatment

The raw signal must be observed in controlled condition in order to identify error due to the acquisition system that are not related to the mechanical reality and apply appropriate solutions, such as frequency filters and thresholds.

4.2.2   Battery supply

The strain signal is directly proportional to the electrical supply voltage. Since battery voltage changes over the operation, the acquisition system was prepared to supply the *Wheatstone* bridge with the same voltage over time, if the battery voltage is larger than a minimal value. Otherwise, the *Wheatstone* bridge is undersupplied and, consequently, the strain signal decreases, even maintaining the same stress on the shafts.

The signal on two measurements points (points 1 and 3) were monitored for successive time intervals. Between the intervals, the batteries were disconnected for voltage measurements.

4.2.3 Definition of run duration, sampling over time and repeatability of experiments

It is necessary to define the runs' duration and of the method to select the data over time. These definitions are related to several questions relevant to the development of the experimental procedure: total duration of the tests, number of battery recharging needed for the total tests, identification of more stable period of data acquisition. These three aspects also concern the repeatability of experiments. Shorter duration of the total number of test and fewer disassembly and assembly batteries for charging diminish the variability coming from the experimental procedure.

4.3 2^4 Full factorial experiment design

The following discussion is about how the 2^k full factorial experiment design was used to answer the second and the third research question, which are: "**Are one box's losses affected by the other boxes' losses belonging to the loop?**" and **"Is it possible to quantify the relation among the power losses of the boxes belonging to the power loop?"**

According to the discussion in chapter "Objective and Approach", the investigation towards the second research question will focus on the dynamic behavior of just one transmission box, which should be in a similar position to the test gearboxes at ITA Test Rig. PRILs transmission boxes at position 1 and 2 satisfy that condition. However, the transmission box at the position 1 is the best choice for this investigation, since it is the only transmission box with two measuring points before the coupling junctions at PRILs.

In order to plan the experiments, responses and factors should be well defined. The direct responses are the measured torques at the shafts on the transmission box 1 (T_1 and T_2). An indirect response will be also considered: the transmission torque loss (BL_1) obtained by subtracting the measured torques. T_1, T_2 and BL_1 can be seen in Figure 4.6. Therefore, one ANOVA analysis will be done for each of the three cited responses.
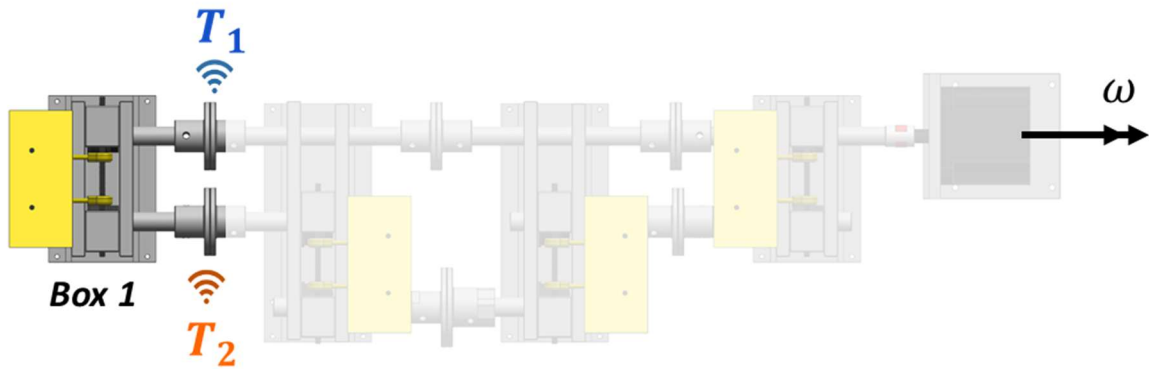
$$Box\ 1: BL_1 = T_2 - T_1$$

Figure 4.6: Responses for the investigation towards the second research question

The factors should be related to variations on the transmission boxes losses, accordingly to the proposed question. Transmission power losses change in different conditions of speed, transmitted load, temperature and lubrication (HÖHN, 2009), but PRILs was designed to replicate losses coming from all those sources by inducing friction losses. Therefore, they are related to the factors. For simplicity, the masses used to induce losses were defined as factors instead of value of friction forces or friction losses. Thus, there are four factors studied and they can be seen in Figure 4.7. The set of masses used for this investigation is made of steel and each one weights 2330 g. Each one of the masses received an identification from 1 to 4. This identification was used to assure that each mass would only be placed on top of one of the boxes. This restriction guaranteed that the boxes would be loaded at the same way whenever it was needed.
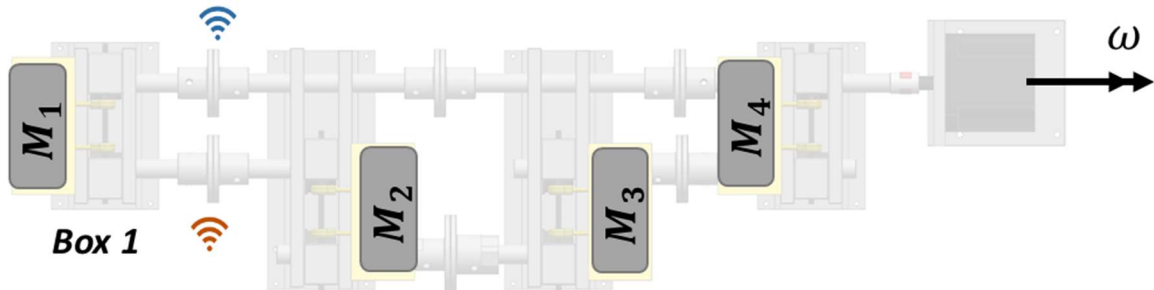
Figure 4.7: The four factors considered for the investigation towards the second research question: M_1, M_2, M_3 and M_4

Since the factors were defined, the other sources of influence on transmission efficiency, speed, load, temperature and lubrication, should be kept constant. The tests will be performed at a rotation velocity of 3 Hz, because of higher power available and the lower vibration observed at this speed. The direction of rotation can be seen in Figure 4.7. Those conditions combined lead to simulation of higher losses and to better data quality, respectively, what is advantageous to the measuring. The engine power curve can be seen in Attachment A.

The transmitted load will vary due to the induction of losses, although the locked-in torque can be kept constant. For this investigation, no locked-in torque will be applied. The conclusions of this investigation will address the no load runs prescribed by the report FVA no. 345. The temperature condition was addressed by the first research question and PRILs does not have a lubrication system.

The tests were done also by acquiring data from other measurements points, since the required efforts were minimal. The responses are the torque on each of the 4 monitored points (input T_1 and output T_2 of box 1 and T_3 between boxes 3 and 4), besides the torque loss BL_1 and efficiency η_1 of box 1, calculated from the torques T_1 and T_2 (Figure 4.7). The statistical analysis followed the six-step method described in Figure 2.11.

The third research question proposes an overview of the behavior of the system of interest. The first investigation done for this last question is to analyze the boxes 2, 3 and 4 under no locked-in torque condition, since the box 1 at the same condition was approached by the second question.

The second investigation required by the third question approaches all the torque and torque losses responses under the applied locked-in torque condition. The same design of experiments was used for the second investigation. Therefore, 16 runs were done under applied locked-in torque condition, but in a new random order. The locked-in torque introduced higher losses on the system. The motor could not supply the total amount of power required by the combination of the locked-in torque and the steel set of masses. Therefore, a new and lighter set of masses was used. Each mass was manufactured from aluminum blocks and weights 433 g.

The described statistic methods require a lot of effort if done manually. For this reason, the analysis was conducted using routines programmed in R language, which is an open source programming language dedicated to statistical computing and graphics. The scripts used can be found in Appendices A, B, C.

5 Results and Discussion

This chapter shows the results and discussion structured into three sections. Each section is dedicated to present the results obtained from the investigation targeted at each one of the three research questions.

5.1 Development of experimental procedure

This section aims to present an answer to the first research question: "Which experimental procedure is suitable to achieve the objective?" The procedure that was elaborated to minimize the variability from the process, such as system operation, environmental conditions, deterioration of components and data treatment. The following topics will approach these concerns. At the end of this section, the proposed procedure for running experiments on PRILs will the described.

5.1.1 Data visualization and data treatment

PRILs' antennas send the values of the *Wheatstone* bridges voltage output, given in mV. These values are converted to torque just after being saved on computer. It was observed that the raw signal received by the master antenna contained some outlier points. For this reason, the raw signal was treated digitally with a threshold function: if a received point value is greater than 2000 mV, it is disregarded, and the previous point is repeated. These thresholds worked for all the executed experiments. This treated signal is recorded in the computer. The signals with and without treatment can be seen in Figure 5.1.
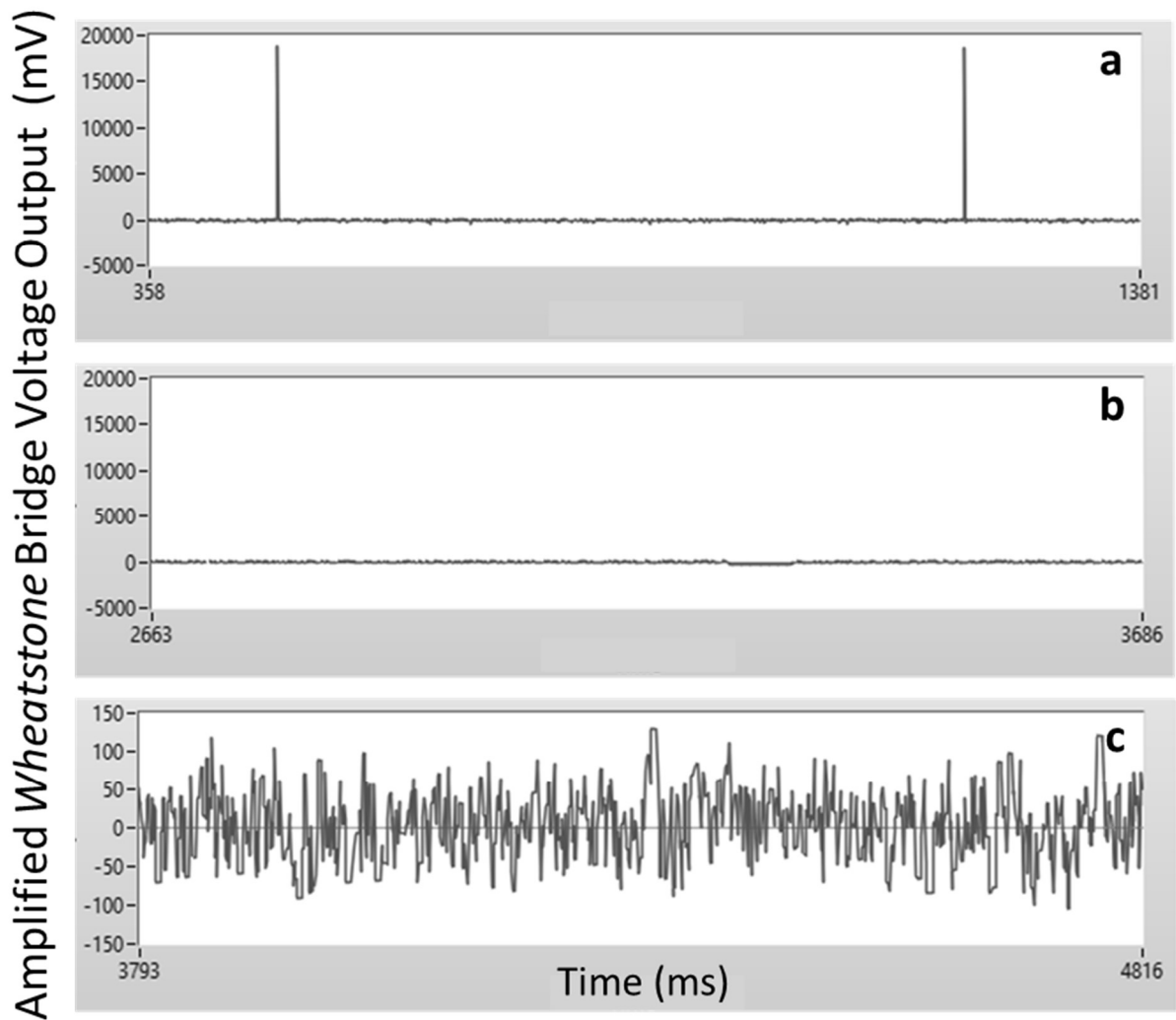
Figure 5.1: (a) Signal without threshold treatment, (b) signal with threshold treatment and (c) signal with threshold treatment with scaled Y-axis.

PRILs acquisition system enables monitoring in real time the data acquisition. It helps the operator to identify any abnormality in data acquisition during the tests, such as loss of signal from some antenna or unexpected signal feature. The observed abnormalities were: loss of some antenna communication and square-shaped signals. Those problems were most of the time related: due to the loss of communication, the last received value was recorded several times producing a square-shaped signal. This problem was always solved by reestablishing lost communication.

The monitoring interface can be seen in Figure 5.2. In order to be more user-friendly, the interface shows the signals smoothed by a moving-average with 1000 points. The signal

coming from the points 1, 2, 3 and 4 are showed in red, dark blue, green and light blue colors, respectively.
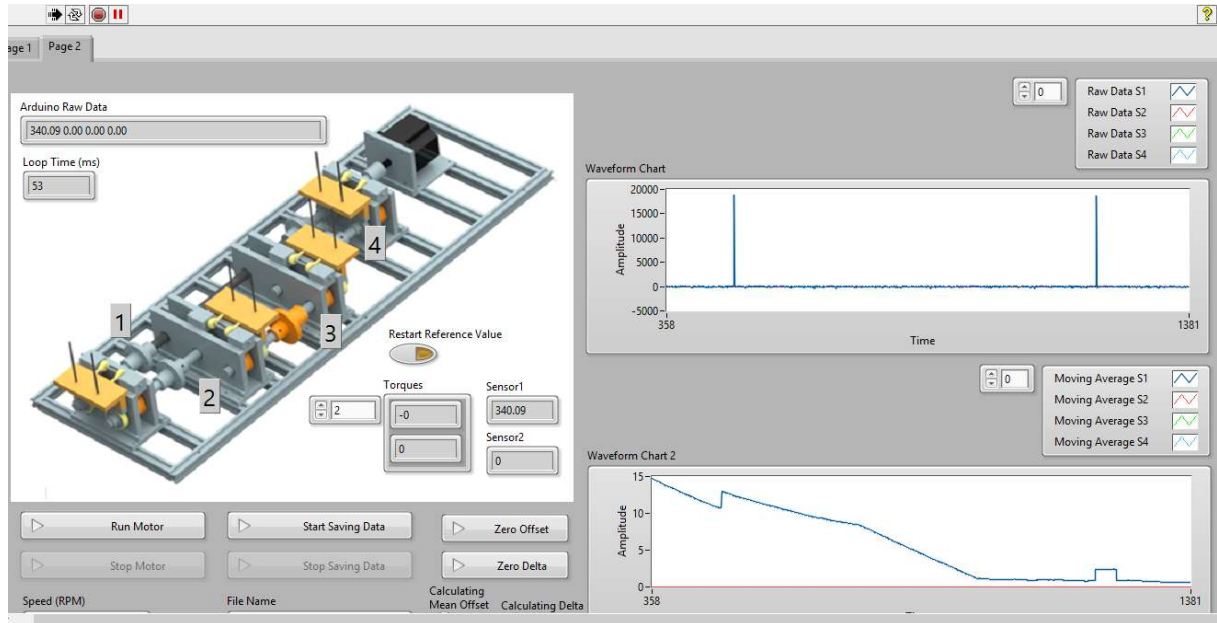
Figure 5.2: Monitoring interface

5.1.2 Battery inspection

The acquisition system working depends on a minimal battery voltage. This system limitation was investigated by monitoring the acquisition system working and the battery voltage simultaneously. The battery voltage of the measuring point at position 3 was measured in between 10 minutes long runs, from which data were recorded for subsequent analysis. The motor was not operating for this test. After 6 runs, the test was finished since it was possible to observe that the measurement signal changed significantly. The battery voltage was 6,95 V after 60 minutes operating. The initial seconds from each data test can be seen in Figure 5.3 and Figure 5.4. In the initial battery voltage of each run are recorded in Table 5.1.
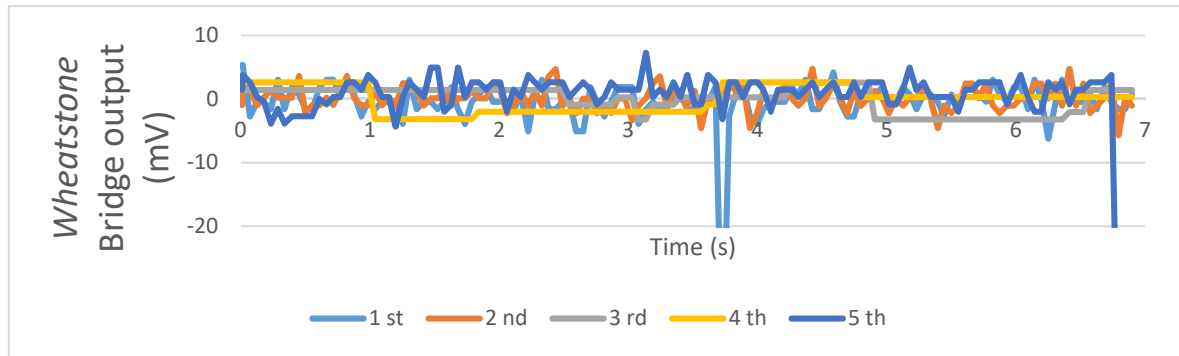
Figure 5.3: Initial data from the first five runs. The acquired signal is measured on the point T_3 and it is showed without in millivolts, which is proportional to the torque at the shaft. The initial seconds from the first to the fifth run is showed above.
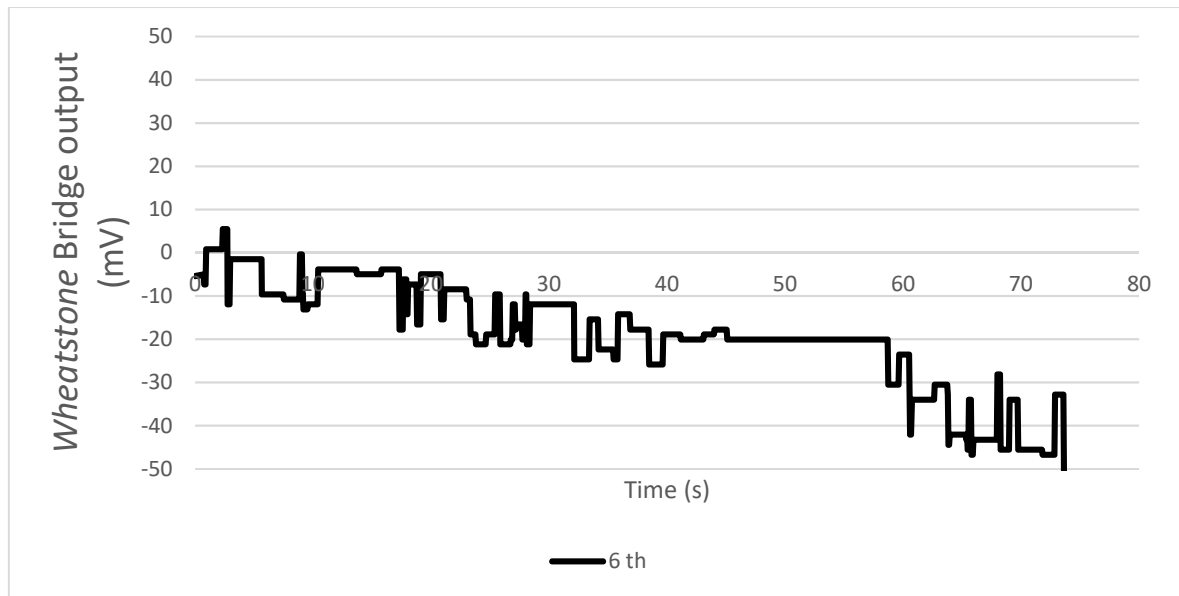
Figure 5.4: Initial data from the sixth run.

Table 5.1: Battery voltage recording.

Run	Initial Battery voltage (V)	Cumulated test time (min)
1	8.80	0
2	8.52	10
3	7.50	20
4	7.43	30
5	7.34	40
6	7.08	50

Since the signals in Figure 5.3 do not present any abnormality, it is possible to state that until the fourth run, the acquisition system was operating properly. The signal of the sixth run (Figure 5.4) presented two evidences that the acquisition did not operate properly: the signal mean declined over the time when it was expected to be zero, since the acquisition system was set to zero at the begging of each run; and there were a lot of plateaus, what indicates that the master antenna was receiving no data for short periods or receiving many points greater than 2000 mV.

The test conclusion is the battery voltage should be at least 7,08 V to guarantee the correct operation of the system. For safety, a minimal value of 7,4 was used. It is also possible to estimate that the batteries can work during 40 minutes before requiring recharge. It is a rough estimation, since the battery charge duration depends on the initial voltage. Additionally, the batteries were identified by a number written on they in order to track if any of them is not working properly. There were five batteries available for testing, although, at maximum four of them were used at the same time.

5.1.3 Signal stability

The signal stability of the acquisition system over the time was verified by experimenting the signals from the points T_1 and T_2, which were acquired during a specific period and their properties were analyzed over this time. The measurement system was set to zero at the beginning of the test and it was expected to be the mean of the signal during all the time. The motor was idle, since the test aimed to analyze just the acquisition system.

The analyzed period is between 30 and 60 seconds. The runs should not be longer, otherwise the reability of the designed experiments would be compromised, since long test schedule may present higher variability (MONTGOMERY, 2013). Considering the design of experiments planned (16 runs), if the run duration is under two minutes, including set up time, it is possible to execute the runs without need for recharging the batteries in between. It avoids variability coming from the processes of disassembly, recharge, which takes twelve hours, and disassembly and assembly of the batteries.

The test result can be seen in Figure 5.5. It is possible to notice that both the signal means increase over the time, mainly after 1000 seconds. However, this duration is longer than the planned for each run of the designed experiments. The stability of the signals during this specific period is shown in Figure 5.6.
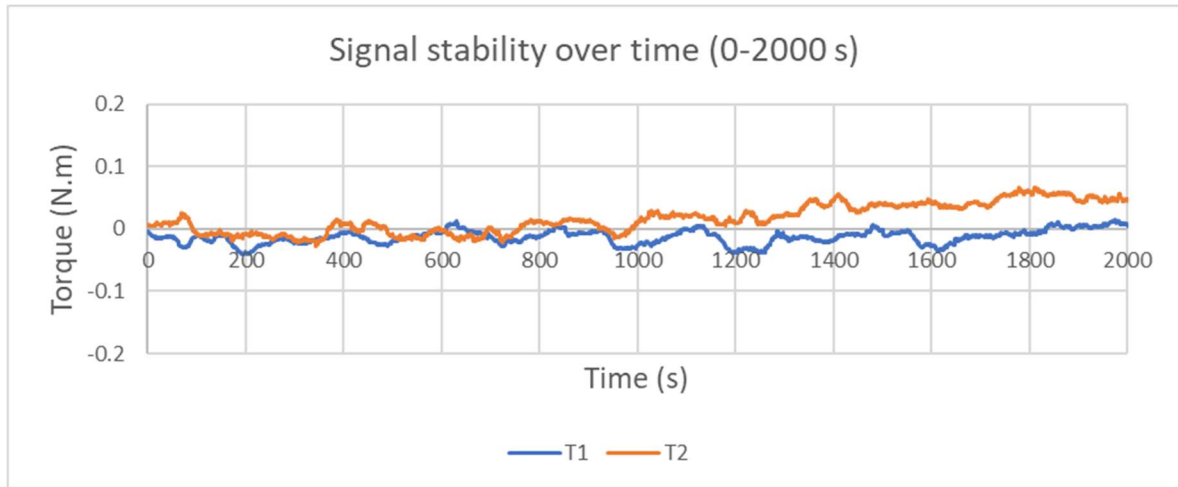
Figure 5.5: Data acquired during 2000 s in order to analyze signal stability over time. The system was set to zero at the test beginning.

.
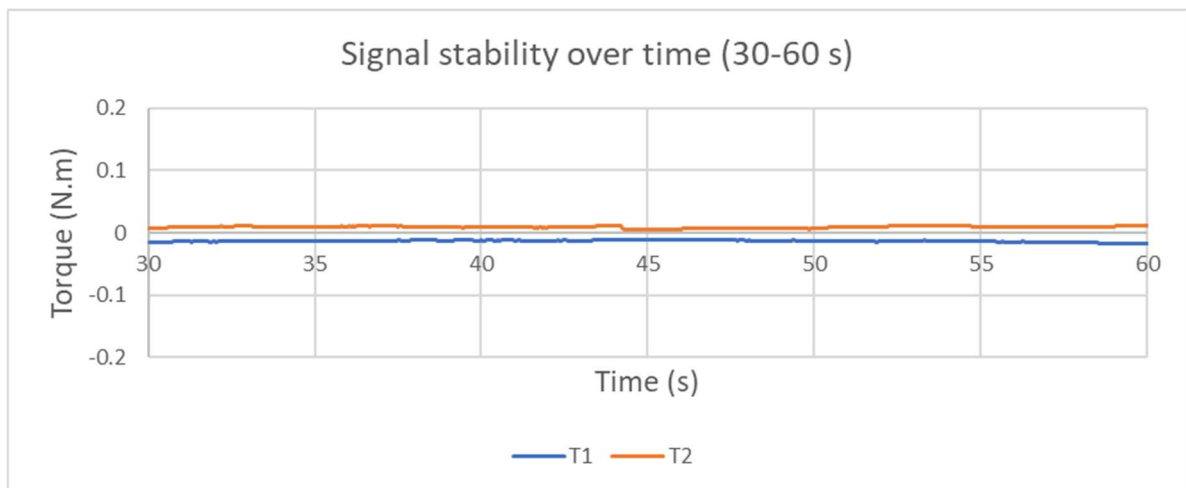
Figure 5.6: Data acquired during the period used for the experiments.

The signal of both the measured torques between 30 and 60 seconds is stable, and no trend could be observed. Therefore, the acquisition system stability is adequate for the proposed test duration: 1 minute long runs, of which the last 30 second are used for statistical assessment and further analysis.

5.1.4 Repeatability of experiments

The repeatability of experiments was analyzed for the case of mass applied to the position one (on box 1), with other platforms kept raised and the motor speed of 3 Hz. It was observed that if platforms with no mass are kept down, they introduce vibration into the system, which leads to poor data quality.

Six runs of the proposed configuration were realized in order to calculate the standard deviation. The results can be seen in Table 5.2. The standard deviation was calculated for the points of each run and for the runs means. Also, a linear fit was calculated for each run and their slopes were recorded. The standard deviation of each run and the slope are a metric for the signal stability. The standard deviation calculated for the runs means is a metric for the repeatability of the experiments. The three metrics are expected to be smaller when compared to the mean of each run in order to classify the data signal quality as good.

Table 5.2: Repeatability tests results

| Run | T_1 | | | T_2 | | |
---	Mean	Std. Deviation	Slope	Mean	Std. Deviation	Slope
1	-0.19365	0.01286	7.00E-05	0.08680	0.01197	6.00E-05
2	-0.10063	0.00202	-5.00E-06	0.09511	0.00820	4.00E-05
3	-0.14936	0.00709	4.00E-05	0.11249	0.01361	7.00E-05
4	-0.15579	0.01477	7.00E-05	0.13408	0.01161	7.00E-05
5	-0.13721	0.00905	1.00E-05	0.05691	0.01238	7.00E-05
6	-0.12251	0.01363	-7.00E-05	0.11322	0.00497	1.00E-05
Mean of the runs	-0.14319			0.09977		
Std. Deviation	0.03168			0.02663		

The slopes are much less than the mean of each run. The standard deviation of the points is approximately one tenth of the mean of each run and the standard deviation between the runs are under one fourth of the mean. Since the considered condition is the one with smaller torques, the signal quality is considered appropriate.

5.1.5 Proposed procedure for experiments

Room temperature might be a source of variability. For this reason, the room temperature was monitored and roughly controlled, although any investigation about the temperature effect on the system has been conducted, due to difficulty of setting temperature as a test variable. At least 24 hours before a set of tests, the air-conditioning system was turned on and the desired temperature was set to 20 °C. The resulting room temperature should be between 22°C and 24°C. The temperature was verified at the beginning at the end of the sets using a thermometer at the PRILs support table.

The deterioration of the loss applier system components was also verified. Considering the pair of materials in friction, aluminum alloy and polyamide polymer, it is expected that the polyamide polymer presents more intense deterioration. At the beginning of each set of test the diameter of the polyamide polymer disc was measured at the same two positions, displaced at 90° from each other.

Planning the experiments includes the preparation of the test form, which includes initial verification and measurement that should be done before the first run test and the tests that should be performed. The initial verifications are: room temperature, battery voltage and which battery was assembled on each position and friction disk diameter. An example of this test form can be seen in Appendix D. Also, the order of runs should be written on this form already randomized. When some test or run presented any abnormality, that run should be redone with a new name, composed by the old name plus "_1" at the end, and a note should be written at the test form.

Each set test received a title. The data file name contains the title, a number to identify replicates and a code to indicate the conditions of the test. The file name should follow the example: "TITLE_REPLICATE_XXXXX", where the first "X" indicates if locked-in torque is applied (1) or not (0); the other "X" points if the masses are on the platforms (1) or not (0) at the positions 1, 2, 3 and 4, respectively. So, the data file named "TITLE_REPLICATE_10101" is related to the test with locked-in torque, with the masses applied on the positions 2 and 4 and platforms 1 and 3 raised.

The procedure to start PRILs is also established and can be found in Appendix E. After conducting the last procedure, it begins the procedure to perform a run. If the run requires applied locked-in torque, it must be done before all the procedure to perform a run. The procedure is presented below:

- Write the data file name;

- If that is the case, apply locked-in torque and save the data referent to the loading process;

- Drop the platforms which will support masses on this run;

- Set to zero all the signals relevant for the current run;

- Start the motor at 3 Hz speed, in case of dynamic testing;

- Place the masses prescribed for this run. Start placing the masses from box 4 to box 1;

- Start saving data;

- After 60 second of acquisition stop saving data;

- Stop the motor;

- Remove all the masses and raise the platforms.

After conducting all the planned runs, if that is the case, loose locked-in torque and save the data referent to the unloading process.

5.1.6 Summary

The first research question aimed the development of a reliable experimental procedure to be used at PRILs. This question leaded to an investigation of the PRILs operation characteristics with the objective of identify limitations and most robust operation conditions. The first question answer is the experimental procedure established on the basis of the observations of PRILs operation at different conditions, and the results obtained from conducted tests, such as battery test and repeatability of acquired data.

The prescribed operation conditions were:

- Platform position: raised position leads to better quality data, when no mass is required over it;

- Rotational speed: 3Hz, due to lower vibration;

- Minimal battery voltage to guarantee the correct operation of the acquisition system: 7,3 V;

- Room temperature and thermal stabilization: room temperature should be between 22 °C and 24 °C aided by the air-conditioning system, that should be started 24 hours before the test beginning.

The procedure also concerns how the operator should start PRILs (Appendix E) and conduct the runs, as listed in the previous topic 0.

5.2   The effect of losses on the power-loop on one box's losses

This section presents the investigation forward the clarification of the second research question: "Is one box's power losses affected by the power losses of other boxes belonging to the power loop?"

The influence of the induced losses in different position of the power loop on one box behavior was investigated. The design of experiments was presented on the previous chapter. Four factors were considered, which were the masses related to the induced losses. The considered responses are related to the box 1: the torque on shafts and the torque loss on box 1, as can be seen in Figure 5.7. The total of runs was $2^4 = 16$, according to the number of factors and to the condition of none replicate. Although it has been pointed out that three responses are object of analysis, only 16 runs were enough, since the two points of torque were operating during all the runs.
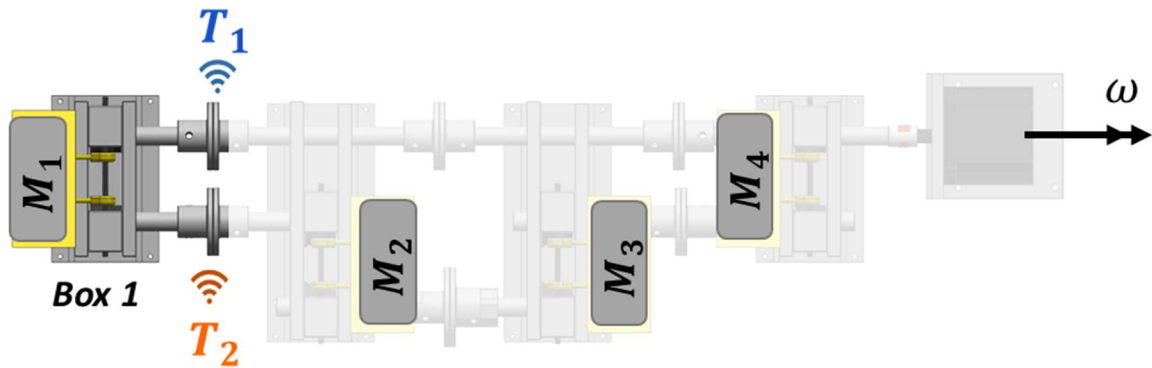
Figure 5.7: Factors M_1, M_2, M_3 and M_4 (in black) and responses T_1, T_2 and BL_1 of the designed experiment

The experiment design was realized according to the procedure described in the previous topic. The system ran for 1 minute with all the losses appliers loaded in order to warm-up. Each run took one minute, and the set-up time was under one minute. Before starting the engine at each run, the acquisition system was reset. It was not necessary to recharge the batteries during the test set. By the end of the set test the battery voltage was higher than 7.3 V.

The set of masses used were made of steel and each one weights approximately 2,300 g. Each mass received one of the following identifications: M_1, M_2, M_3 or M_4, following the number identification of the boxes. The mass M_1 was placed only on box 1 platform and never occupied one of the other platforms. The same procedure was adopted to the other masses.

The runs were named according to the masses placed on the boxes. The first digit is always 0, since the locked-in torque effect was not explored by this design. The following digits indicate if there were masses placed on the boxes. The following digits represent the presence of the masses on each respective box, starting with the box 1. The digit 1 indicates that the mass on that position was placed on the box, while the digit 0 indicates that there was no mass placed on that position. When any of the masses was not required for the run, the platform at that position was kept raised. The data was recorded for one minute.

There were four abnormalities due to lost communication during the execution of this test set. During the tests 16runs5_00001, 16runs5_00110, 16runs5_01101 and 16runs5_01111, it was observed that the signals of some measuring points were square-shaped, what indicated loss of communication, since the batteries' voltages were above 7.3 V. Those runs were done again, and a new data file was saved and renamed accordingly to the proposed procedure. The mean of the last 30 seconds signal was calculated for each run. Table 5.3 presents the results.

Table 5.3: 2^4 design of experiments results.

M_1	M_2	M_3	M_4	T_1 $(N.m)$	T_2 $(N.m)$	T_3 $(N.m)$	T_4 $(N.m)$	BL_1 $(N.m)$	BL_2 $(N.m)$	BL_3 $(N.m)$	BL_4 $(N.m)$
0	0	0	0	-0.92	2.56	2.64	4.75	3.48	0.08	2.11	-5.67
0	0	0	1	0.63	2.86	5.11	6.35	2.23	2.26	1.23	-5.72
0	0	1	0	-1.25	1.70	3.33	6.68	2.94	1.63	3.35	-7.92
0	0	1	1	0.00	2.03	2.66	5.92	2.03	0.63	3.26	-5.92
0	1	0	0	-2.66	-0.39	5.76	8.26	2.26	6.15	2.50	-10.92
0	1	0	1	-0.30	1.72	5.13	5.97	2.02	3.41	0.84	-6.27
0	1	1	0	-2.95	-0.77	5.46	10.90	2.18	6.23	5.44	-13.85
0	1	1	1	-2.70	-0.32	6.47	11.39	2.39	6.79	4.92	-14.09
1	0	0	0	-2.64	3.21	5.98	9.75	5.85	2.77	3.77	-12.40
1	0	0	1	-0.01	6.51	7.21	7.28	6.52	0.69	0.07	-7.28
1	0	1	0	-2.24	2.77	5.35	10.54	5.01	2.57	5.20	-12.78
1	0	1	1	-0.72	5.76	7.31	9.72	6.49	1.55	2.41	-10.44
1	1	0	0	-2.40	3.40	9.25	11.91	5.80	5.85	2.65	-14.30
1	1	0	1	-2.75	1.80	8.26	10.24	4.55	6.46	1.99	-12.99
1	1	1	0	-3.23	2.10	8.30	12.89	5.33	6.20	4.59	-16.12
1	1	1	1	-2.58	2.40	9.71	13.80	4.98	7.30	4.10	-16.38

5.2.1 Statistical Assessment

The exposed data is analyzed according to the method 6-step ANOVA proposed in chapters 2 and 4 (Figure 2.11). All the calculation steps were done using the R programming language. The first step (Step 1) is Estimate Factor Effects. This step is showed for the three considered responses in Appendix F. The relevant factors were those which effects estimated by the metric E were higher than 0,03 (see Figure 2.11). The factors considered relevant according to the criteria are highlighted on the tables on Appendix F.

The Step 2 is the proposition of the first model based on the estimated effect. The first model is composed by the factors considered relevant and their interactions, since, according to the principle of sparsity of effects, it is unlikely for a factor to present no relevance while one of its interactions present any relevance.

The second step is to propose the first model using the relevant factors and interactions. The first model for each of the responses followed the criteria proposed in chapter "Materials and Methods": the most relevant factors and their interaction. The most relevant factors are shown in Figure 5.8. The first models proposed for T_1 and T_2 are composed by M_1, M_2, M_4 and their interactions. The first model proposed for BL_1 is composed by M_1, M_2 and their interactions.
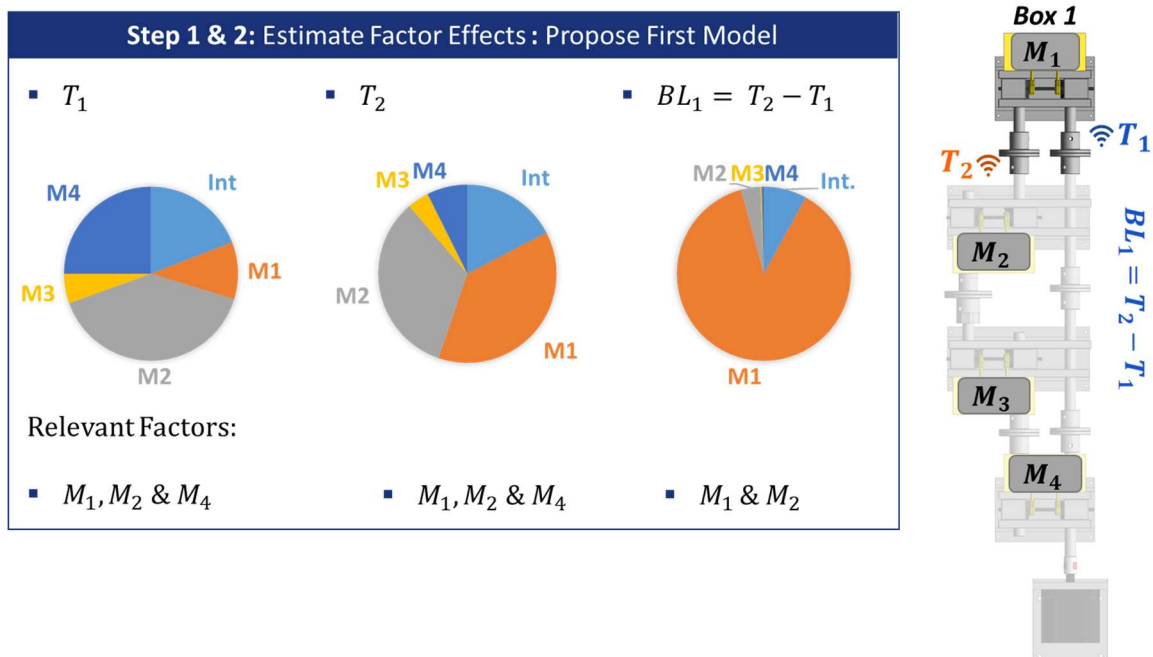
Figure 5.8: Step 1 of 6-step ANOVA

The third step is to perform the F-test in order to identify significant factors or interactions with a 95% confidence level, which is verified by a p-value of less than 0.05. The results are shown below, in Figure 5.9 for each of the proposed models.
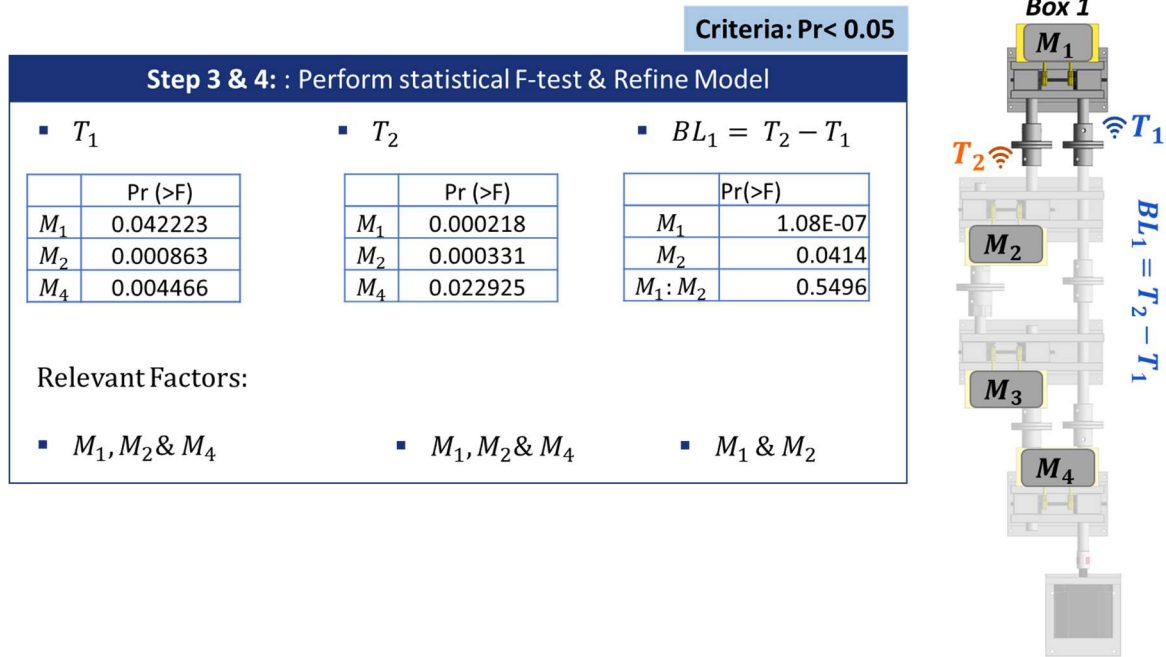
Figure 5.9: Refined model after the execution of Steps 3 and 4.

The test indicates that only M_2, M_4 and M_1 are relevant for T_1 and T_2. For BL_1, M_1 is the most influential factor. M_2 is also relevant, but the interaction between these factors cannot be considered relevant for the response BL_1.

The Step 5 of the method checks for the validity of the proposed models, with relation to the normality and random distribution hypotheses. The normality criteria can be analyzed using the normal probability plot or the *Shapiro-Wilk* test. The random criteria are analyzed aided by the plotted residuals in run order. The results can be seen in Figure 5.10, Figure 5.11 and Figure 5.12.
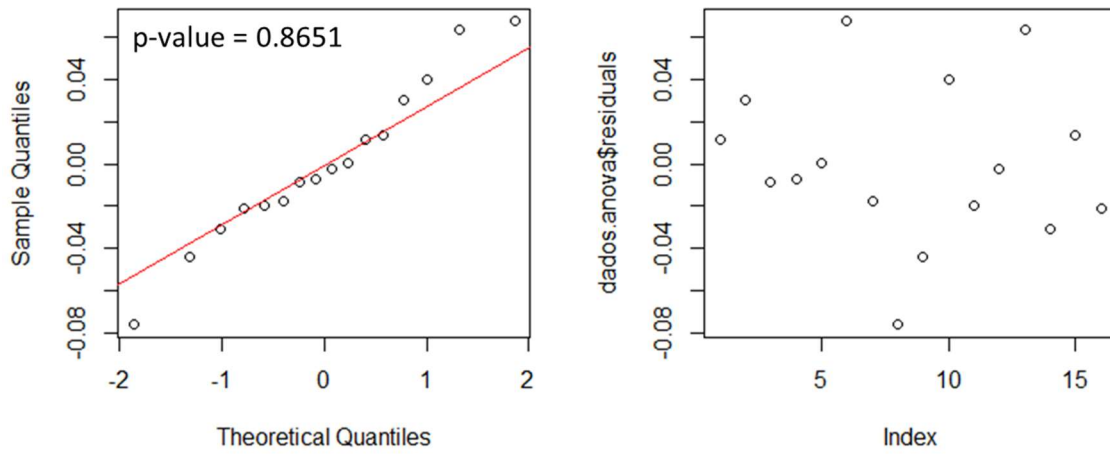
Figure 5.10: Residuals analysis for the proposed model for the response T_1
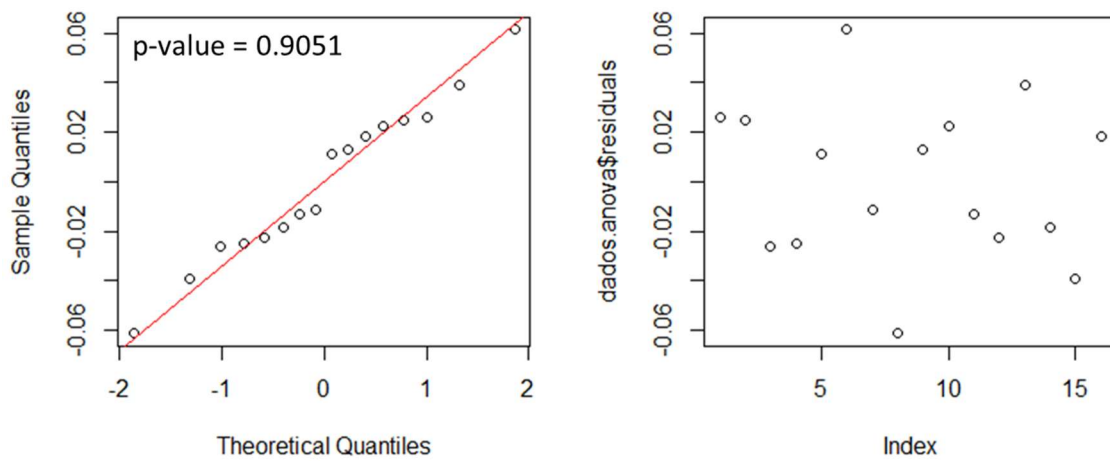
Figure 5.11: Residuals analysis for the proposed model for the response T_2
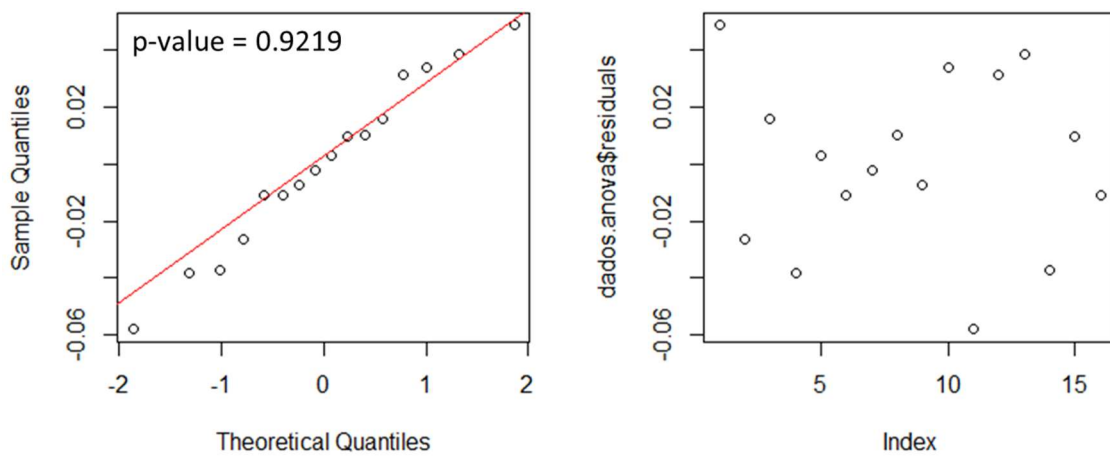
Figure 5.12: Residuals analysis for the proposed model for the response BL_1

According to the *Shapiro-Wilk* test, one cannot reject the hypothesis that the residuals of the three models have a normal distribution ($p - value \geq 0.05$). Also, no temporal trend was observed in the residuals in run order graph. The analysis of residuals indicates that the proposed models are adequate. The sixth step will the discussed separately on the next topic.

5.2.2   Step 6: Provide Results' Interpretation

The results obtained from the current investigation are illustrated in Figure 5.13. For each of the considered responses, T_1, T_2 and BL_1, the relevant masses are showed.
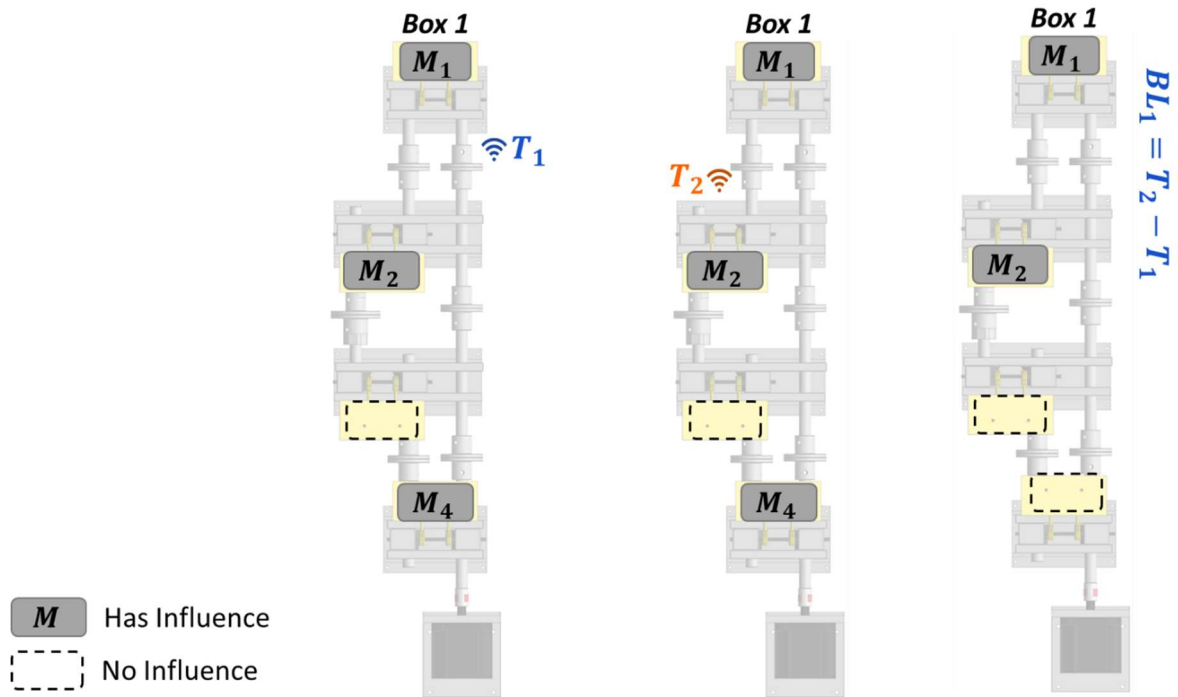
Figure 5.13: Summary of the results obtained from 6-step ANOVA.

According to Equations 2.2 and 2.3, the amount of losses (P_L) influences directly on the efficiency, which requires either input or output torque to change (XU, 2005). Placing M_1 on the box 1 platform introduces a power loss between measuring points T_1 and T_2. Therefore, the influence of M_1 on T_1, T_2 and BL_1 was observed, as expected. BL_1 increases with M_1, as does T_2, which means T_1 decreases. Placing M_1 not only decreases the torque output, but also increases the torque input. It shows that when a box requires more power, the motor provides it to the system.

M_4 equally increases T_1 and T_2. This effect will be further discussed in Section 5.3.3. The effect of the losses due to M_2 on the measured T_1 and T_2 indicates that the losses on each box may not be independent from the behavior of other boxes losses. The power loss on box 1 (BL_1) is showed to be affected by M_1 the most, and by M_2. However, M_2 effect is lighter than M_1 effect, the first one is considered relevant with a higher than 95% confidence level. M_4 has no effect, since it influences equally T_1 and T_2.

The second question aims to identify if the losses on box 1 are affected by other boxes' losses. The conducted investigation showed that the measured torques at the shafts of box 1, T_1 and T_2, are influenced by variations of power losses at boxes 1, 2 and 4, with relation to M_1, M_2 and M_4. Additionally, the power loss on box 1 is affect not only by the load applied directly at the box, but also by the losses of the close box 2. Therefore, the answer for the second question is that box 1's losses behavior is affected by the power losses of other boxes belonging to the power loop.

All the experiments discussed until this point were realized at a condition of no locked-in torque. The results showed might be relevant considering the report FVA no. 345 (DOLESCHEL et al., 2002), used as reference for gear efficiency testing. According to this procedure, part of the experiment is prescribed to be no-load runs or almost no-load runs. It has been shown that the behavior of the power losses at the boxes are not independent. So, it indicates that variation coming from the most vary sources, such as assembly (ANDERSSON et. al, 2014), may affect the measured efficiency of the box of interest.

This conclusion leads to further investigations proposed by the third question, which aims to observe the dynamic behavior of all the four boxes with and without applied locked-in torque. The phenomenological discussion will be conducted considering this overall investigation.

5.3   The relation among the losses of the power loop boxes

This section aims to present the results obtained from investigations related to the third research question: "Is it possible to quantify the relation among the power losses of the boxes belonging to the power loop?"

Two investigation were conducted to answer the third question. One investigation aimed the dynamic behavior of the power losses at boxes 2, 3 and 4 when no locked-in torque is applied. The behavior of box 1 at this condition was already explored by the second research

question. A final investigation was conducted in order to explore the dynamic behavior of the power losses on the four boxes when locked-in torque was applied.

5.3.1 Torque distribution for no locked-in torque condition

This section aims to discuss the power losses dynamic behavior when no locked-in torque is applied. The design of experiments was presented on the previous chapter. The considered factors were four, the masses related to the induced losses. The total of runs was $2^4 = 16$, according to the number of factors and to the condition of none replicate.

The considered responses are eight and related to all the boxes: the torques on shafts $(T_1, T_2, T_3$ and $T_4)$ and the torque loss on all the boxes $(BL_!, BL_2, BL_3$ and $BL_4)$, as can be seen in Figure 5.14. The same runs were used for acquiring the data used in the following analysis and the data used for the investigation proposed by the second question.

$$\text{Box 1: } BL_1 = T_2 - T_1 \qquad \text{Box 3: } BL_3 = T_4 - T_3$$
$$\text{Box 2: } BL_2 = T_3 - T_2 \qquad \text{Box 4: } BL_4 = T_1 - T_4$$
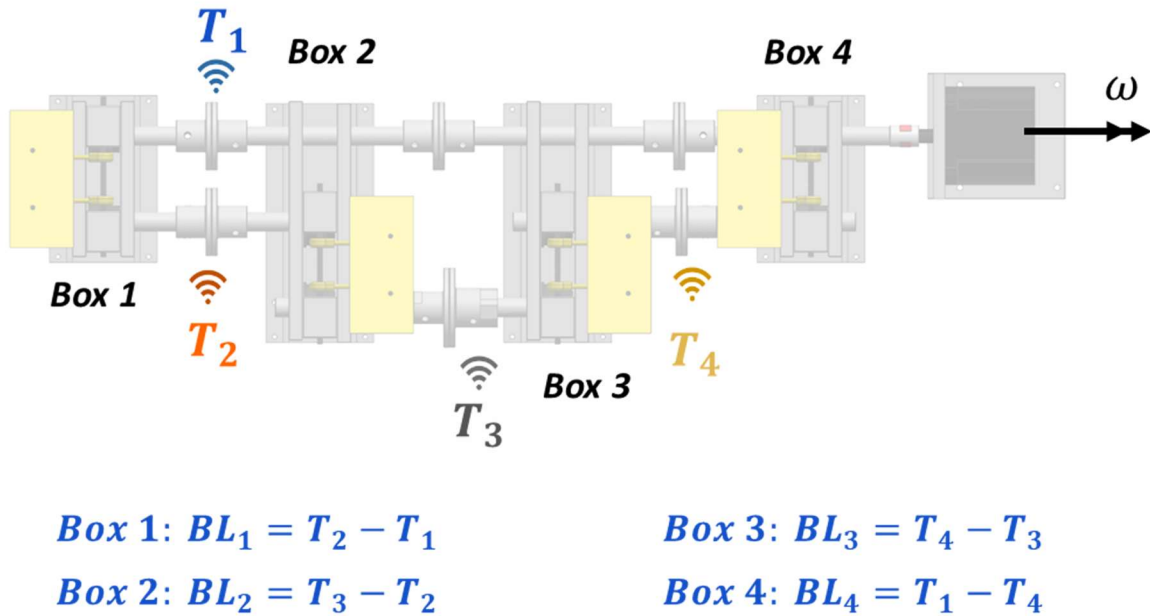
Figure 5.14: Responses of the analyzed experiments: four measured torques and four measured torque losses.

The results from 6-step ANOVA for the responses of power losses are presented after the results for the torque responses. In order to produce an overview of studied condition, the second question's results $(T_1$ and $T_2)$ are shown together with the results for T_3 and T_4. The used procedure is similar to the already used for the second research question.

The data is analyzed according to the proposed method 6-step ANOVA (Figure 2.11). All the calculation steps were done using the R programming language (Appendix C). The first step (Step 1) is Estimate Factor Effects and the second is the proposition of the first model. The estimated effects are shown in Appendix G, where the factors considered relevant are highlighted on the tables. The relevant factors and their contribution to the total observed effects can be seen also in Figure 5.15. They and their combination compose the first model proposition.
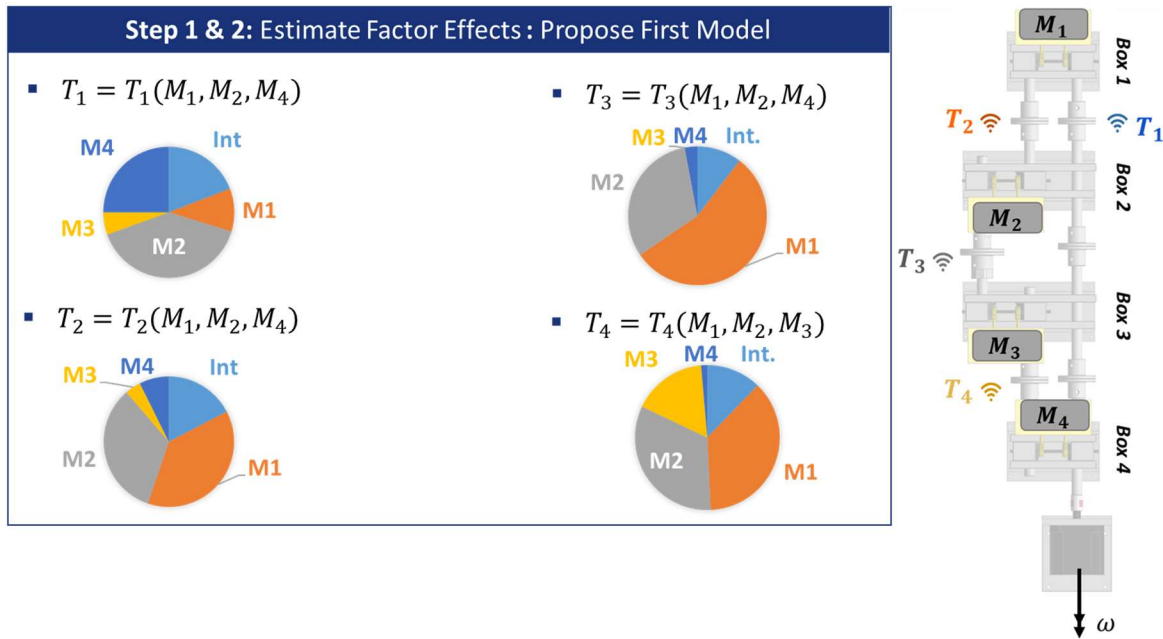
Figure 5.15: Step 1 of 6-step ANOVA for measured torques T_1, T_2, T_3 and T_4 under no locked-in torque condition

The Step 3 is the statistical test (F-test) for the proposed models. Significant factors or interactions with a 95% confidence level are verified by a p-value of less than 0.05. The results are shown below, in Figure 5.16, for each of the proposed models. The final models were: $T_3 = T_3(M_1, M_2)$ and $T_4 = T_4 (M_1, M_2, M_3)$.
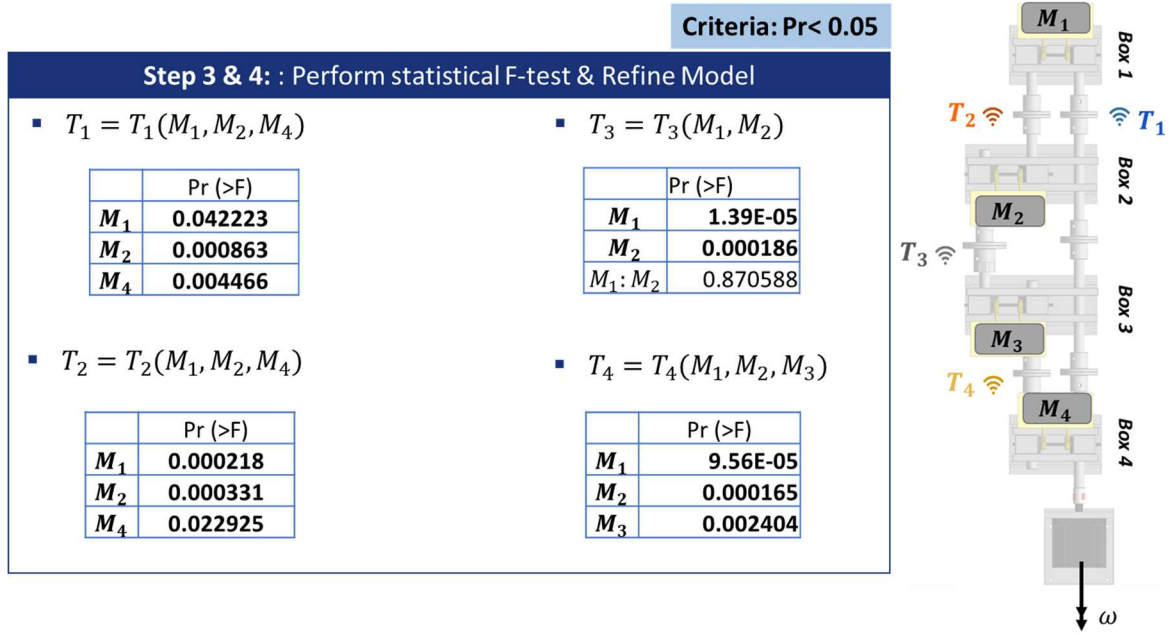
Figure 5.16: Refined models and results from F-test for the measured torque responses.

The adequacy of the proposed models is verified in Step 5. The residuals must be verified with relation to normality and random distribution. *Shapiro-Wilk* test and the graph Normal probability plot are used for checking the normality distribution: if the p-value of the *Shapiro-Wilk* is higher than 0.05 and if the if the residuals fit a line in Normal probability plot graph, the hypothesis of normal distribution cannot be rejected. The random distribution is verified by a lacking trend in the residuals plot in run order. The *Shapiro-Wilk* tests and Normal probability plot graph pointed that the hypothesis of normal distribution cannot be rejected, and none trend was noticed in the residual plot in run order. These results can be seen in Figure 5.17 and in Figure 5.18.
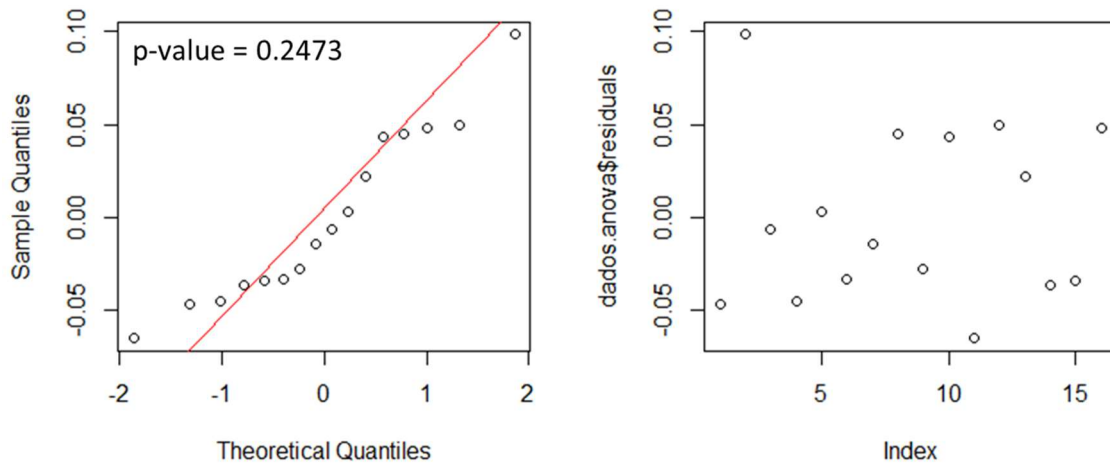
Figure 5.17: Residuals analisys of the proposed model $T_3 = T_3 (M_1, M_2)$
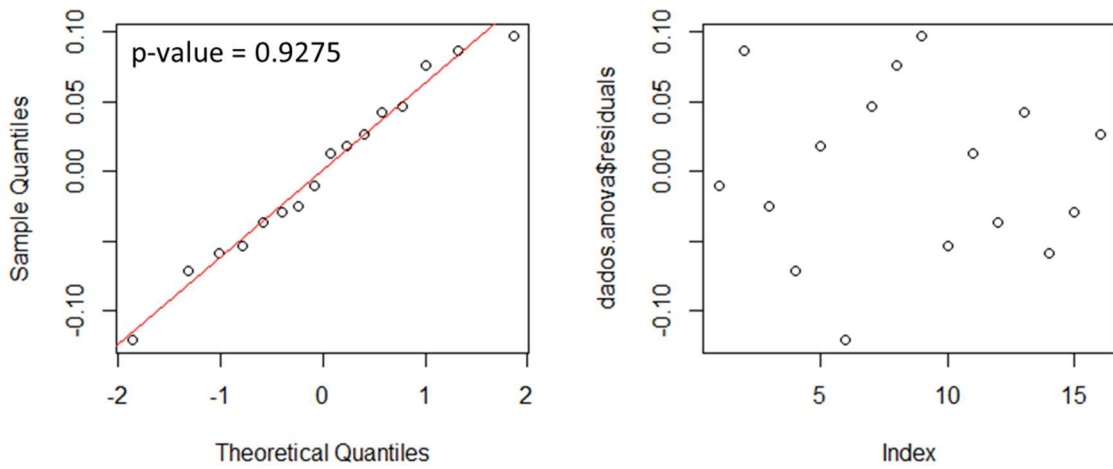
Figure 5.18: Residuals analisys of the proposed model $T_4 = T_4(M_1, M_2, M_3)$

The final step is analyzing the results. A summary can be found in Figure 5.19. It is possible to notice that the measured torque depends on the mass applied directly on the shaft where the measurement point is installed. Thus, T_1 depends on M_1 and M_4, T_2 depends on M_1 and M_2, as well as T_3 depends on M_2 and T_4 depends on M_3. The influences of M_3 on T_3 and of M_4 on T_4 were not verified.
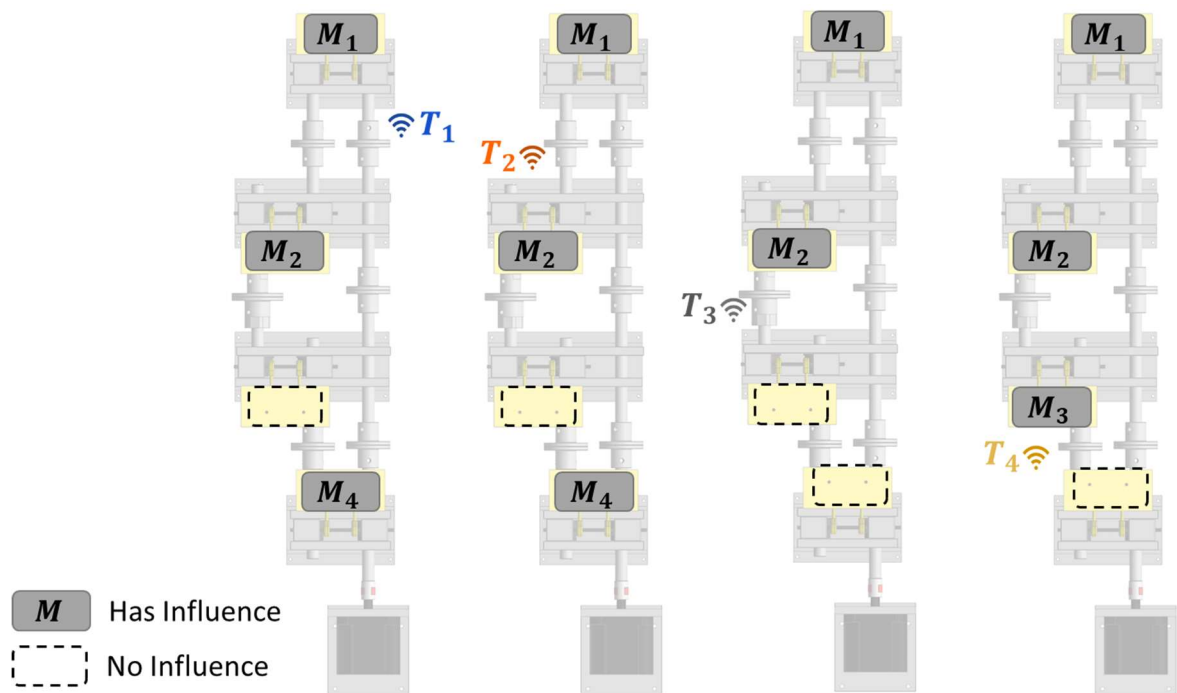
Figure 5.19: Summary of the results for the analysis of the behavior of the measured torques under no locked-in torque condition.

It is noticed that the measured torques are affected by masses applied directly on the instrumented shaft. Thus, T_1 is affected by M_1 and M_4, T_2 is affected by M_1 and M_2, T_3 is affected by M_2 and T_4 is affected by M_3. All the torques depend on M_1, since it acts directly on the system input power. Some measured torques are related to masses applied on other shafts, what would suggest that the dynamic behaviors of the boxes are interdependent. The losses due to M_4 are directly related to the power available to the power loop, since it is located at the power input point of the system. This can be observed for T_1 and T_2.

The relevance of this results concerns the no-load gear efficiency test prescribed by the report FVA no. 345 (DOLESCHEL et. al., 2002), used as reference for gear efficiency testing. Even if the torque losses were not yet analyzed, the presented results with relation to the torques indicate that variation on other boxes losses changes the power and load available to the boxes of interest. The usual procedure of measuring different gear pairs efficiency and comparing the measured results can be affected negatively, once the power and load available in different runs may be not comparable.

5.3.2 Power losses assessment for no-load condition

The investigation herein presented is based on the same data used for the past analysis. The responses considered now are: torque losses on box 1, defined as: $BL_1 = T_2 - T_1$; torque losses on box 2, defined as $BL_2 = T_3 - T_2$; torque losses on box 3, defined as $BL_3 = T_4 - T_3$; and torque losses on box 4, defined as $BL_4 = T_1 - T_4$. The factors and levels are the same used for the past analysis.

The statistical assessment method is the same used for the last analysis. The results from each step will be briefly commented herein, and their interpretation will be on focus. Appendix I presents the tables with the estimation of effects for the torque losses responses. Those results are illustrated in Figure 5.20. The estimation of effects showed that the masses applied on the top of each box have a substantial effect on the box loss. It occurs to M_1 and BL_1, M_2 and BL_2, M_3 and BL_3 and, in a lighter way, to M_4 and BL_4. Additionally, some masses present a substantial effect on neighbor boxes: M_4 has a considerable estimated effect on BL_3 and on BL_1.
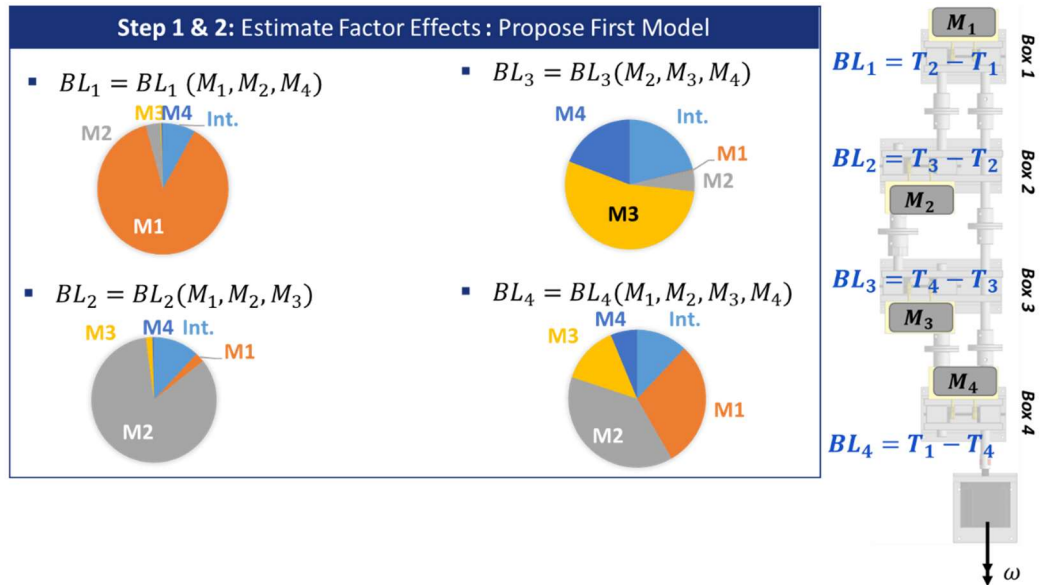
Figure 5.20: Step 1 of 6-step ANOVA for measured box losses BL_1, BL_2, BL_3 and BL_4.

The factors which effects were considered relevant were M_1 and M_2 and M_4 for BL_1; M_1, M_2 and M_3 for BL_2; M_2, M_2, M_3 and M_4 for BL_3; and all the masses for BL_4. They and their interactions were used for the first proposed model. It was performed statistical F-test on the first model. The factors and interaction which were not considered relevant with 95% confidence level were excluded from the model, and a new one composed by the relevant factors and interactions was tested again. The refined model can be seen in Figure 5.21.
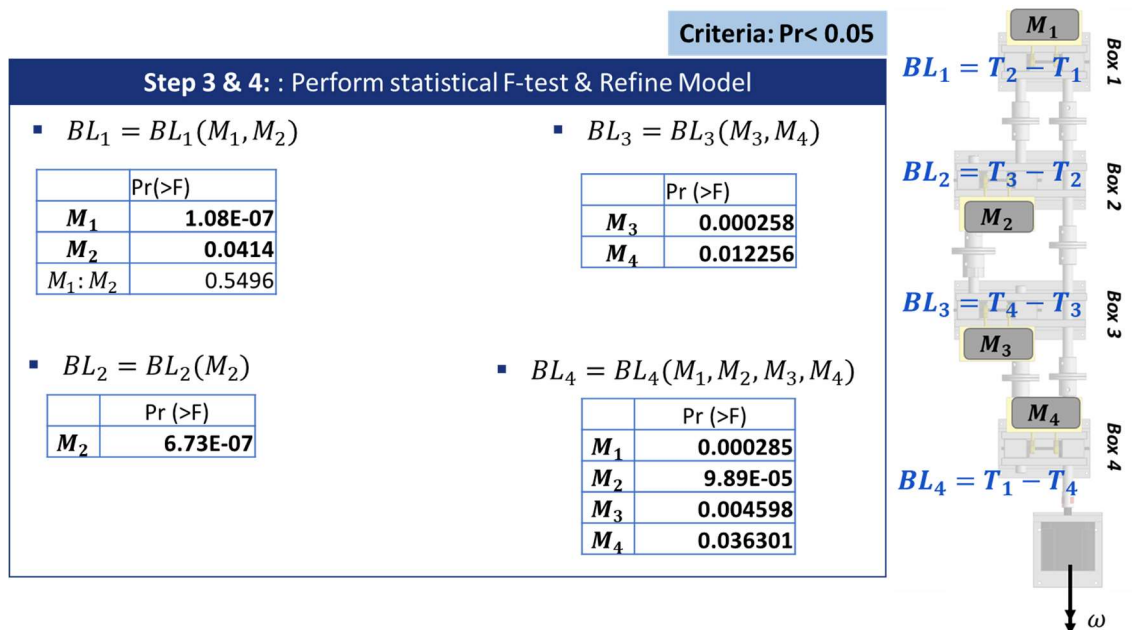
Figure 5.21: Refined models and results from F-test for the responses measured box losses.

BL_4 depends on all the factors. This is reasonable, since in this study BL_4 is mathematically defined as the sum of BL_1, BL_2 and BL_3. The losses on boxes 1 and 3 depend on the masses placed directly over them, M_1 and M_3, respectively, and on masses that induced extra losses on the neighbor boxes. Remarkably, box 2 is not affected by losses induced at other points of the power loop, only by the mass placed on itself. Thus, at PRILs, the optimal box, with concern to reliable dynamic behavior of the losses, to conduct efficiency tests is box 2.

It was still necessary to test the residuals of each model to validate the normality and random distribution hypothesis. The results of this step are shown in Figure 5.22, Figure 5.23 and Figure 5.24. No violation of the hypothesis was found for the three performed analysis: the *Shapiro-Wilk* test of the three models residuals does not reject the null hypothesis of normality with 95% confidence level and no trend was found considering the order of the runs.
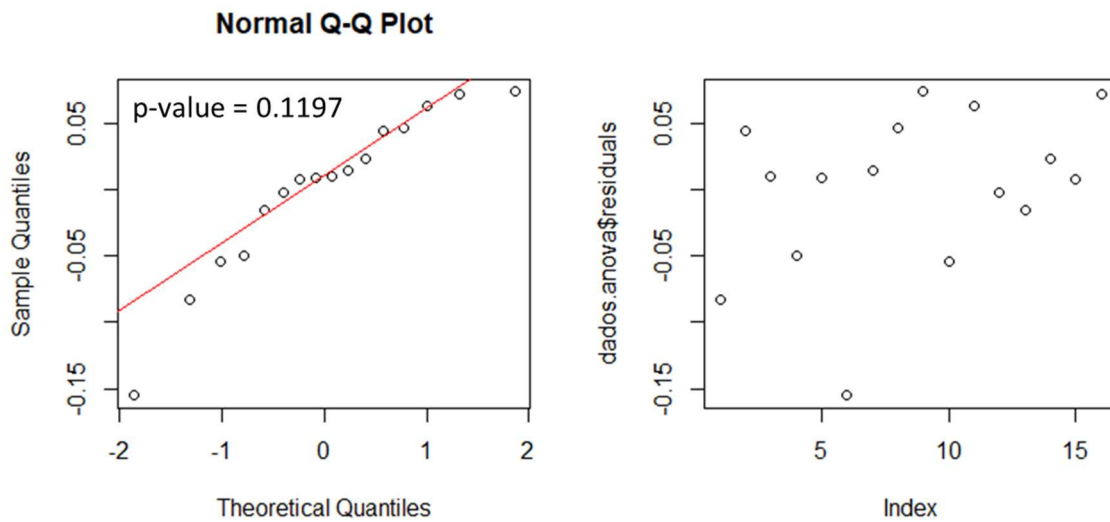
Figure 5.22: Residuals analisys of the proposed model $BL_2 = BL_2\ (M_1, M_2)$.
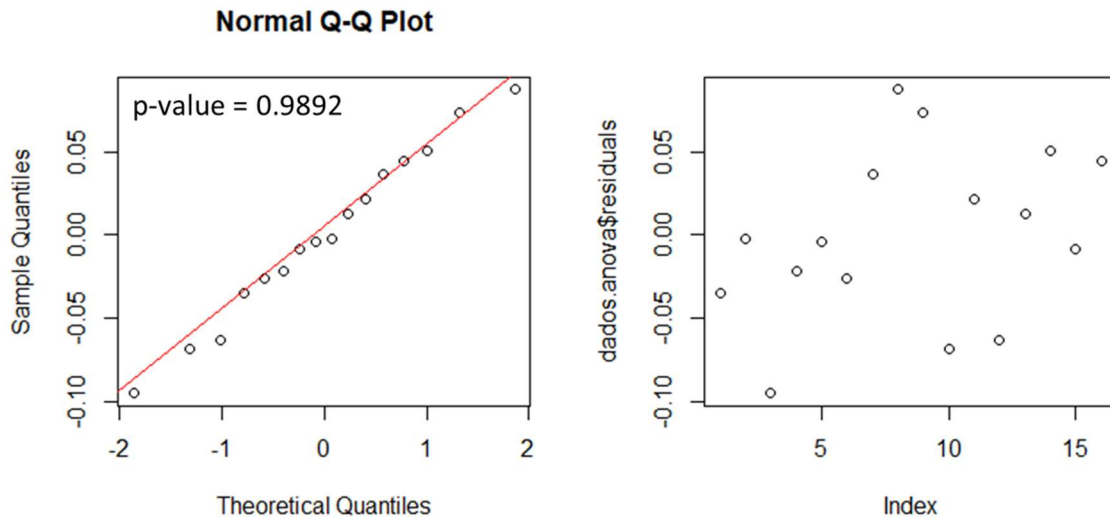
Figure 5.23: Residuals analisys of the proposed model $BL_3 = BL_3\ (M_3, M_4)$.
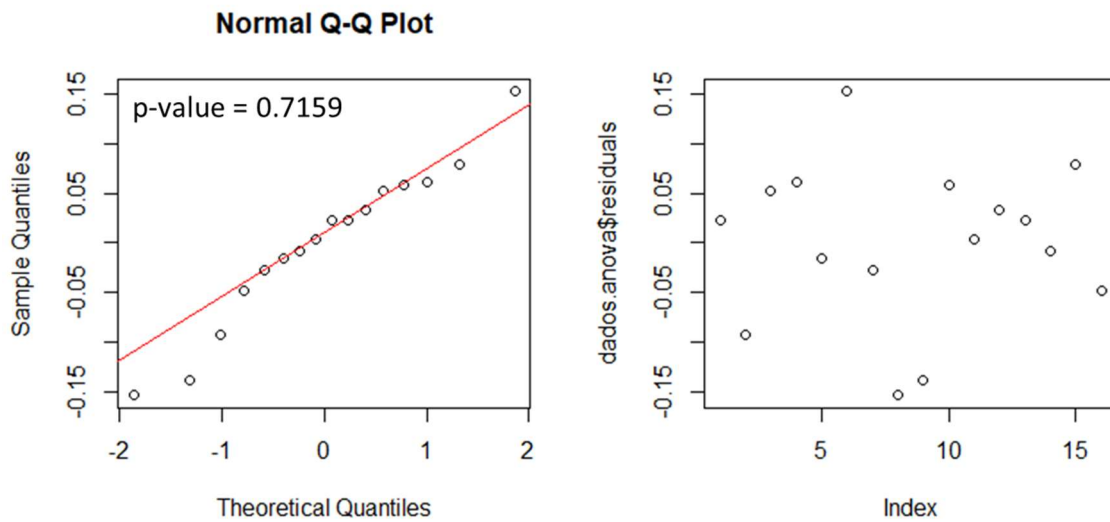
Figure 5.24: Residuals analisys of the proposed model $BL_4 = BL_4\ (M_1, M_2, M_3, M_4)$

A summary of the investigation with relation to the boxes torque losses is presented in Figure 5.25. The result of the dependency of the box loss on the mass applied directly on it was already expected.
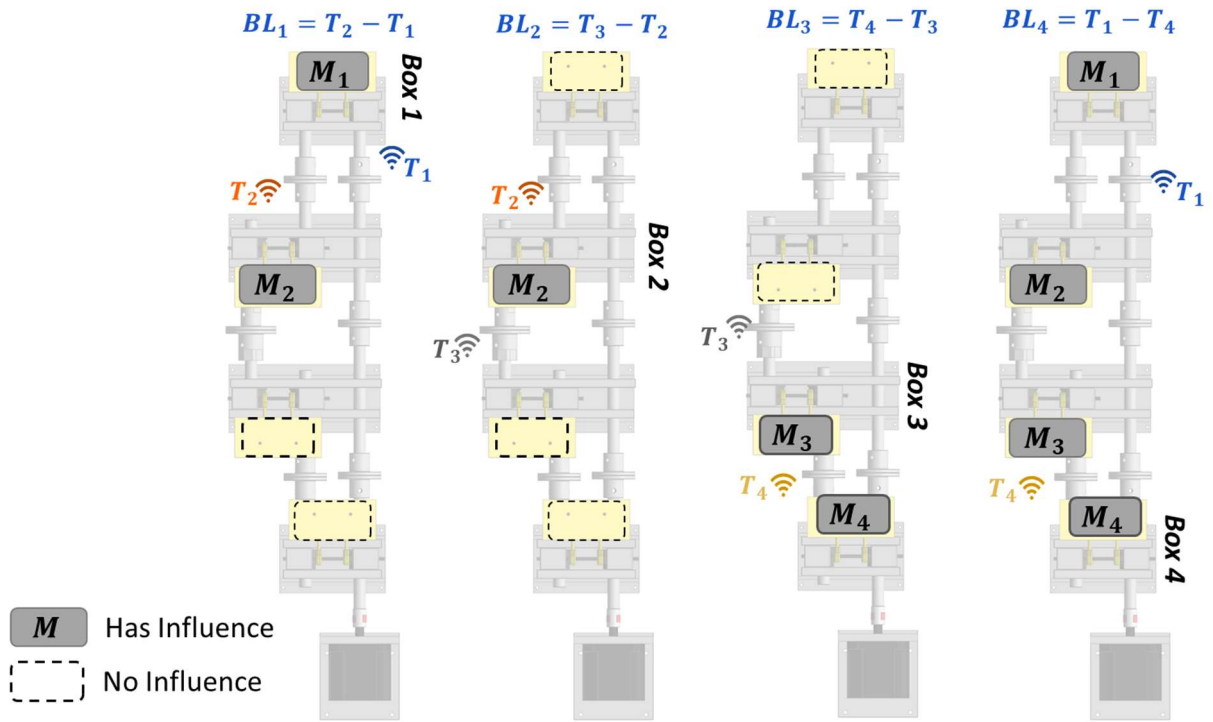
Figure 5.25: Summary of the results for the analysis of the behavior of the measured boxes' losses under no locked-in torque condition.

The losses on box 1 and box 3 depend on M_2 and M_4, respectively, besides the mass applied direct on them. This result shows that the power available to each box and, consequently, the loss on each box can be affected by variation of losses in other points of the loop. During the tests, those variations were intentionally induced in a controlled way. However, during gear test efficiency it can come from uncontrolled sources, such as assembly errors (ANDERSSON et. al, 2014) or wear of other parts which are not the object of the study. This may alter the measurements (ANDERSSON et. al, 2014) and affect negatively the comparison among the measured efficiencies of the gear pairs prescribed by the FVA nº 345 (DOLESCHEL et. al, 2002).

The box 2 is the only one that seems to be not affected by the other boxes' losses. It is possible to that at PRILs there is a box which is less sensitive to changes on the power loss distribution inside the power loop. It indicates that there may be an optimal position in the loop the conduct efficiency tests. At PRILs, it occurs at the box 2.

Observing Figure 5.26, it is possible to see how T_2, T_3 and BL_2 behave at different conditions of induced losses. The first graph shows the tests in which M_2 was not placed on box 2. All other masses' variations are presented in X-axis. It is possible to observe that BL_2 presents a variation between 0 and 0.16 N.m, while T_2 varies between 0.10 and 0.40 N.m and

T_3 varies from 0.16 to 0.44 N.m. The second graph in Figure 5.26 presents the tests in which M_2 was placed on box 2. BL_2 is greater at the second graph due to the induction of losses caused by M_2, although the maximum variation is roughly the same: 0.22 N.m. Moreover, the torque values present comparable variations: T_2 and T_3 vary 0.24 N.m.
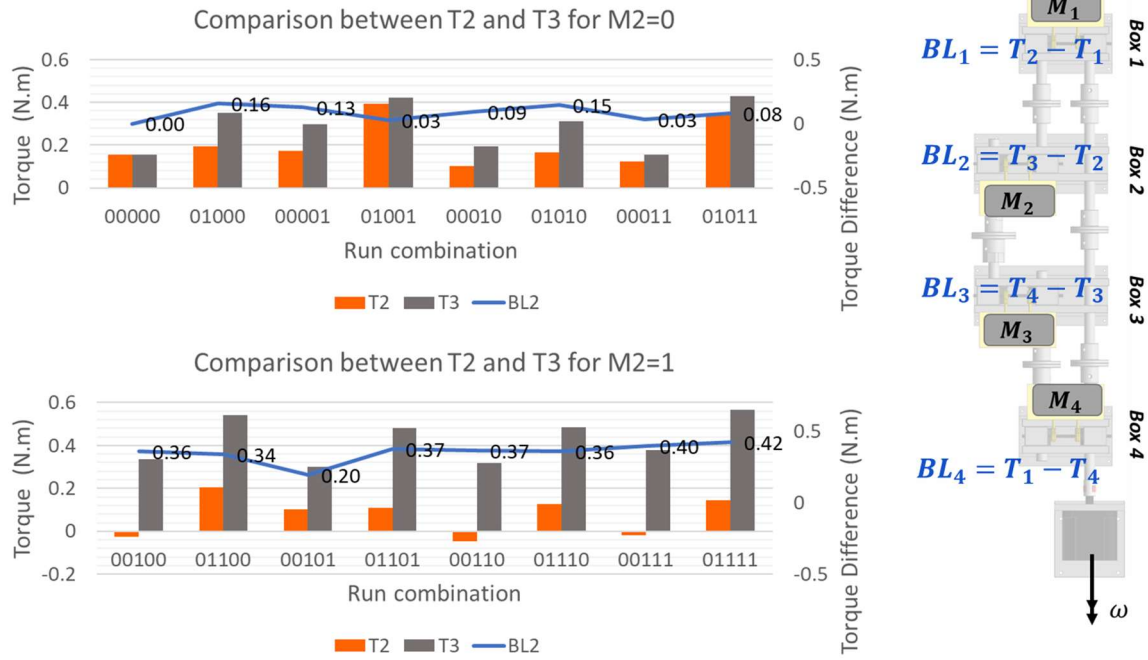
Figure 5.26: Dynamic behavior of T_2, T_3 and BL_2 at different conditions of power loss distribution at the loop. The X-axis presents all tested conditions, where the first digit 0 means that there is no locked-in torque applied, the following digits mean if masses M_1, M_2, M_3 and M_4 are placed on the boxes (1) or not (0), respectively.

The graphs in Figure 5.26 reveal that, although T_2 and T_3 vary due to variation on the power loss distribution on the power loop, both torques follow the same trend. Due to this fact, BL_2 is not affected by the induction of losses on different points of the power loop, other than the ones that occur in box 2 itself, such as M_2.

The next section will discuss which PRILs characteristics may justify this observation, so that it can be extended to other power-circulating test rigs.

5.3.3 The overall phenomenological interpretation of the no locked-in torque condition

The results obtained by applying the 6-step ANOVA method to the data from the no locked-in torque condition tests indicate which torques and boxes' losses are affected by variations at different points of the power loop. The following discussion aims to explain which PRILs features lead to the fact that only box 2 is not affected by loss variations at other boxes.

The first phenomenological observation concerns how the power flows through the system. A consistent order in the values of measured torque can be observed throughout all runs: $T_1 < T_2 < T_3 < T_4$. The data is plotted in Figure 5.27. This behavior indicates the preferential direction in which the power flows in the system: from the motor to box 4, then to box 3 and so on, as the torque decreases with successive losses
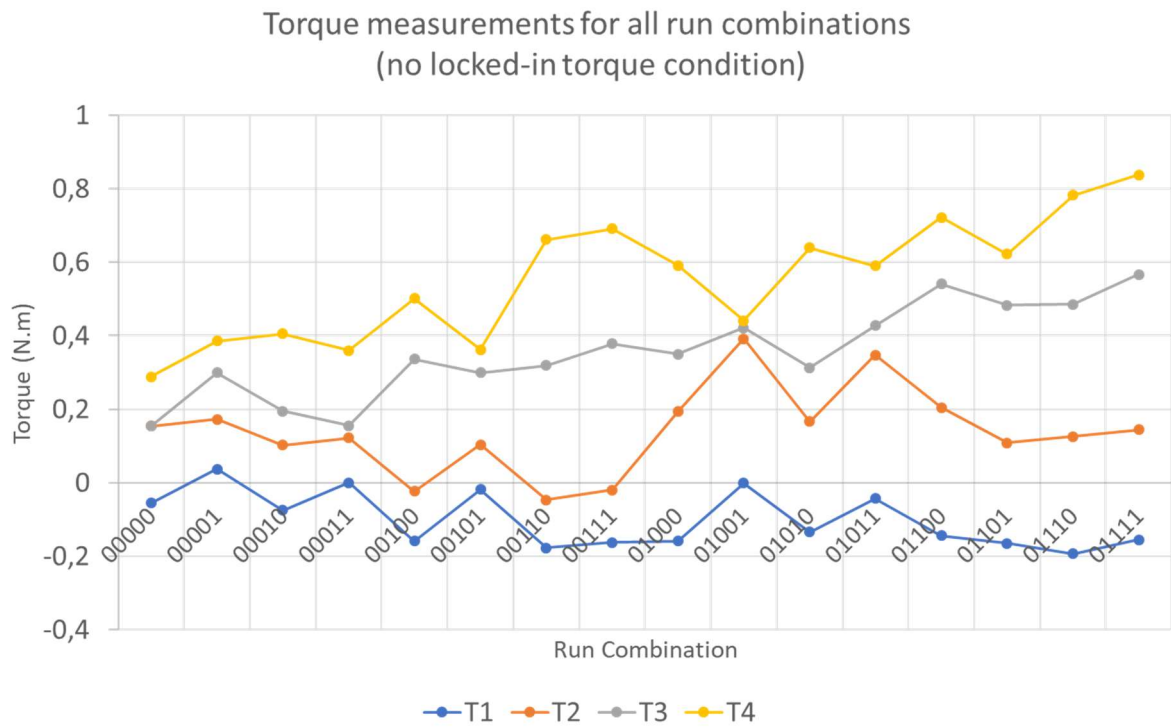
Figure 5.27: Measured torques under no locked-in torque condition. The X-axis presents all tested conditions named according to the standard stablished on section 0, where the first digit 0 means that there is no locked-in torque applied, the following digits mean if the masses M_1, M_2, M_3 and M_4 are placed on the boxes (1) or not (0), respectively.

The distribution of the induced losses at PRILs does not change the power flow direction. For this reason, it is suggested that other factors, not addressed by this study, are

responsible for establishing the preferential way in which the power flows. The rotational speed direction is a candidate for a future investigation, since it was kept constant and it is closely related to the system kinematics. The induced losses are much greater than those observed at gear pairs or than extra power losses due to assembly errors or wear of components, so it is unlikely that variations in the loss distribution at a power-circulating gear test rig lead to changes on the power flow direction due to variations in the power loss distribution. The following discussion will be aided by the reference direction stablished by the power flow, as can been seen in Figure 5.28. The upstream direction is opposite to the power flow direction, while the downstream direction coincides with the power flow direction.

$$\text{Box 1: } BL_1 = T_2 - T_1 \qquad \text{Box 3: } BL_3 = T_4 - T_3$$
$$\text{Box 2: } BL_2 = T_3 - T_2 \qquad \text{Box 4: } BL_4 = T_1 - T_4$$
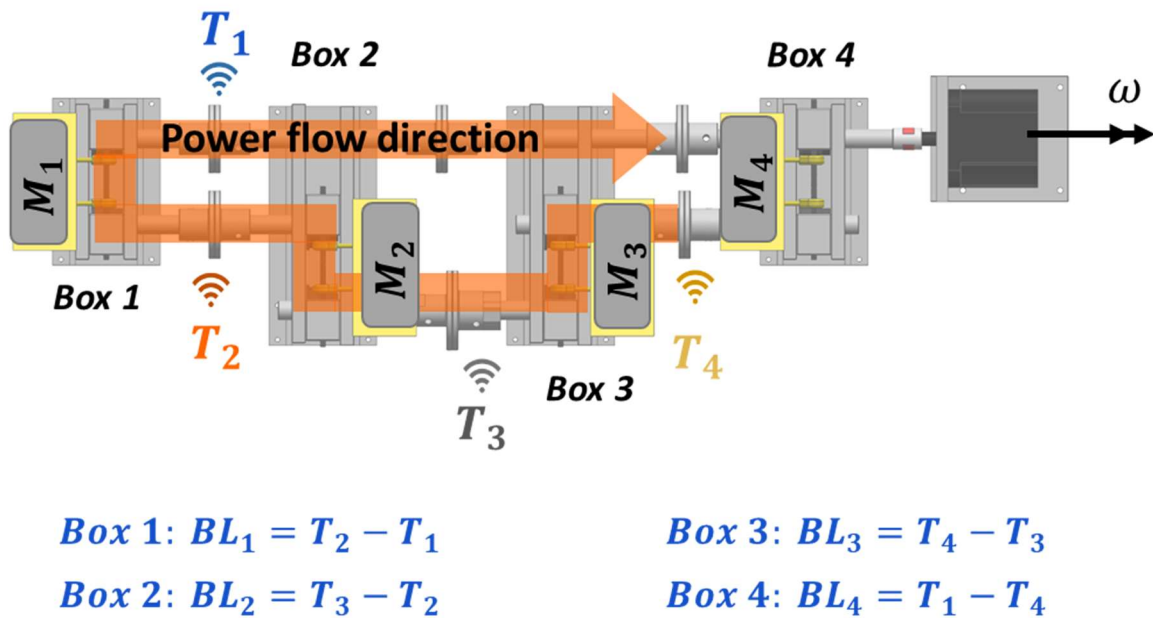
Figure 5.28: Power flow direction at PRILs

The second observation concerns the relation between the measured torques and the masses. It was observed that, when a power loss is introduced inside the power loop, there is an increase in the torques upstream of the point where the loss was added. This behavior can be seen quantitatively in Figure 5.29 and qualitatively in Figure 5.30. The color blue indicates that there is a positive relation with 95% confidence level between the measured torque and the application of the mass: if the mass is placed on the system, the torque increases. The color orange indicates that there is a negative relation, with 95% confidence level, between the mass and the measured torque. The color grey indicates that the relation cannot be defined as positive or negative with 95% confidence level.
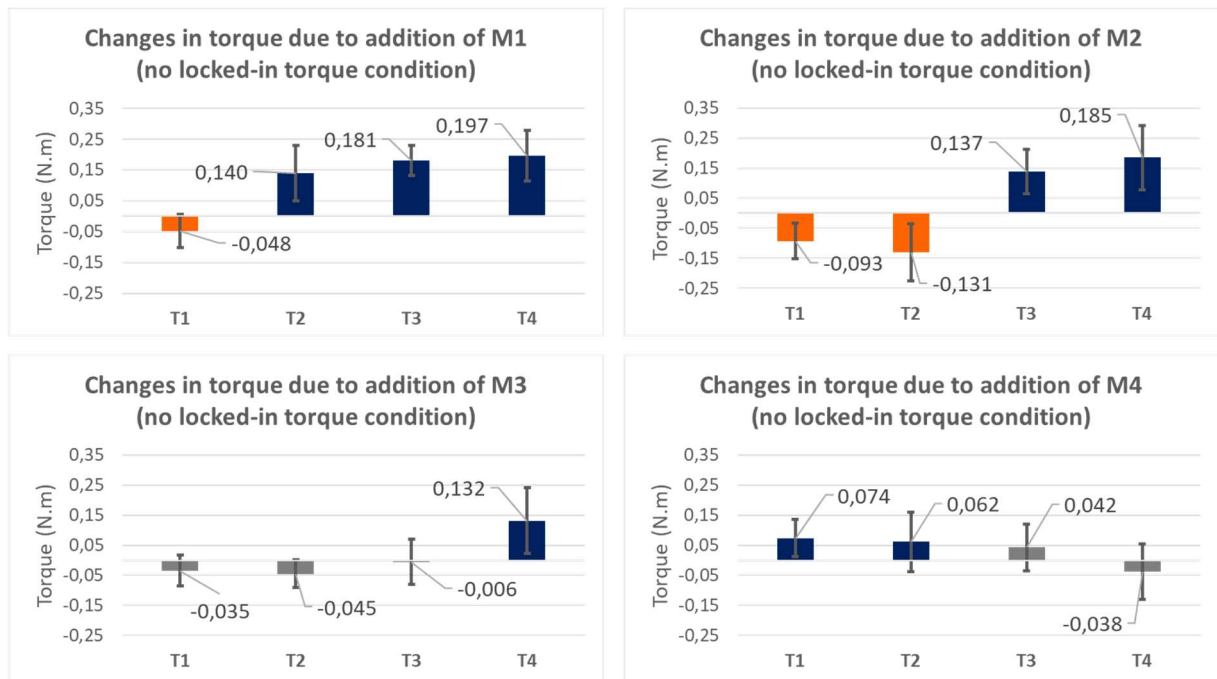
Figure 5.29: The average influences of each mass on the measured torques. The columns represent the average influence considering all the run combinations and the bars represent the standard deviation.
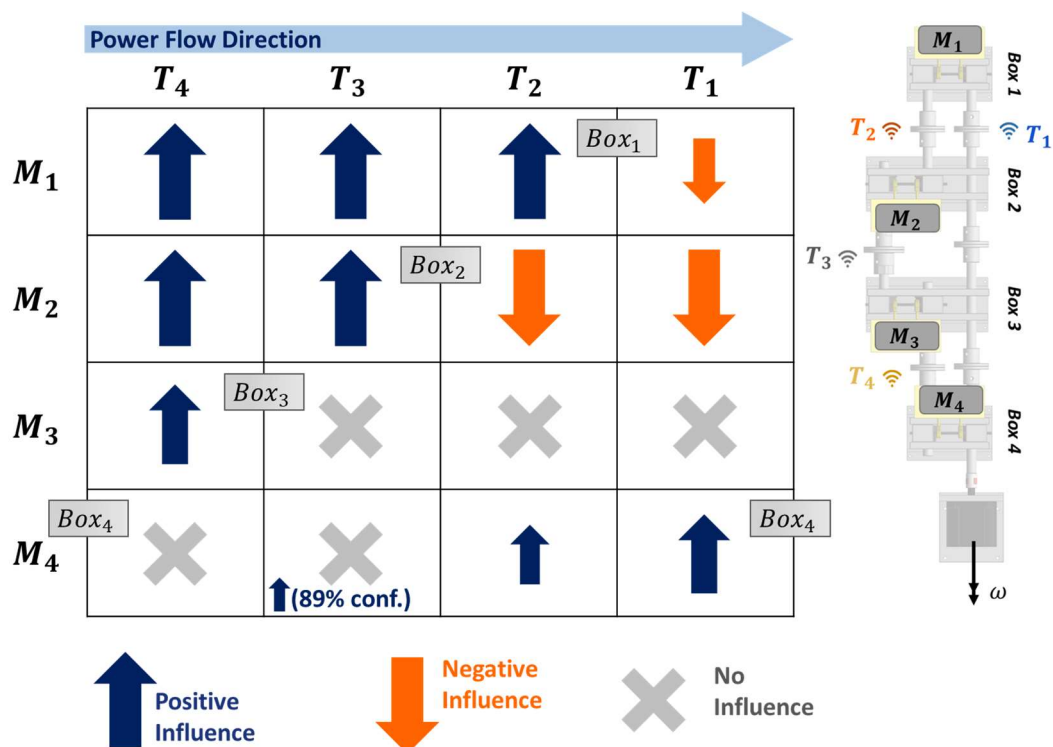
Figure 5.30: Summary of the average influence of the masses on the measured torques.

The motor supplies all the power loop losses (DOLESCHEL, 2002), thus, when an extra amount of power losses is introduced, the motor delivers more power. The motor control imposes a constant rotational speed, therefore, to increase the power delivered, it is necessary to increase the motor output torque. This effect will be herein called *upstream effect*.

The *upstream effect* is more evident the further the added loss is downstream. When M_1 is added to the system, the increase in T_4 is bigger than when M_2 is added, as can be seen in Figure 5.29. The same happens if one compares T_4 when M_2 is applied and T_4 when M_3 is applied.

This occurs because of the load-dependent losses (HÖHN et al., 2009) of the boxes upstream the induced loss. The load-dependent losses increase as the input torque increases, Thus, when more power is delivered by the motor, more power is lost at the shafts where the torque increased.

On the other hand, for a given mass position, the torques downstream decrease and it causes a decrease of load-dependent losses and, as a consequence, the total losses also decrease. Additionally, this effect is attenuated downstream. As each box decreases the torque available for the following box, the losses on successive boxes also decrease. The addition of M_1 increases T_4 by 0.197 N.m, T_3 by 0.181 N.m and T_2 by 0.140 N.m. It can be seen in Figure 5.29.

Any amount of energy loss added to the system demands an equal amount of extra energy from the motor. It was observed that when the loss point is near the power input, the extra power is supplied, and the rest of the loop is not affected. At PRILs, this behavior is observed up to measurement point T_3. When M_3 is placed on box 3, only T_4 increases, and the remaining torques are not affected.

However, when losses are applied further downstream, all transmission stages and components before the loss point are subjected to the torque increase, while torques after this point decrease. According to Höhn et al. (2009), at this condition, one would observe an increase in load-dependent losses with the torque increase, and the opposite behavior with torque decrease. A possible explanation for this fact is that the system converges to a state of minimum energy by balancing the increased losses upstream with decreasing losses downstream. Although, if the extra power loss is induced near the motor output, the extra power is delivered to that point and a smaller compensation between the power loss upstream and downstream is required. At this condition, the torques downstream should change less.

The observations lead to the hypothesis that a power-circulating test rig will have a point, here called *threshold point*, up to where all upstream added losses will not influence the efficiency downstream, considering the power flow direction. The best position to perform an efficiency test in such a rig will be in the box immediately after the *threshold point*, where the torque input is less sensitive, and, as a consequence, the power loss is less sensitive.

Further investigation must be done towards this hypothesis. It is suggested the study of the relation between the motor power output and the position where the same amount of loss is induced. For this purpose, it is necessary a power-circulating test rig with torque measuring points inside the power loop and a torque measuring point at the motor shaft, outside the power loop. Additionally, it is necessary to guarantee that the exact same amount of power loss be induced at different points. The absolute power loss can be measured by performing tests using an open power loop configuration, in order to avoid the interference of the closed power loop.

5.3.4 The influence of the locked-in torque

The influence of the induced losses in different positions of the power loop on the boxes belonging to the loop behavior was investigated in running conditions. Here, it will be presented the results from the experiments designed to study the mentioned behavior in condition of locked-in torque applied. The design of experiments is similar to the one used for the investigation with no locked-in torque: the 2^4 full factorial design. The order of the runs was different, since it was randomized again for this investigation.

There were considered four factors, which were the masses related to the induced losses, and there were eight responses analyzed: the torque on shafts and the torque loss on the boxes, as can be seen in Figure 5.31. The total of runs was $2^4 = 16$, accordingly to the number of factors and to the condition of none replicate.
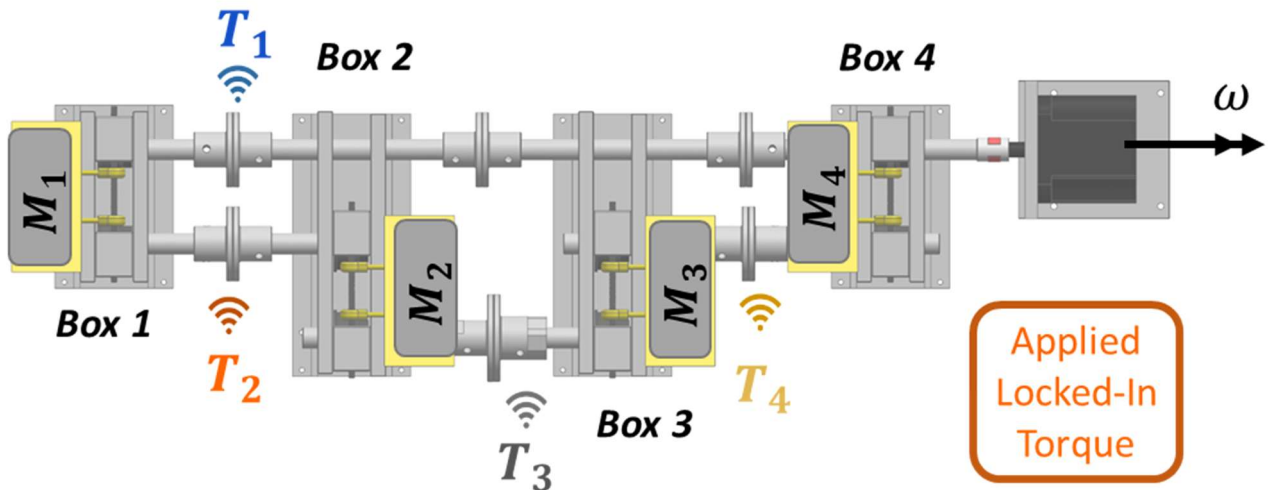
$$Box\ 1: BL_1 = T_2 - T_1 \qquad Box\ 3: BL_3 = T_4 - T_3$$
$$Box\ 2: BL_2 = T_3 - T_2 \qquad Box\ 4: BL_4 = T_1 - T_4$$

Figure 5.31: Factors masses and responses torques and torque losses of the designed experiment.

The locked-in torque introduced higher losses on the system. The lighter set of masses made of aluminum was used due to the limitation of the maximum power output of the electric motor. In order to keep the procedure step of setting to zero all the signals before each run, the loading locked-in torque process was monitored, from that data the locked-in torque was obtained, and this value was added to the torque measures for the statistical assessment. The measured locked-in torque was 5.2 N.m.

The results from 6-step ANOVA for the measured torques is shown in Appendix J and illustrated in and Figure 5.32. The results are very different from the ones obtained under no locked-in torque condition. Single factors present less significance, with the majority of the effects being distributed among higher order interactions.

When the model is refined, most of the significant interactions are deemed non-influential on the responses. This behavior was observed on all torques, for which the only significant interaction of the refined model was $M_1: M_3$, as shown in Figure 5.32.

The results from 6-step ANOVA for torque losses are shown below in Appendix K and illustrated in Figure 5.33.
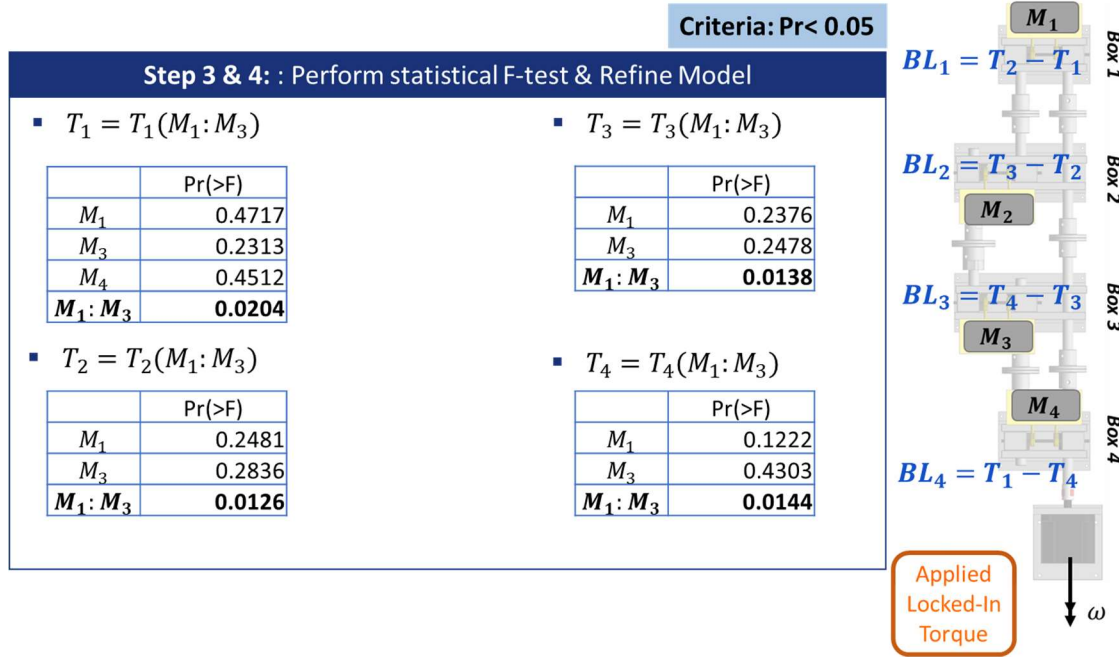
Figure 5.32: Refined models and results from F-test for the responses measured torque.

The effects are well distributed among several terms, including higher order interactions, as has been observed for the torque measurements. After refining the models, all the effect of single factors is diminished. BL_1 and BL_2 maintain dependence on $M_1:M_3$, while BL_3 and BL_4 do not depend on any factor or interaction with 95% confidence level, as summarized in Figure 5.33.
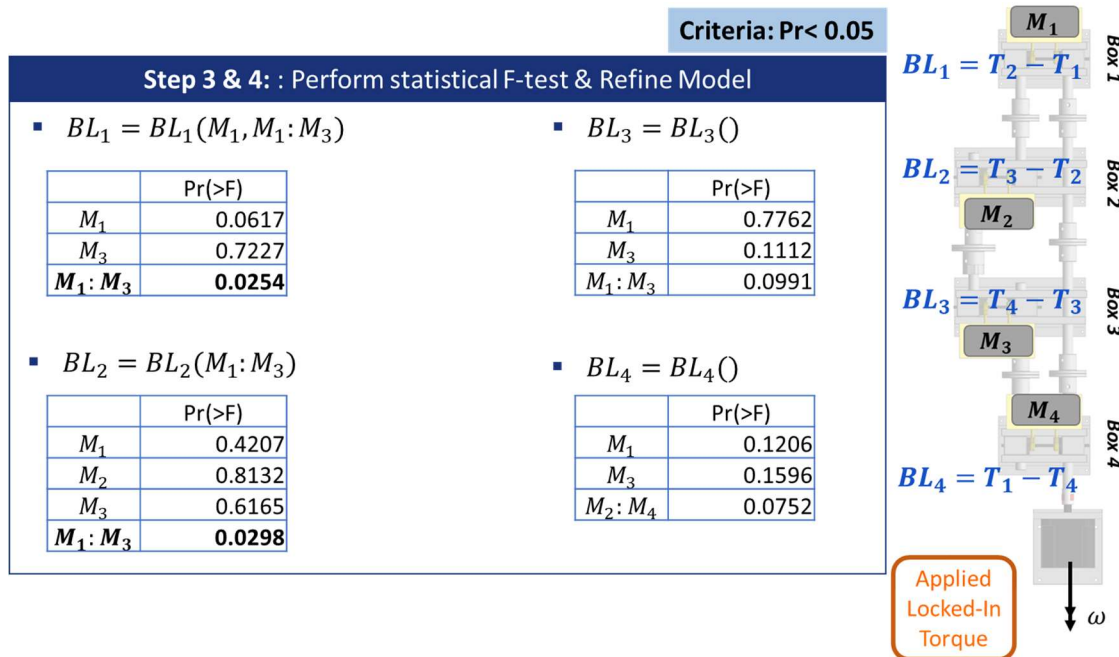
Figure 5.33: Refined models and results from F-test for the responses measured box losses.

Due to the inconclusive 6-step ANOVA, further verifications were done. A comparison of the losses due to the masses and the losses inherent to the system was done. The losses inherent to the system occurs singly when no mass is placed on PRILs: run 0000. The total losses due to the masses is the difference between the losses recorded during run 1111 (when all the masses are placed on PRILs) and the losses recorded during run 0000. According to BL_4 definition, it is already the power available to the other boxes. For this reason, the values of BL_4 were used for this analysis. These results are shown in Table 5.4 and in Figure 5.34.

Table 5.4: Losses inherent to the system and losses due the masses

	X0000		X1111	
	No locked-in torque	Applied locked-in torque	No locked-in torque	Applied locked-in torque
BL_4	-0.3400	-0.4575	-0.9830	-0.6299
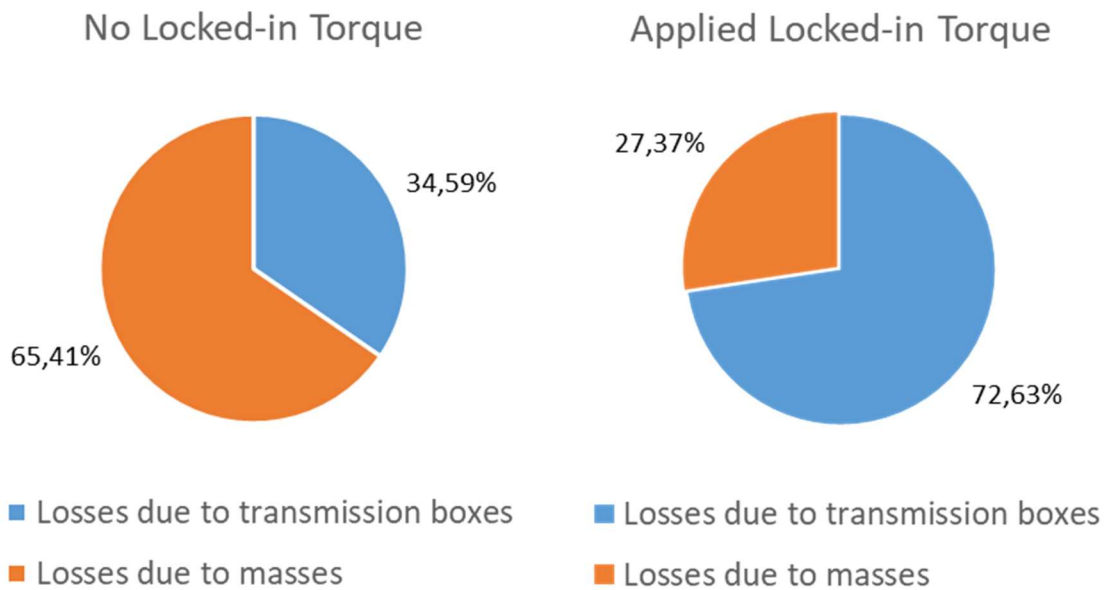
Figure 5.34: Losses distribution under different condition of locked-in torque.

It is possible to notice that the masses account for a much smaller fraction of the measured losses when the aluminum set is used, and the locked-in torque is applied. Therefore, the data acquired is not appropriate to investigate the effects of the masses under this condition with relation to the trade-off between the locked-in torque and the masses weights. Further

investigations of this conditions will require modification on PRILs: use of a more powerful motor and a heavier set of masses or modification of the coupling to apply less locked-in torque.
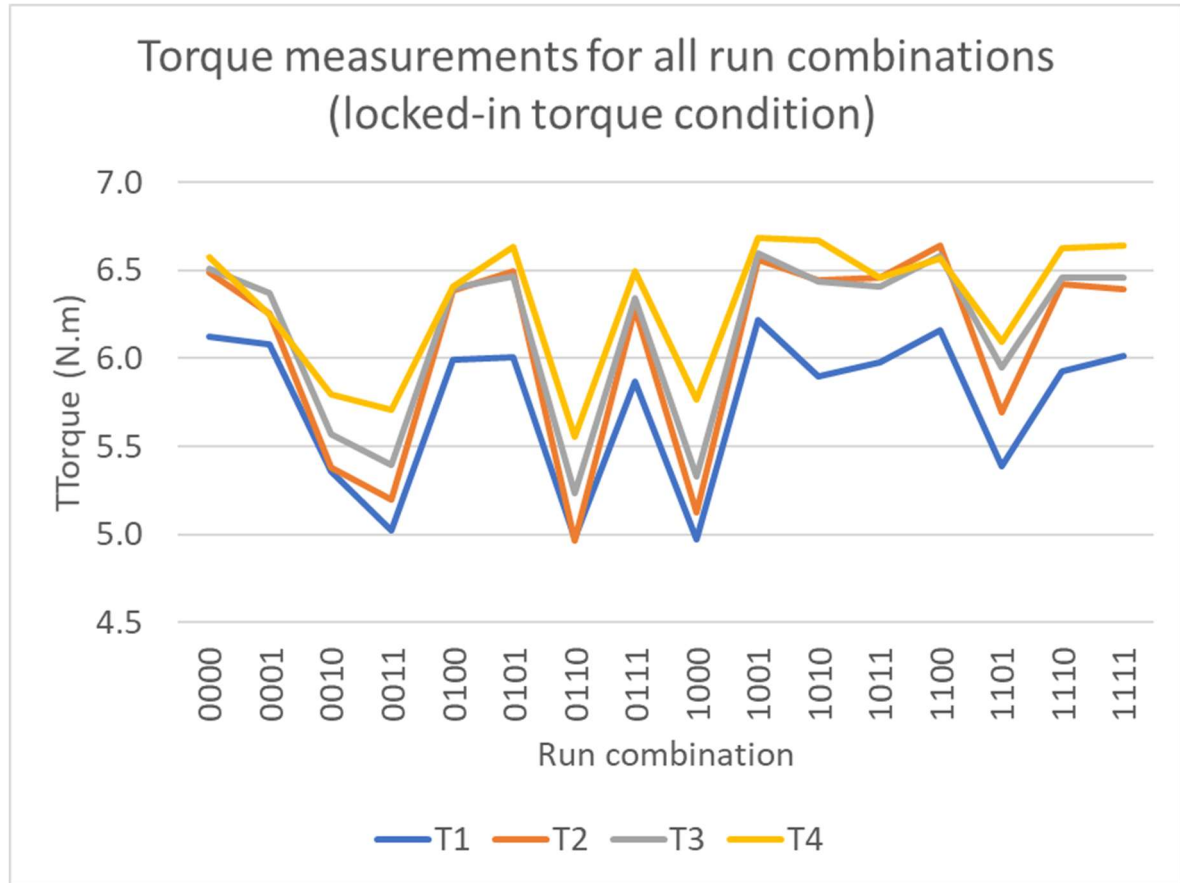
Figure 5.35: Measured torques under applied locked-in torque condition.

Despite the inconclusive results from 6-step ANOVA, for the majority of runs, the measured torques presented the same rank in their values: $T_1 < T_2 < T_3 < T_4$. The data can be seen in Figure 5.35. Since T_4 is always bigger than T_1, it indicates that the power input system is still the shaft where T_4 is measured and that This behavior was also observed for the tests with no locked-in torque (Figure 5.27) and indicates that the direction of the power flow is kept when the locked-in torque is applied.

6   Conclusion and Outlook

Gear power losses depends on five factors: lubricant, type of lubrication, speed, temperature and load. Traditional test rigs, which have two gear boxes, perform normalized tests, varying the cited factors. It is assumed that the boxes contribute equally to the total losses, which are measured at the output engine shaft, outside the power loop. In order to use these simplification, high level of symmetry between the boxes is required. When it is not possible to build or assembly the rig with the required level of symmetry or it is suspected that the difference of efficiency among the compared specimens is smaller than the error possibly coming from the assumption, it is necessary to assess torque efficiency more accurately.

The objective of this study is more reliable efficiency measurements at a power-circulating rig. In order to achieve this objective, it was necessary to develop a test procedure and execute an experimental investigation of the dynamic behavior of the power losses at a power-circulating test rig. The investigation was divided strategically into three research questions.

The first research question aimed the development of an experimental procedure to be used at PRILs, a four-box power-circulating rig conceived in a previous work. This test rig project simplifies the losses coming from factors related to lubricant, speed and temperature, in the form of induced friction losses. They can be independently induced on each separate box and there are four point of torque measurement inside the power loop. The development of the procedure aimed to promote reability of the tests by prescribing a proper test method. The proposed test method was based on experimental observation of PRILs mechanical and electronic operation and its limitations. The developed procedure prescribes how to start PRILs, how to set the acquisition system and how to execute the 60-second long runs.

The second research question investigate the behavior of box 1 under condition of no locked-in torque applied and a constant speed of 3 Hz. Since there is not much knowledge about this behavior, a 2^4 full factorial exploratory design of experiments was proposed. The four factors are the masses on each box. The responses are torques on the box 1's shafts and box 1's torque loss. The 6-step ANOVA analysis lead to the following conclusions:

- The torques (T_1 and T_2) depend on the mass applied on box 1 (M_1);
- The torques (T_1 and T_2) depend on masses applied on other boxes (M_2 and M_4);
- The torque loss (BL_1) depend on the mass applied on box 1 (M_1);

- The torque loss (BL_1) depend on masses applied on other boxes (M_2).

These conclusions are important for further investigation on gear load independent losses efficiency. The available power, related to the torque input, and the power losses on a given box are shown to depend on losses of other boxes. Although induced in a controlled fashion for this experiment, it has been shown that such differences also occur in existing systems due to assembly variations (ANDERSSON et al., 2014).

The third question proposed an overall observation of the dynamic behavior of the losses. Two conditions were tested: no locked-in torque applied and applied locked-in torque. The conclusion for the investigation under no locked-in torque are:

- The torques (T_3 and T_4) do not depend on the masses applied on boxes 3 and 4, respectively (M_3 and M_4);
- The torques (T_3 and T_4) depend on masses applied on other boxes (M_1 and M_2);
- The torque loss (BL_2) depends exclusively on the mass applied on box 2 (M_2);
- The torque loss (BL_3) depends on masses applied both on box 3 (M_3) and on other boxes (M_4).
- The torque loss (BL_4) depends on masses applied on all boxes (M_1, M_2, M_3 and M_4).
- The power flows first from T_4 to T_3, then to T_2 and T_1.

At PRILs, there are both a unique power flow direction and an optimal box of the power loop for efficiency studies under no locked-in torque condition. The optimal box is box 2, since it was showed with 95% confidence level that its torque loss depends only on the loss present on itself. Additionally, it was observed that when an extra loss is induced near the motor output, it is supplied by the motor and no relevant effect is observed downstream the point where the loss was induced, with relation to the power flow direction. However, when the extra loss is induced further downstream, the torque upstream that position increase, while the torques downstream decrease. Based on this observation, a hypothesis was proposed: there is an energy balance on the system between the increasing losses due to the increased torque upstream and the decreasing losses due to the decreased torques downstream.

Further investigation of this hypothesis requires the study of the relation between the power delivered by the motor and the position of the loss induction. Currently, the motor power is not measured at PRILs, thus, this future work will require the installation of a new torque measurement point, besides other experimental plan and previous investigations of the factors.

The investigation under applied locked-in torque condition was inconclusive according to 6-step ANOVA for a given 95% confidence level. The main reason that explains this behavior is the smaller contribution of the lighter set of masses to the total losses of the system. The most relevant conclusion of the investigation with applied locked-in torque is the rank of torques observed in the investigation under no locked-in torque condition was also observed under locked-in torque condition. Thus, at PRILs, there are a preferential way to flow the power through the system. Conditions not addressed by this study, and kept constant for this reason, may be responsible for stablishing the preferential power flow direction. As future works, the relation among the directions of locked-in torque, rotational speed and power flow be investigated.

Future works include further investigation on the condition of applied locked-in torque and verification of the hypothesis of energy balance at PRILs. It is expected that the conclusions presented for PRILs help achieve more accurate measurements of gear efficiency executed on other power-circulating test rigs. Therefore, future works also include the verification of the behaviors already observed at PRILs at other rigs, such as ITA test rig, and the application of the developed knowledge to other power-circulating test rigs.

References

ANDRADE, N. M. **Projeto de bancada de recirculação de potência análoga em escala reduzida para ensaio de eficiência de transmissões**. 2017. 60f. Trabalho de Conclusão de Curso (Graduação) - Instituto Tecnológico de Aeronáutica, São José dos Campos.

ANDERSSON, Martin et al. Effect of assembly errors in back-to-back gear efficiency testing. In: **International Gear Conference, August 26-28 2014, Lyon, France**. Woodhead Publishing Limited, 2014. p. 784-793.

BP LONDON. **BP Statistical Review of World Energy June 2016**. 2016.

CHANGENET, Christophe; VELEX, Philippe. Housing influence on churning losses in geared transmissions. **Journal of Mechanical Design**, v. 130, n. 6, p. 062603, 2008.

CHASE, D. R. **Development of an efficiency test methodology for high-speed gearboxes**. Tese de Doutorado. The Ohio State University, 2005.

CHIARA, Fabio; CANOVA, Marcello. A review of energy consumption, management, and recovery in automotive systems, with considerations of future trends. **Proceedings of the Institution of Mechanical Engineers, Part D: Journal of Automobile Engineering**, v. 227, n. 6, p. 914-936, 2013.

CONTI, J.; HOLTBERG, P.; DIEFENDERFER, J.; LAROSE, A.; TURNURE, J. T.; WESTFALL, L. **International energy outlook 2016 with projections to 2040**. USDOE Energy Information Administration (EIA), Washington, DC (United States). Office of Energy Analysis, 2016.

DALLY, James W.; RILEY, William F. Experimental stress analysis. 1965.

DAVIS, Joseph R. (Ed.). **Gear materials, properties, and manufacture**. ASM Internacional, 2005.

DOLESCHEL, A.; MICHAELIS, K.; HÖHN, B. R. **Method to determine the frictional behaviour of lubricants using a fzg gear test rig**. Forschungsvereinigung Antriebstechnik Frankfurt, FVA Information Sheet, v. 345, 2002.

DRESSELHAUS, M. S.; THOMAS, I. L. **Alternative energy technologies**. Nature, v. 414, n. 6861, p. 332, 2001.

EUROPEAN ENVIRONMENT AGENCY. **Europe's onshore and offshore wind energy potential**. 2009.

EUROPEAN PARLIAMENT AND THE COUNCIL OF THE EUROPEAN UNION. **Regulation (EC) No. 443/2009 of the European Parliament and of the Council of 23 April 2009, setting emission performance standards for new passenger cars as part of the community's integrated approach to reduce CO_2 emissions from light-duty vehicles.** Official Journal of the European Union, L Series., v. 140, 2009.

EUROPEAN PARLIAMENT**. Regulation (EU) No 333/2014 of the European Parliament and of the Council of 11 March 2014 amending Regulation (EC) No 443/2009 to define the modalities for reaching the 2020 target to reduce CO2 emissions from new passenger cars.** Official Journal of the European Union, L103/15, 2014.

HEADWATERS MB. **Gear suppliers need to diversify their application range as a hedge against exposure to cyclical end-markets**. Drive Technology - Gears, Sector Report, 2016.

HÖHN, B.; MICHAELIS, K.; HINTERSTOISSER, M. **Optimization of gearbox efficiency**. Goriva i maziva, Hrvatsko Drustvo za Goriva i Maziva (Croatian Society for Fuels and Lubricants), v. 48, n. 4, p. 462, 2009.

HÖHN, Bernd-Robert; MICHAELIS, Klaus; DOLESCHEL, Andreas. Limitations of bench testing for gear lubricants. In: **Bench Testing of Industrial Fluid Lubrication and Wear Properties Used in Machinery Applications**. ASTM International, 2001.

HÖHN, Bernd-Robert; MICHAELIS, Klaus; OTTO, Hans-Philipp. Flank load carrying capacity and power loss reduction by minimized lubrication. **Gear Technol., May**, p. 53-62, 2011.

ISO, DIN. 14635-1. FZG-Prüfverfahren A/8, 3/90 zur Bestimmung der relativen Fresstragfähigkeit von Schmierölen (ISO 14635-1: 2000), Deutsches Institut für Normung eV.

JOACHIM, Franz; KURZ, Norbert; GLATTHAAR, Bernhard. Influence of coatings and surface improvements on the lifetime of gears. **Gear Technology**, v. 21, n. 4, p. 50-56, 2004.

JUVINALL, R. C.; MARSHEK, K. M. **Fundamentals of machine component design**. J. Wiley, 1991.

LECHNER, G.; NAUNHEIMER, H. **Automotive transmissions**: fundamentals, selection, design and application. [S.l.]: Springer Science & Business Media, 1999.

LI, S., VAIDYANATHAN, A.; HARIANTO, J.; KAHRAMAN, A. **Influence of design parameters on mechanical power losses of helical gear pairs.** Journal of Advanced Mechanical Design, Systems, and Manufacturing, *3* (2), 146-158, 2009.

LI, Zhengminqing et al. Analytical impact of the sliding friction on mesh stiffness of spur gear drives based on Ishikawa model. **Vibroengineering Procedia**, v. 4, p. 29-33, 2014.

KLOCKE, Fritz; BRECHER, Christian. **Zahnrad-und Getriebetechnik: Auslegung– Herstellung–Untersuchung–Simulation**. Carl Hanser Verlag GmbH Co KG, 2016.

MAIA, André Hemerly et al. **A method for evaluating the dynamic behavior of a gear test rig**. SAE Technical Paper, 2014.

MARQUES, P. M.; FERNANDES, C. M.; MARTINS, R. C.; SEABRA, J. H. **Efficiency of a gearbox lubricated with wind turbine gear oils**. Tribology International, 71, 7-16, 2014.

MARTINS, R. et al. Friction coefficient in FZG gears lubricated with industrial gear oils: biodegradable ester vs. mineral oil. **Tribology international**, v. 39, n. 6, p. 512-521, 2006.

MENEGHETTI, G.; TERRIN, A.; GIACOMETTI, S. A twin disc test rig for contact fatigue characterization of gear materials. **Procedia Structural Integrity**, v. 2, p. 3185-3193, 2016.

MICHAELIS, Klaus; HÖHN, Bernd-Robert; OSTER, Peter. Influence of lubricant on gear failures—test methods and application to gearboxes in practice. **Tribotest**, v. 11, n. 1, p. 43-56, 2004.

MONTGOMERY, Douglas C. **Design and analysis of experiments**. Eighth edition. John Wiley & Sons, 2013.

PETRY-JOHNSON, Travis T. et al. An experimental investigation of spur gear efficiency. **Journal of Mechanical Design**, v. 130, n. 6, p. 062601, 2008.

SWART, R. J. et al. **Europe's onshore and offshore wind energy potential: An assessment of environmental and economic constraints**. European Environment Agency, 2009.

THIES, C.; KIECKHAEFER, K.; SPENGLER, T. S. **Market introduction strategies for alternative powertrains in long-range passenger cars under competition**. Transportation Research Part D: Transport and Environment, v. 45, p. 4-27, 2016.

XU, H. **Development of a generalized mechanical efficiency prediction methodology for gear pairs**. 2005. 258 p. Thesis (Mechanical Engineering) - The Ohio State University, Ohio.

WANG, C.; WANG, S.; WANG, G. **A method for calculating gear meshing efficiency by measured data from gear test machine**. Measurement, v. 119, p. 97-101, 2018.

WARD JR., W. C.; TIPTON, C. D.; MURRAY, K. A. **Lubrication fluids for reduced air entrainment and improved gear protection.** U.S. Patent n. 6,251,840, 26 jun. 2001.

ZHANG, X.; MA, C.; ZHAN, S.; CHEN, W. **Assessing powder emission risk on large open-air yard of coal energy**. V 11, p. 3047-3053, 01 2011.

ZHANG, X.; MYHRVOLD, N. P.; CALDEIRA, K. **Key factors for assessing climate benefits of natural gas versus coal electricity generation.** Environmental Research Letters, IOP Publishing, v. 9, n. 11, p. 114022, 2014.l: Phase transformations and mechanical properties. **Materials & Design**, v. 56, p. 258–263, 2014.

Appendix A - Script for the second research question in R language under no locked-in torque condition

```
##################Remover todos os objetos
rm(list=ls(all=TRUE))
#################Listar objetos
ls()

##################Ler Arquivo
arq = file.choose()
dados = read.table(arq,header=TRUE)

summary(dados)
attach(dados)

M1 = factor(M1)
M2 = factor(M2)
M3 = factor(M3)
M4 = factor(M4)

#Step 1 & 2 - T1
dados.anova = aov(T1 ~ M1*M2*M3*M4)
summary(dados.anova)

#Step 1 & 2 - T2
dados.anova = aov(T2 ~ M1*M2*M3*M4)
summary(dados.anova)

#Step 1 & 2 - BL1
dados.anova = aov(BL1 ~ M1*M2*M3*M4)
summary(dados.anova)

#Step 3 & 4 - T1
dados.anova = aov(T1 ~ M1*M2*M4)
summary(dados.anova)

#Gráficos para a analise dos residuos e normalidade
par(mfrow=c(2,1))
qqnorm(dados.anova$residuals)
qqline(dados.anova$residuals,col="red")
plot(dados.anova$residuals)
shapiro.test(dados.anova$residual)

   ##FINAL MODEL
dados.anova = aov(T1 ~ M1+M2+M4)
summary(dados.anova)

#Gráficos para a analise dos residuos e normalidade
par(mfrow=c(1,2))
qqnorm(dados.anova$residuals)
qqline(dados.anova$residuals,col="red")
plot(dados.anova$residuals)
shapiro.test(dados.anova$residual)

#Step 3 & 4 - T2
dados.anova = aov(T2 ~ M1*M2*M4)
```

```
summary(dados.anova)

par(mfrow=c(2,1))
qqnorm(dados.anova$residuals)
qqline(dados.anova$residuals,col="red")
plot(dados.anova$residuals)
shapiro.test(dados.anova$residual)

##FINAL MODEL
dados.anova = aov(T2 ~ M1+M2+M4+M1:M2:M4)
summary(dados.anova)

par(mfrow=c(1,2))
qqnorm(dados.anova$residuals)
qqline(dados.anova$residuals,col="red")
plot(dados.anova$residuals)
shapiro.test(dados.anova$residual)


#Step 3 & 4 - BL1
dados.anova = aov(BL1 ~ M1*M2)
summary(dados.anova)

par(mfrow=c(2,1))
qqnorm(dados.anova$residuals)
qqline(dados.anova$residuals,col="red")
plot(dados.anova$residuals)
shapiro.test(dados.anova$residual)

dados.anova = aov(BL1 ~ M1+M2)
summary(dados.anova)

par(mfrow=c(2,1))
qqnorm(dados.anova$residuals)
qqline(dados.anova$residuals,col="red")
plot(dados.anova$residuals)
shapiro.test(dados.anova$residual)

##FINAL MODEL

dados.anova = aov(BL1 ~ M1*M2)
summary(dados.anova)

par(mfrow=c(1,2))
qqnorm(dados.anova$residuals)
qqline(dados.anova$residuals,col="red")
plot(dados.anova$residuals)
shapiro.test(dados.anova$residual)


###########################################################
```

Appendix B - Script for the third research question in R language under no locked-in torque condition

```
##################Remover todos os objetos
rm(list=ls(all=TRUE))
##################Listar objetos
ls()

#################Ler Arquivo
arq = file.choose()
dados = read.table(arq,header=TRUE)

summary(dados)
attach(dados)

M1 = factor(M1)
M2 = factor(M2)
M3 = factor(M3)
M4 = factor(M4)

#ANOVA Reduzida

#Step 1 & 2 - T3
dados.anova = aov(T3 ~ M1*M2*M3*M4)
summary(dados.anova)

#Step 1 & 2 - T4
dados.anova = aov(T4 ~ M1*M2*M3*M4)
summary(dados.anova)

#Step 3 & 4 - T3
dados.anova = aov(T3 ~ M1*M2*M4)
summary(dados.anova)

#Gráficos para a analise dos residuos e normalidade
par(mfrow=c(1,2))
qqnorm(dados.anova$residuals)
qqline(dados.anova$residuals,col="red")
plot(dados.anova$residuals)
shapiro.test(dados.anova$residual)


##FINAL MODEL
dados.anova = aov(T3 ~ M1*M2)
summary(dados.anova)

#Gráficos para a analise dos residuos e normalidade
par(mfrow=c(1,2))
qqnorm(dados.anova$residuals)
qqline(dados.anova$residuals,col="red")
plot(dados.anova$residuals)
shapiro.test(dados.anova$residual)
```

```
#Step 3 & 4 - T4
dados.anova = aov(T4 ~ M1*M2*M3)
summary(dados.anova)

#Gráficos para a analise dos residuos e normalidade
par(mfrow=c(1,2))
qqnorm(dados.anova$residuals)
qqline(dados.anova$residuals,col="red")
plot(dados.anova$residuals)
shapiro.test(dados.anova$residual)

##FINAL MODEL
dados.anova = aov(T4 ~ M1+M2+M3)
summary(dados.anova)

par(mfrow=c(1,2))
qqnorm(dados.anova$residuals)
qqline(dados.anova$residuals,col="red")
plot(dados.anova$residuals)
shapiro.test(dados.anova$residual)


#Step 1 & 2 - BL2
dados.anova = aov(BL2 ~ M1*M2*M3*M4)
summary(dados.anova)

#Step 1 & 2 - BL3
dados.anova = aov(BL3 ~ M1*M2*M3*M4)
summary(dados.anova)

#Step 1 & 2 - BL4
dados.anova = aov(BL4 ~ M1*M2*M3*M4)
summary(dados.anova)

#Step 3 & 4 - BL2
dados.anova = aov(BL2 ~ M1*M2*M3)
summary(dados.anova)

par(mfrow=c(2,1))
qqnorm(dados.anova$residuals)
qqline(dados.anova$residuals,col="red")
plot(dados.anova$residuals)
shapiro.test(dados.anova$residual)

##FINAL MODEL
dados.anova = aov(BL2 ~ M2)
summary(dados.anova)

par(mfrow=c(1,2))
qqnorm(dados.anova$residuals)
qqline(dados.anova$residuals,col="red")
plot(dados.anova$residuals)
shapiro.test(dados.anova$residual)

#Step 3 & 4 - BL3
dados.anova = aov(BL3 ~ M3*M2*M4)
summary(dados.anova)
```

```
par(mfrow=c(2,1))
qqnorm(dados.anova$residuals)
qqline(dados.anova$residuals,col="red")
plot(dados.anova$residuals)
shapiro.test(dados.anova$residual)

##FINAL MODEL
dados.anova = aov(BL3 ~ M3+M4)
summary(dados.anova)

par(mfrow=c(1,2))
qqnorm(dados.anova$residuals)
qqline(dados.anova$residuals,col="red")
plot(dados.anova$residuals)
shapiro.test(dados.anova$residual)

#Step 3 & 4 - BL4
dados.anova = aov(BL4 ~ M1+M2+M4+M3+M2:M3)
summary(dados.anova)

par(mfrow=c(2,1))
qqnorm(dados.anova$residuals)
qqline(dados.anova$residuals,col="red")
plot(dados.anova$residuals)
shapiro.test(dados.anova$residual)

##FINAL MODEL
dados.anova = aov(BL4 ~ M1+M2+M3+M4)
summary(dados.anova)

par(mfrow=c(1,2))
qqnorm(dados.anova$residuals)
qqline(dados.anova$residuals,col="red")
plot(dados.anova$residuals)
shapiro.test(dados.anova$residual)


###############################################################
```

Appendix C - Script for the third research question in R language under applied locked-in torque condition

```
##################Remover todos os objetos
rm(list=ls(all=TRUE))
##################Listar objetos
ls()

##################Ler Arquivo
arq = file.choose()
dados = read.table(arq,header=TRUE)

summary(dados)
attach(dados)

M1 = factor(M1)
M2 = factor(M2)
M3 = factor(M3)
M4 = factor(M4)

#ANOVA Reduzida

#Step 1 & 2 - T1
dados.anova = aov(T1 ~ M1*M2*M3*M4)
summary(dados.anova)

#Step 1 & 2 - T2
dados.anova = aov(T2 ~ M1*M2*M3*M4)
summary(dados.anova)

#Step 1 & 2 - T3
dados.anova = aov(T3 ~ M1*M2*M3*M4)
summary(dados.anova)

#Step 1 & 2 - T4
dados.anova = aov(T4 ~ M1*M2*M3*M4)
summary(dados.anova)

#Step 1 & 2 - BL1
dados.anova = aov(BL1 ~ M1*M2*M3*M4)
summary(dados.anova)

#Step 1 & 2 - BL2
dados.anova = aov(BL2 ~ M1*M2*M3*M4)
summary(dados.anova)

#Step 1 & 2 - BL3
dados.anova = aov(BL3 ~ M1*M2*M3*M4)
summary(dados.anova)

#Step 1 & 2 - BL4
dados.anova = aov(BL4 ~ M1*M2*M3*M4)
summary(dados.anova)
```

```
#Step 3 & 4 - T1
dados.anova = aov(T1 ~ M1:M3+M2:M3:M4+M1:M3:M4)
summary(dados.anova)

#Gráficos para a analise dos residuos e normalidade
par(mfrow=c(1,2))
qqnorm(dados.anova$residuals)
qqline(dados.anova$residuals,col="red")
plot(dados.anova$residuals)
shapiro.test(dados.anova$residual)

dados.anova = aov(T1 ~ M1:M3+M1+M3+M4)
summary(dados.anova)

#Gráficos para a analise dos residuos e normalidade
par(mfrow=c(1,2))
qqnorm(dados.anova$residuals)
qqline(dados.anova$residuals,col="red")
plot(dados.anova$residuals)
shapiro.test(dados.anova$residual)

#Step 3 & 4 - T2

dados.anova = aov(T2 ~ M1:M3+M2:M3:M4+M1:M3:M4)
summary(dados.anova)

#Gráficos para a analise dos residuos e normalidade
par(mfrow=c(1,2))
qqnorm(dados.anova$residuals)
qqline(dados.anova$residuals,col="red")
plot(dados.anova$residuals)
shapiro.test(dados.anova$residual)

##FINAL

dados.anova = aov(T2 ~ M1+M3+M1:M3)
summary(dados.anova)

#Gráficos para a analise dos residuos e normalidade
par(mfrow=c(1,2))
qqnorm(dados.anova$residuals)
qqline(dados.anova$residuals,col="red")
plot(dados.anova$residuals)
shapiro.test(dados.anova$residual)

#Step 3 & 4 - T3

dados.anova = aov(T3 ~ M1:M3+M2:M3:M4+M1:M3:M4)
summary(dados.anova)

#Gráficos para a analise dos residuos e normalidade
par(mfrow=c(1,2))
qqnorm(dados.anova$residuals)
qqline(dados.anova$residuals,col="red")
plot(dados.anova$residuals)
shapiro.test(dados.anova$residual)
```

```
###FINAL

dados.anova = aov(T3 ~ M1+M3+M1:M3)
summary(dados.anova)

par(mfrow=c(1,2))
qqnorm(dados.anova$residuals)
qqline(dados.anova$residuals,col="red")
plot(dados.anova$residuals)
shapiro.test(dados.anova$residual)

#Step 3 & 4 - T4

dados.anova = aov(T4 ~ M1:M3+M2:M3:M4+M1:M3:M4)
summary(dados.anova)

#Gráficos para a analise dos residuos e normalidade
par(mfrow=c(1,2))
qqnorm(dados.anova$residuals)
qqline(dados.anova$residuals,col="red")
plot(dados.anova$residuals)
shapiro.test(dados.anova$residual)

###FINAL
dados.anova = aov(T4 ~ M1+M2+M3+M1:M3)
summary(dados.anova)

par(mfrow=c(1,2))
qqnorm(dados.anova$residuals)
qqline(dados.anova$residuals,col="red")
plot(dados.anova$residuals)
shapiro.test(dados.anova$residual)

#Step 3 & 4 - BL1
dados.anova = aov(BL1 ~ M1*M2+M1:M3)
summary(dados.anova)

par(mfrow=c(1,2))
qqnorm(dados.anova$residuals)
qqline(dados.anova$residuals,col="red")
plot(dados.anova$residuals)
shapiro.test(dados.anova$residual)

#Step 3 & 4 - BL2
dados.anova = aov(BL2 ~ M2+M1)
summary(dados.anova)

par(mfrow=c(1,2))
qqnorm(dados.anova$residuals)
qqline(dados.anova$residuals,col="red")
plot(dados.anova$residuals)
shapiro.test(dados.anova$residual)

##FINAL MODEL
dados.anova = aov(BL2 ~ M2)
summary(dados.anova)

par(mfrow=c(1,2))
```

```
qqnorm(dados.anova$residuals)
qqline(dados.anova$residuals,col="red")
plot(dados.anova$residuals)
shapiro.test(dados.anova$residual)

#Step 3 & 4 - BL3
dados.anova = aov(BL3 ~ M3+M4)
summary(dados.anova)

par(mfrow=c(1,2))
qqnorm(dados.anova$residuals)
qqline(dados.anova$residuals,col="red")
plot(dados.anova$residuals)
shapiro.test(dados.anova$residual)

#Step 3 & 4 - BL4
dados.anova = aov(BL4 ~ M1+M2+M4+M3)
summary(dados.anova)

par(mfrow=c(1,2))
qqnorm(dados.anova$residuals)
qqline(dados.anova$residuals,col="red")
plot(dados.anova$residuals)
shapiro.test(dados.anova$residual)

############################################################
```

Appendix D - Test form

Date:					
Operator:					
	Start	**Finish:**			
Time:					
Room Temp. (°C):					
Test ID Number/:					
Objective:					

DIAMETER & BATTERY VOLTAGE MEASUREMENTS

Measument equipment		Beginning Diameter 1 @Sc(mm)	Beginning Diameter 2 (mm)	Final Diameter 1 @Sc(mm)	Final Diameter 2 (mm)	Battery Nº	Beginning Battery Voltage (V)	Final Battery Voltage (V)
[mm]	Calliper							
[V]	Voltmeter							
Position 1								
Position 2								
Position 3				-		-	-	
Position 4								
Position 5				-		-	-	
Position 6				-		-	-	
Position 7				-		-	-	
Position 8								

TEST TABLE

Run	Torque	M1	M2	M3	M4	Check
1	0	2	0	0	0	
2	0	2	0	0	0	
3						

Appendix E - Procedure to start PRILs in portuguese

```
Inicialização de Ensaio:

Abrir e iniciar Programa Principal (State Machine)

Verificar se o motor energizado

Conectar Baterias

Resetar Placas = Desligar e Ligar Chave 1

Certifique que a chave 6 está ligada

Rotacionar eixos manualmente para verificar interferêcias
mecânicas

Conectar Arduino+Xbee ao PC, verificar o reconhecimento da porta
COM

Iniciar Conexão

Alterar para aba "Page 2"

Atualizar nome do arquivo nos quais serão salvo os dados

Iniciar log de dados, se desejado

Rotacionar para acomadação elástica

Iniciar o offset dos sensores

Aplicar o torque desejado

Ajustar velocidade do motor

Iniciar o motor
-------------------------------------------------------------
---
Finalização de Ensaio:

Parar Motor

Aliviar torque

Parar o log de dados

Pasta com os dados: C:\Data

Fechar Conexeção

Parar o programa
```

Appendix F - Estimation of effects for responses T_1, T_2 and BL_1 under no locked-in torque condition

Table F.1: Estimation of factors effects (Step 1) for response T_1

	Degree of Freedom	Sum Square (SS)	E	$E_{Cumulative}$
M1	**1**	**0.00922**	**0.106001**	**0.106001**
M2	**1**	**0.03459**	**0.397678**	**0.503679**
M3	1	0.00478	0.054955	0.558634
M4	**1**	**0.02174**	**0.249943**	**0.808577**
M1:M2	1	0.00067	0.007703	0.81628
M1:M3	1	0.00161	0.01851	0.83479
M2:M3	1	0.00099	0.011382	0.846172
M1:M4	1	0.0002	0.002299	0.848471
M2:M4	1	0.00366	0.042079	0.89055
M3:M4	1	0.00143	0.016441	0.90699
M1:M2:M3	1	0.00042	0.004829	0.911819
M1:M2:M4	1	0.00301	0.034606	0.946424
M1:M3:M4	1	0.00118	0.013566	0.959991
M2:M3:M4	1	0.00002	0.00023	0.960221
M1:M2:M3:M4	1	0.00346	0.039779	1
SS_T		0.08698		

Table F.2: Estimation of factors effects (Step 1) for response T_2

	Degree of Freedom	Sum Square (SS)	E	$E_{Cumulative}$
M1	**1**	**0.07815**	**0.378615**	**0.378615**
M2	**1**	**0.06906**	**0.334577**	**0.713192**
M3	1	0.0081	0.039242	0.752434
M4	**1**	**0.01522**	**0.073737**	**0.826171**
M1:M2	1	0.00003	0.000145	0.826317
M1:M3	1	0.00112	0.005426	0.831743
M2:M3	1	0.00001	4.84E-05	0.831791
M1:M4	1	0.00073	0.003537	0.835328
M2:M4	1	0.00725	0.035124	0.870452
M3:M4	1	0	0	0.870452
M1:M2:M3	1	0.00033	0.001599	0.872051
M1:M2:M4	1	0.02052	0.099414	0.971465
M1:M3:M4	1	0.00236	0.011434	0.982898
M2:M3:M4	1	0.00006	0.000291	0.983189
M1:M2:M3:M4	1	0.00347	0.016811	1
SS_T		0.20641		

Table F.3: Estimation of factors effects (Step 1) for response BL_1

	Degree of Freedom	Sum Square (SS)	E	$E_{Cumulative}$
M1	**1**	**0.14106**	**0.876312**	**0.876312**
M2	**1**	**0.0059**	**0.036653**	**0.912965**
M3	1	0.00043	0.002671	0.915636
M4	1	0.00058	0.003603	0.91924
M1:M2	1	0.00043	0.002671	0.921911
M1:M3	1	0.00004	0.000248	0.922159
M2:M3	1	0.00078	0.004846	0.927005
M1:M4	1	0.00169	0.010499	0.937504
M2:M4	1	0.00061	0.00379	0.941293
M3:M4	1	0.00141	0.008759	0.950053
M1:M2:M3	1	0.00001	6.21E-05	0.950115
M1:M2:M4	1	0.00782	0.04858	0.998695
M1:M3:M4	1	0.0002	0.001242	0.999938
M2:M3:M4	1	0.00001	6.21E-05	1
M1:M2:M3:M4	1	0	0	1
SS_T		0.16097		

Appendix G - Estimation of effects for responses T_3 and T_4 under no locked-in torque condition

Table G.1: Estimation of factors effects (Step 1) for response T_3

	Degree of Freedom	Sum Square (SS)	E	$E_{Cumulative}$
M1	**1**	**0.13131**	**0.550843**	**0.550843**
M2	**1**	**0.07505**	**0.314833**	**0.865677**
M3	1	0.00012	0.000503	0.86618
M4	**1**	**0.00715**	**0.029994**	**0.896174**
M1:M2	1	0.00007	0.000294	0.896468
M1:M3	1	0.0001	0.000419	0.896887
M2:M3	1	0.00313	0.01313	0.910018
M1:M4	1	0.00043	0.001804	0.911821
M2:M4	1	0.00378	0.015857	0.927678
M3:M4	1	0.00058	0.002433	0.930112
M1:M2:M3	1	0.00069	0.002895	0.933006
M1:M2:M4	1	0.00039	0.001636	0.934642
M1:M3:M4	1	0.00461	0.019339	0.953981
M2:M3:M4	1	0.00889	0.037293	0.991274
M1:M2:M3:M4	1	0.00208	0.008726	1
SS_T		0.23838		

Table G.2: Estimation of factors effects (Step 1) for response T_4

	Degree of Freedom	Sum Square (SS)	E	$E_{Cumulative}$
M1	**1**	**0.15465**	**0.370694**	**0.370694**
M2	**1**	**0.13671**	**0.327692**	**0.698387**
M3	**1**	**0.06919**	**0.165848**	**0.864235**
M4	1	0.00576	0.013807	0.878041
M1:M2	1	0.00038	0.000911	0.878952
M1:M3	1	0.00072	0.001726	0.880678
M2:M3	1	0.0142	0.034037	0.914715
M1:M4	1	0.00219	0.005249	0.919965
M2:M4	1	0	0	0.919965
M3:M4	1	0.00499	0.011961	0.931926
M1:M2:M3	1	0.00634	0.015197	0.947122
M1:M2:M4	1	0.0062	0.014861	0.961984
M1:M3:M4	1	0.00333	0.007982	0.969966
M2:M3:M4	1	0.00845	0.020255	0.99022

M1:M2:M3:M4	1	0.00408	0.00978	1
SS_T		0.41719		

Appendix I - Estimation of effects for responses BL_2, BL_3 and BL_4 under no locked-in torque condition

Table I.1: Estimation of effects for BL_2.

	Degree of Freedom	Sum Square (SS)	E	$E_{Cumulative}$
M1	**1**	**0.00686**	**0.019944**	**0.019944**
M2	**1**	**0.28811**	**0.837602**	**0.857546**
M3	1	0.00622	0.018083	0.875629
M4	1	0.00151	0.00439	0.880019
M1:M2	1	0.00001	2.91E-05	0.880048
M1:M3	1	0.00054	0.00157	0.881618
M2:M3	1	0.00353	0.010263	0.89188
M1:M4	1	0.00004	0.000116	0.891996
M2:M4	1	0.00056	0.001628	0.893624
M3:M4	1	0.0006	0.001744	0.895369
M1:M2:M3	1	0.00197	0.005727	0.901096
M1:M2:M4	1	0.01525	0.044335	0.945431
M1:M3:M4	1	0.00038	0.001105	0.946536
M2:M3:M4	1	0.00747	0.021717	0.968253
M1:M2:M3:M4	1	0.01092	0.031747	1
SS_T		0.34397		

Table I.2: Estimation of effects for BL_3.

	Degree of Freedom	Sum Square (SS)	E	$E_{Cumulative}$
M1	1	0.00095	0.006759	0.006759
M2	**1**	**0.00917**	**0.065244**	**0.072003**
M3	**1**	**0.07519**	**0.53497**	**0.606973**
M4	**1**	**0.02575**	**0.183209**	**0.790181**
M1:M2	1	0.00079	0.005621	0.795802
M1:M3	1	0.00137	0.009747	0.80555
M2:M3	1	0.004	0.02846	0.834009
M1:M4	1	0.00456	0.032444	0.866453
M2:M4	1	0.0036	0.025614	0.892067
M3:M4	1	0.00217	0.015439	0.907506
M1:M2:M3	1	0.00285	0.020277	0.927784
M1:M2:M4	1	0.00971	0.069086	0.996869
M1:M3:M4	1	0.0001	0.000711	0.997581
M2:M3:M4	1	0.00001	7.11E-05	0.997652

M1:M2:M3:M4	1	0.00033	0.002348	1
SS$_T$		0.14055		

Table I.3: Estimation of effects for BL$_4$.

	Degree of Freedom	Sum Square (SS)	E	E$_{Cumulative}$
M1	**1**	**0.23941**	**0.297356**	**0.297356**
M2	**1**	**0.30883**	**0.383578**	**0.680934**
M3	**1**	**0.11036**	**0.137071**	**0.818005**
M4	**1**	**0.04989**	**0.061965**	**0.87997**
M1:M2	1	0.00205	0.002546	0.882516
M1:M3	1	0.00449	0.005577	0.888093
M2:M3	1	0.02268	0.028169	0.916262
M1:M4	1	0.00107	0.001329	0.917591
M2:M4	1	0.00349	0.004335	0.921926
M3:M4	1	0.01177	0.014619	0.936544
M1:M2:M3	1	0.01004	0.01247	0.949014
M1:M2:M4	1	0.01785	0.02217	0.971185
M1:M3:M4	1	0.00055	0.000683	0.971868
M2:M3:M4	1	0.00759	0.009427	0.981295
M1:M2:M3:M4	1	0.01506	0.018705	1
SS$_T$		0.80513		

Appendix J - Estimation of effects for responses T_1, T_2, T_3 and T_4 under applied locked-in torque condition

Table J.1: Estimation of factors effects (Step 1) for response T_1

	Degree of Freedom	Sum Square (SS)	E	$E_{Cumulative}$
M1:M3	1	1.0293	0.347255	0.347255491
M1:M2:M4	1	0.6805	0.229581	0.576836139
M2:M3:M4	1	0.6331	0.213589	0.790425424
M3	1	0.2255	0.076077	0.86650248
M4	1	0.0857	0.028913	0.895415134
M1	1	0.078	0.026315	0.921730036
M1:M2:M3	1	0.0577	0.019466	0.941196316
M1:M3:M4	1	0.0489	0.016497	0.957693735
M1:M2:M3:M4	1	0.0462	0.015587	0.973280254
M2:M4	1	0.0335	0.011302	0.984582167
M2	1	0.03	0.010121	0.994703283
M2:M3	1	0.0087	0.002935	0.997638406
M3:M4	1	0.0046	0.001552	0.999190311
M1:M2	1	0.0016	0.00054	0.999730104
M1:M4	1	0.0008	0.00027	1
SS_T		2.9641		

Table J.2: Estimation of factors effects (Step 1) for response T_2

	Degree of Freedom	Sum Square (SS)	E	$E_{Cumulative}$
M1:M3	1	1.8842	0.368173	0.368173
M1:M2:M4	1	1.149	0.224515	0.592688
M2:M3:M4	1	0.7624	0.148973	0.741661
M1	1	0.3234	0.063192	0.804854
M3	1	0.2766	0.054048	0.858901
M1:M3:M4	1	0.1954	0.038181	0.897083
M4	1	0.1384	0.027043	0.924126
M2	1	0.118	0.023057	0.947183
M1:M2:M3	1	0.1001	0.01956	0.966743
M1:M2:M3:M4	1	0.0891	0.01741	0.984153
M3:M4	1	0.035	0.006839	0.990992

M2:M4	1	0.0216	0.004221	0.995213
M1:M4	1	0.0182	0.003556	0.998769
M1:M2	1	0.0041	0.000801	0.99957
M2:M3	1	0.0022	0.00043	1
SS$_T$		5.1177		

Table J.31: Estimation of factors effects (Step 1) for response T$_3$

	Degree of Freedom	Sum Square (SS)	E	E$_{Cumulative}$
M1:M3	1	1.2689	0.355873	0.355873
M1:M2:M4	1	0.7049	0.197695	0.553567
M2:M3:M4	1	0.5676	0.159188	0.712755
M1	1	0.2363	0.066272	0.779027
M3	1	0.2256	0.063271	0.842299
M1:M3:M4	1	0.1727	0.048435	0.890734
M4	1	0.1344	0.037694	0.928427
M2	1	0.1022	0.028663	0.95709
M1:M2:M3	1	0.0842	0.023615	0.980705
M1:M2:M3:M4	1	0.047	0.013182	0.993886
M2:M4	1	0.0098	0.002748	0.996635
M3:M4	1	0.0067	0.001879	0.998514
M1:M4	1	0.0042	0.001178	0.999691
M2:M3	1	0.0006	0.000168	0.99986
M1:M2	1	0.0005	0.00014	1
SS$_T$		3.5656		

Table J.4: Estimation of factors effects (Step 1) for response T$_4$

	Degree of Freedom	Sum Square (SS)	E	E$_{Cumulative}$
M1:M3	1	0.809	0.3464	0.34636297
M1:M2:M4	1	0.4784	0.2048	0.5511838
M2:M3:M4	1	0.2738	0.1172	0.66840776
M1	1	0.2736	0.1171	0.78554609
M1:M3:M4	1	0.1591	0.0681	0.85366271
M1:M2:M3:M4	1	0.0803	0.0344	0.88804213
M2	1	0.0769	0.0329	0.92096588
M3	1	0.0659	0.0282	0.94918012
M4	1	0.0612	0.0262	0.97538211
M1:M4	1	0.0158	0.0068	0.98214668
M1:M2	1	0.0104	0.0045	0.98659931
M2:M4	1	0.0104	0.0045	0.99105193

M1:M2:M3	1	0.0098	0.0042	0.99524768
M3:M4	1	0.0069	0.003	0.99820182
M2:M3	1	0.0042	0.0018	1
SS_T		2.3357		

Appendix K - Estimation of effects for responses BL_1, BL_2, BL_3 and BL_4 under applied locked-in torque condition

Table K.1: Estimation of effects for BL_1.

	Degree of Freedom	Sum Square (SS)	E	$E_{Cumulative}$
M1:M3	1	0.12827	0.284368	0.284368
M1	1	0.08371	0.185581	0.469949
M1:M2:M4	1	0.06099	0.135212	0.605161
M1:M3:M4	1	0.04885	0.108298	0.713459
M2	1	0.029	0.064292	0.777751
M1:M4	1	0.02642	0.058572	0.836323
M2:M3	1	0.01972	0.043718	0.880041
M3:M4	1	0.01425	0.031592	0.911632
M1:M2	1	0.01091	0.024187	0.935819
M1:M2:M3:M4	1	0.00697	0.015452	0.951271
M4	1	0.00629	0.013945	0.965216
M2:M3:M4	1	0.006	0.013302	0.978518
M1:M2:M3	1	0.0058	0.012858	0.991376
M3	1	0.0026	0.005764	0.99714
M2:M4	1	0.00129	0.00286	1
SS_T		0.45107		

Table K.2: Estimation of effects for BL_2.

	Degree of Freedom	Sum Square (SS)	E	$E_{Cumulative}$
M1:M3	1	0.06062	0.340868	0.340868
M1:M2:M4	1	0.05396	0.303419	0.644287
M2:M3:M4	1	0.01434	0.080634	0.724921
M3:M4	1	0.01104	0.062078	0.787
M1:M2	1	0.0074	0.04161	0.82861
M1	1	0.00682	0.038349	0.866959
M1:M2:M3:M4	1	0.00666	0.037449	0.904408
M2:M3	1	0.00516	0.029015	0.933423
M1:M4	1	0.00498	0.028003	0.961426
M3	1	0.00259	0.014564	0.97599
M2:M4	1	0.00229	0.012877	0.988866

M1:M3:M4	1	0.0007	0.003936	0.992803
M1:M2:M3	1	0.00068	0.003824	0.996626
M2	1	0.00057	0.003205	0.999831
M4	1	0.00003	0.000169	1
SS$_T$		0.17784		

Table K.3: Estimation of effects for BL$_3$.

	Degree of Freedom	Sum Square (SS)	E	E$_{Cumulative}$
M2:M3:M4	1	0.05298	0.18021	0.18021
M1:M3	1	0.05152	0.175244	0.355454
M3	1	0.04765	0.16208	0.517535
M2:M4	1	0.04056	0.137964	0.655498
M1:M2:M3	1	0.03662	0.124562	0.780061
M1:M2:M4	1	0.02189	0.074458	0.854519
M1:M2	1	0.01534	0.052179	0.906698
M4	1	0.01423	0.048403	0.955101
M1:M2:M3:M4	1	0.00441	0.015001	0.970101
M1:M4	1	0.00374	0.012722	0.982823
M2	1	0.00179	0.006089	0.988911
M2:M3	1	0.00162	0.00551	0.994422
M1	1	0.00136	0.004626	0.999048
M1:M3:M4	1	0.00028	0.000952	1
M3:M4	1	0	0	1
SS$_T$		0.29399		

Table K.4: Estimation of effects for BL$_4$.

	Degree of Freedom	Sum Square (SS)	E	E$_{Cumulative}$
M2:M4	1	0.08129	0.199534	0.199533628
M2:M3:M4	1	0.07424	0.182229	0.381762396
M1	1	0.05937	0.145729	0.527491409
M3	1	0.04761	0.116863	0.644354443
M1:M3:M4	1	0.03162	0.077614	0.721968581
M1:M4	1	0.02343	0.057511	0.779479627
M1:M2	1	0.02025	0.049705	0.829185076
M1:M2:M3	1	0.01998	0.049043	0.878227786
M1:M2:M4	1	0.01777	0.043618	0.921845852
M1:M3	1	0.01324	0.032499	0.954344624
M2	1	0.01082	0.026559	0.980903289
M1:M2:M3:M4	1	0.00467	0.011463	0.992366225
M4	1	0.00206	0.005056	0.99742268
M2:M3	1	0.00081	0.001988	0.999410898
M3:M4	1	0.00024	0.000589	1
SS$_T$		0.4074		

Attachment A - Eletric Motor Datasheet

neo motion

AK34/42F8FN1.8

ESPECÍFICAÇÕES GERAIS

Especificação	Valor
Ângulo do passo	1,8°
Número de passos	200
Enrolamento	bifilar
Temperatura de operação máx.	80°C
Temperatura ambiente	-10°C ~ 50°C
Resistência de isolação	100VAC / 500VDC
Rigidez dielétrica	500 VAC / 1 min
Classe de isolação	B
Quantidade de fios	8
Peso	2,3kg

Bipolar Série	
Fio do motor	Terminal do driver
Vermelho	A+
Preto	A-
Branco	B+
Verde	B-
Amarelo / Azul	Unidos*
Laranja / Marrom	Unidos*

*Para ligação unipolar, conectar à comum fase A e comum fase B respectivamente.

Bipolar Paralela	
Fio do motor	Terminal do driver
Vermelho / Azul	A+
Preto / Amarelo	A-
Branco / Marrom	B+
Verde / Laranja	B-

TABELA DE SELEÇÃO

NEMA	MODELO	CONEXÃO		HOLDING TORQUE (kgf.cm)	CORRENTE (A/fase)	TENSÃO (V/fase)	RESISTÊNCIA (Ω/fase)	INDUTÂNCIA (mH/fase)	PESO (kg)
34	AK34/42F8FN1.8	Bipolar	Série	42	2,94	4,7	0,4	14	2,3
			Paralelo		5,88	2,35	1,6	3,5	
		Unipolar		29,4	4,2	3,36	0,8	3,5	

INFORMAÇÕES TÉCNICAS

AK34/42F8FN1.8

Fonte: 60VDC
Corrente: 3,08A
Meio passo
Bipolar série

Ligação paralela

Ligação unipolar

Ligação série
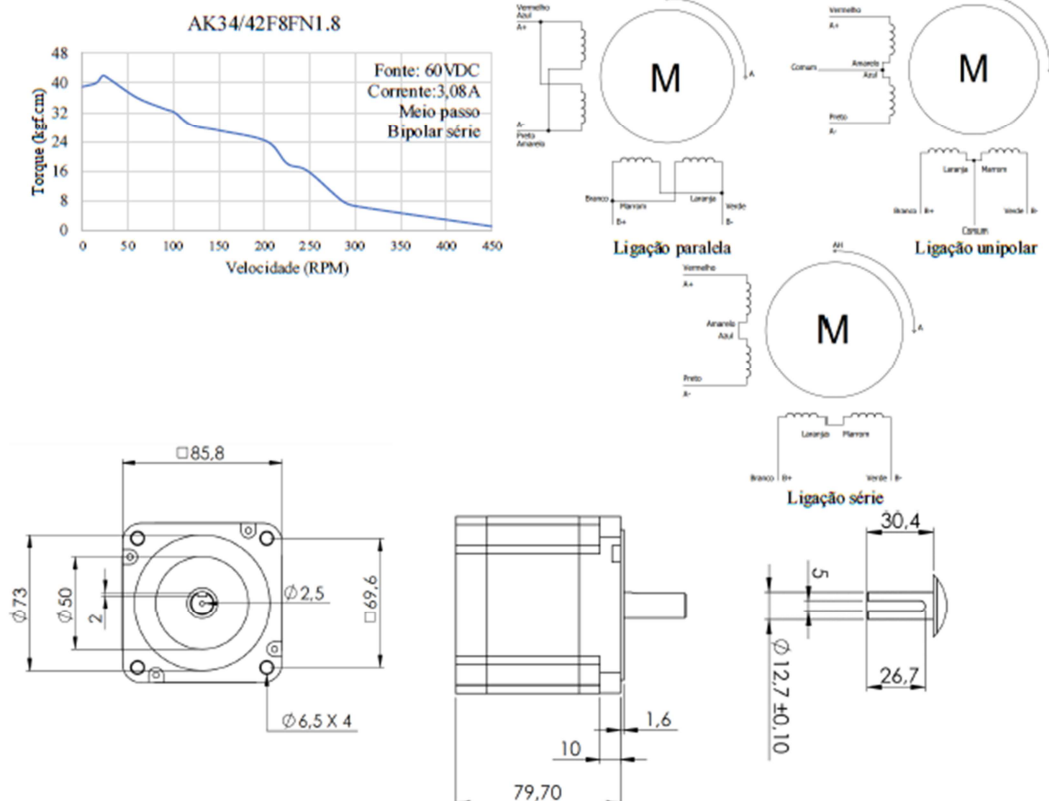
FOLHA DE REGISTRO DO DOCUMENTO

¹· CLASSIFICAÇÃO/TIPO	²· DATA	³· REGISTRO N°	⁴· N° DE PÁGINAS
DM	27 de fevereiro de 2019	DCTA/ITA/DM-006/2019	124

⁵· TÍTULO E SUBTÍTULO:

Dynamic behavior of power losses in a power-circulating rig for gear testing.

⁶· AUTOR(ES):

Nathianne de Moura de Andrade

7. INSTITUIÇÃO(ÕES)/ÓRGÃO(S) INTERNO(S)/DIVISÃO(ÕES):

Instituto Tecnológico de Aeronáutica – ITA

⁸· PALAVRAS-CHAVE SUGERIDAS PELO AUTOR:

Power-circulating; Gear; Efficiency; Mechanical Engineering

9.PALAVRAS-CHAVE RESULTANTES DE INDEXAÇÃO:

Energia; Sistemas dinâmicos; Engrenagens; Eficiência: Dissipação de energia; Circuitos de controle; Torques; Engenharia mecânica.

¹⁰· APRESENTAÇÃO: **X Nacional   Internacional**

ITA, São José dos Campos. Curso de Mestrado. Programa de Pós-Graduação em Engenharia Aeronáutica e Mecânica. Área de Materiais, Manufatura e Automação. Orientador: Prof. Dr. Jefferson de Oliveira Gomes. Defesa em 15/02/2019. Publicada em 2019.

¹¹· RESUMO:

This work presents a structured investigation whose objective is more reliable efficiency measurements at a power-circulating rig. The German Research Association for Drive Technology (FVA) has established a method to measure gear efficiency for this rig concept, assuming that each of the two boxes dissipates half of the amount of power delivered by the motor. An experimental investigation was designed and conducted in order to verify the impacts of transmission boxes with different power losses over the dynamic behavior of the power losses inside the loop. A power-circulating rig was conceived with torque measurements inside the power loop and with a system able to induce controlled losses independently on each transmission box. A 2^4 full factorial design was used to identify significant factors and interactions and this experiment plan was applied under two conditions: with and without locked-in torque. From the experiment results, it was possible to establish the power flow direction and draw conclusions about the relation among the transmission boxes' losses. In the test rig used for this study, it was shown that losses on boxes depend on loss variations on other boxes belonging to the power loop, mainly on those located upstream with relation to the power flow direction. Remarkably, one of the boxes was less susceptible to other boxes' loss variations. A hypothesis for the determination of the less susceptible point to variations in other points of the loop was proposed based on the literature review and the experimental observations.

¹²· GRAU DE SIGILO:

(X) OSTENSIVO ( ) RESERVADO( ) SECRETO